ACTIVE - PASSIVE
MOTION COMPENSATION SYSTEMS
FOR MARINE TOWING

by

PETER ANDREW STRICKER

B. Eng. McGill University
Montreal, 1971.

A THESIS SUBMITTED IN PARTIAL FULFILLMENT OF
THE REQUIREMENTS FOR THE DEGREE OF
MASTER OF APPLIED SCIENCE

in the Department
of
Mechanical Engineering

We accept this thesis as conforming to the
required standard

THE UNIVERSITY OF BRITISH COLUMBIA
VANCOUVER CANADA
January 1975

In presenting this thesis in partial fulfilment of the requirements for an advanced degree at the University of British Columbia, I agree that the Library shall make it freely available for reference and study. I further agree that permission for extensive copying of this thesis for scholarly purposes may be granted by the Head of my Department or by his representatives. It is understood that copying or publication of this thesis for financial gain shall not be allowed without my written permission.

Department of MECHANICAL ENGINEERING

The University of British Columbia
Vancouver 8, Canada

Date APRIL 2, 1975.

ABSTRACT

The dynamic behaviour of an active-passive motion compensation system for handling towed marine vehicles is examined, and a mathematical model developed. In the analysis, the passive system considered is pneumatic, while the active system is electro-hydraulic. The towed body is assumed to be a point mass subjected to hydrodynamic drag, and attached to the motion compensator by means of a linear spring representing the cable. It is not intended, in this project, to model the towed body in greater detail.

The equations of the passive, active, and towed body systems are derived, and linearized to permit a relatively simple frequency-domain solution. A time simulation based on the nonlinear equations, including Coulomb friction in the compensator, is developed for use on an IBM System/370 computer.

A laboratory model is used to conduct experiments at three frequencies, and the results indicate good agreement between the linear, simulation, and real models. Extension of the equations to cover multi-frequency inputs, two-dimensional towing cables, and slow-acting servovalves is also discussed to facilitate application to marine systems.

TABLE OF CONTENTS

LIST OF ILLUSTRATIONS

LIST OF SYMBOLS

SYMBOL	MEANING
A	area of piston
A_A	area of active cylinder piston
A_P	area of passive cylinder piston
C_o	throttling valve coefficient
C_r	capillary coefficient
C_H	hydrodynamic drag factor
C_L	linear drag factor
C_{sv}	servovalve flow coefficient
D	differential operator d/dt
f	friction force in ram
F_A	active cylinder force
F_{NET}	cable tension
F_P	passive cylinder force
F_{RAM}	total ram force
$F_B(s)$	body transfer function
$F_C(s)$	cable transfer function
$G_P(s)$	passive system transfer function
$H(s)$	open loop transfer function
$H_{FB}(s)$	feedback loop transfer function
$H_{FF}(s)$	feedforward loop transfer function
$H_{sv}(s)$	servovalve transfer function
$H_y(s)$	ram centering loop transfer function
K_1	displacement feedback gain
K_2	velocity feedback gain
K_3	acceleration feedback gain
K_{FF}	feedforward static gain
K_{MA}	mechanical advantage
K_P	passive system static gain
K_S	gas spring stiffness
K_{sv}	servo-amplifier gain
m	mass of gas in passive cylinder
M	mass of towed body
N	passive system volume ratio
P	pressure
P_o	initial pressure in passive system
P_1, P_2	passive cylinder pressures
P_d	pressure downstream throttling valve
P_u	pressure upstream throttling valve
P_s	supply pressure in active system
ΔP	pressure drop in active cylinder
Q_A	oil flow into active cylinder
Q_L	leakage flow
Q_v	servovalve flow
r	low level servo signal
R	gas constant for nitrogen
s	Laplace variable
t	time
T	absolute gas temperature
u	disturbance input displacement
V	volume
V_{c1}, V_{c2}	passive cylinder volumes
V_{t1}, V_{t2}	passive tank volumes

$\dot{W}$	power consumption
x	body displacement
x_1	tow point displacement
y	piston displacement
y_c	tow pt displacement relative to ship
z	servovalve actuating current
γ	ratio of specific heats
δ	small piston displacement
ζ	passive system critical damping ratio
ζ_{sv}	servovalve critical damping ratic
λ_1	servovalve flow gain
λ_2	servovalve flow-pressure coefficient
λ_3	bypass valve flow coefficient
τ_1 τ_2	passive system time constants
τ_{sv}	servovalve time constant
ω_o	design frequency
ω_n	passive system natural frequency
ω_{sv}	servovalve natural frequency

ACKNOWLEDGEMENT

I am most grateful for the patient help and encouragement of my supervisor, Dr. R. McKechnie. Special thanks is due to Dr. Keefer of B. C. Research Council who initially gave me the idea for this project, and for his subsequent assistance. Thanks are also due to Mr. Johnson of Fleck Brothers for donating a servovalve and amplifier; to Dr. Vickers for making the valve work; to Messrs. Hoar and Hurren and their crew for building the apparatus and lending equipment; to the Department of Electrical Engineering for the use of their analogue computer; and to Miss Wendy Allen for keypunching the manuscript. All computing was done at the University of British Columbia Computing Centre. The project was funded by the National Research Council of Canada under Grant #67-8183.

CHAPTER I

INTRODUCTION

1.1 Problem Description

The safety and performance of towed submersible vehicles depend, to a large extent, on the ability of the handling gear to decouple wave induced motions of the surface ship from the towing cable. This decoupling is usually accomplished by a motion compensation system -- essentially a special class of a vibration isolator.

Vibration isolating devices are employed in systems where a mass is to be isolated from an external force or motion disturbance. Some common examples are automobile suspensions, earthquake absorbers, and rocket-borne instrumentation cushions.

The marine towing isolation problem has three distinguishing features. First, the frequency of surface ship motion is low, in the order of 0.1 Hz, while the associated amplitude may be in the order of fifteen feet. Second, the mass of the submersible, including the water it entrains, is large -- typically in excess of 30,000 pounds-mass. Finally, the vertical displacement of the stern of the ship consists of the superposition of several harmonic functions of different amplitudes and frequencies as defined by a spectral density function. Thus, the input disturbance is somewhat more

predictable than the forms of vibration present in the previous examples.

The marine towing motion compensation system is usually designed to maintain constant towing cable tension. Once this requirement is met, it then follows that the acceleration of the submersible will be zero, and all undesirable motion will be eliminated. To provide this constant cable tension, all systems attempt to pay out or haul in cable as the ship moves up or down, thus decoupling the motion of the ship from the cable.

The index of performance of such a motion compensation system is the ratio of the amplitude of towed body to ship displacement. It is generally stipulated that the performance index must be less than a given value at the frequency which contains the greatest energy as taken from the sea state spectral density function. This is then considered the primary design frequency. In addition, the minimum acceptable index of performance for other frequencies within the spectrum may be specified. Once the overall physical constraints are met (e.g. weights, geometries, etc., over which the designer has little or no control) the problem then becomes that of determining the physical characteristics of the system. Some of the design considerations include simplicity, reliability, initial cost, and power consumption.

Three of the more popular motion compensation systems are

shown in Fig. 1.1.1. Although very different in appearance, each employs a pneumatic spring in the form of a gas accumulator to operate a hydraulically actuated positioner. With systems (a) and (b), the positioner is a cylinder which controls the vertical displacement of a sheave over which the cable is reeved. System (c) uses a hydraulic winch to haul in and pay out cable. In each case, the cable tension is balanced by a passively-acting pneumatic spring[1]. As will be seen in Section 1.2, such systems, under certain conditions, can be tuned to perform adequately over a narrow frequency range.

It is possible to design a purely active system, in which a significant amount of energy is expended to achieve the stabilization effect. In such a system, a transducer monitors the motion of the load and after suitable signal processing, controls the flow of oil to a hydraulic actuator. Active systems are superior to passive ones in that they are capable of good motion isolation over a wider frequency range. However, because they require a bulky power source and consume a large amount of energy when controlling a massive load, they are not suitable for marine applications.

To improve the performance of a passive system without a large expenditure of power, a hybrid active-passive system is

---

[1] In a passive system, the sum of the potential energy in the spring and kinetic energy of the load is conserved, apart from some dissipation due to damping and friction. Thus, no external energy is required to operate the system.

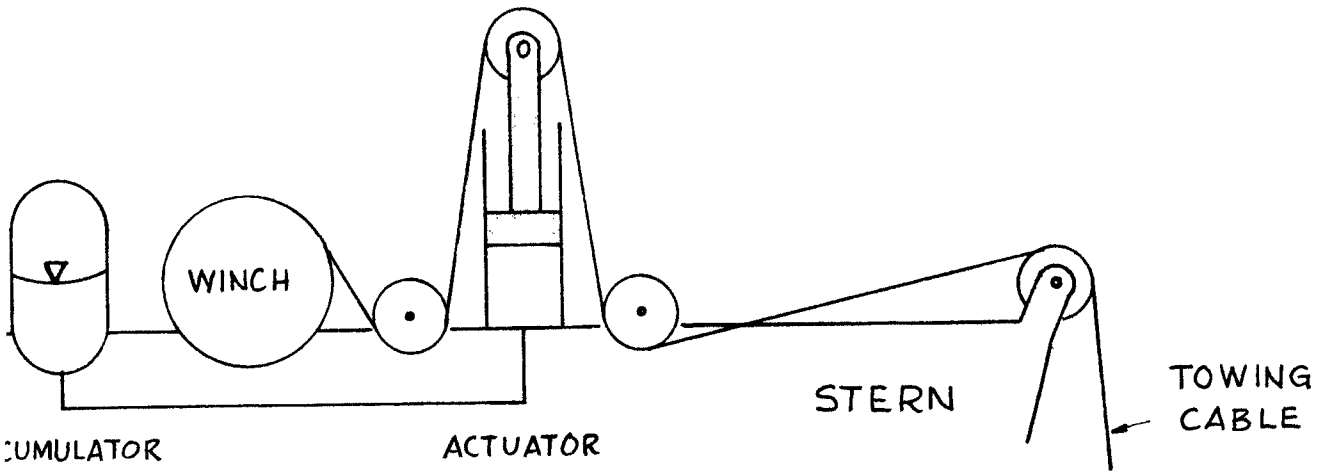

(a) RAM TENSIONER

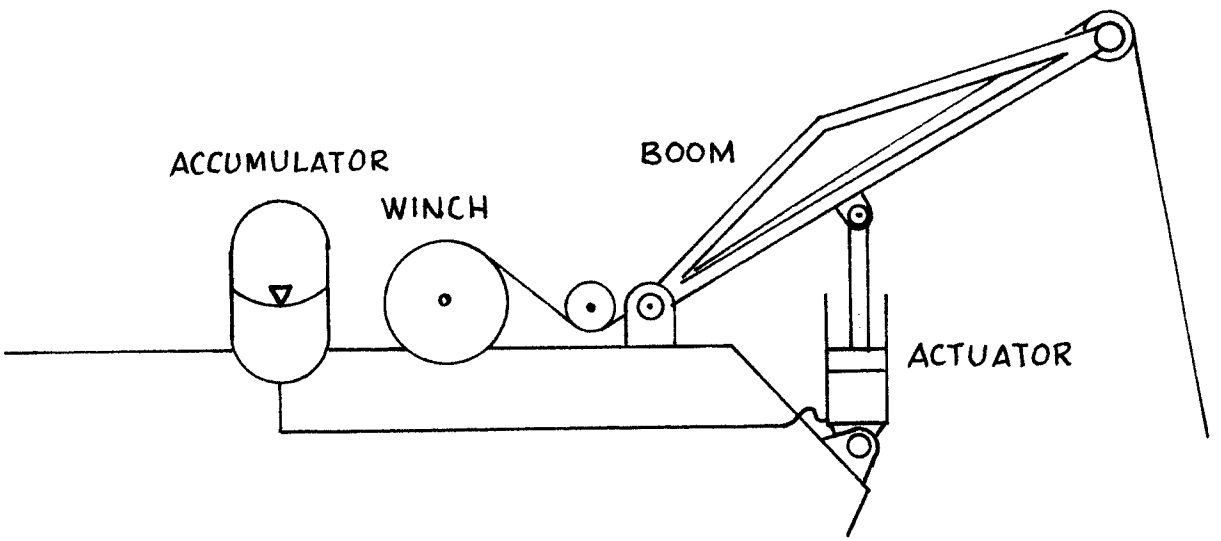

(b) BOOM BOBBER

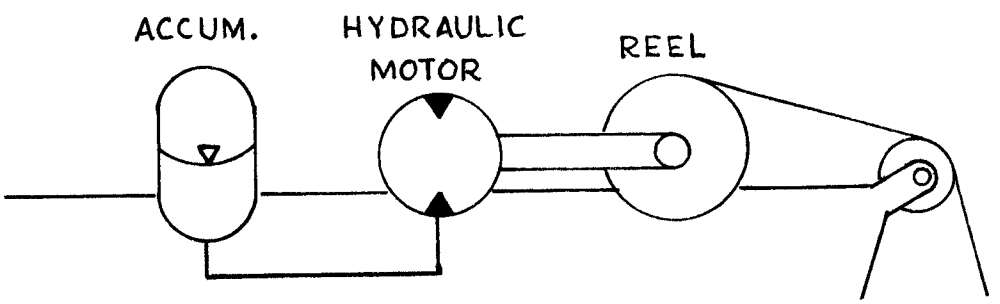

(c) TENSIONING WINCH

FIG. 1.1.1 MOTION COMPENSATION SYSTEMS

proposed. Such systems have been successfully used to isolate small components from an environment of severe shock and vibration. However, as outlined in the next section, no work was found related to the application of such systems to the marine towing field.

1.2 State of the Art

Vibration isolation systems, both active and passive, have been widely investigated in the past decade. In general, it appears that there were two distinct methods of dealing with the problem; one being highly theoretical, and the other being the analysis of a particular problem. The latter method, especially in the field of ocean engineering, has been very empirical in nature, with little or no mathematical justification of the ideas presented.

This section will discuss some of the relevant work that has been done, first, in vibration isolation, and second, in the field of ocean engineering applications.

In general, there are two distinct vibration reduction methods available: absorption and isolation.[1] Isolation involves placing a resilient material between the disturbance source and the receiver (the system to be protected), whereas absorption involves the attachment of an energy absorbing device to either the source or receiver (Fig. 1.2.1). Isolation can be achieved either actively or passively, and can be made effective over a wide range of frequencies. Absorption is generally achieved passively using a spring-mass system which is in resonance with the source and receiver at one particular frequency. At that frequency, the receiver experiences no input at all, but this

---

[1] See Ref. (15)

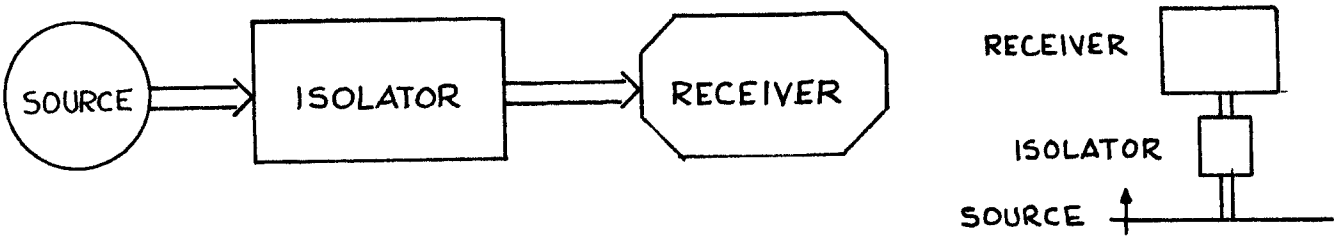

(a) ISOLATION

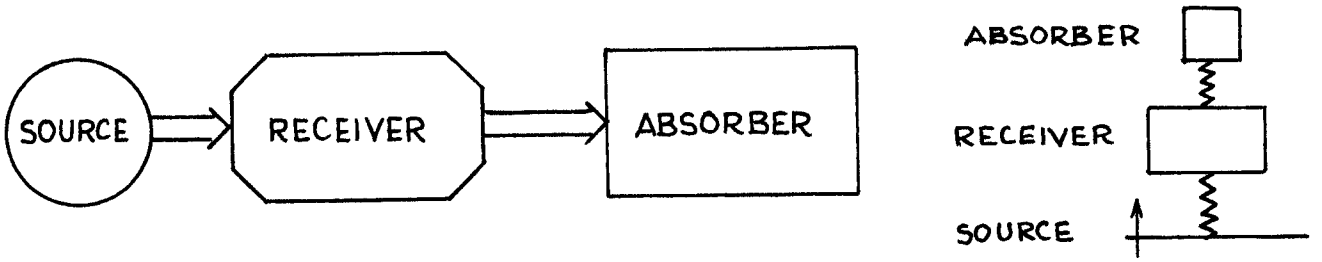

(b) ABSORPTION

FIG. 1.2.1 VIBRATION ISOLATION & ABSORPTION

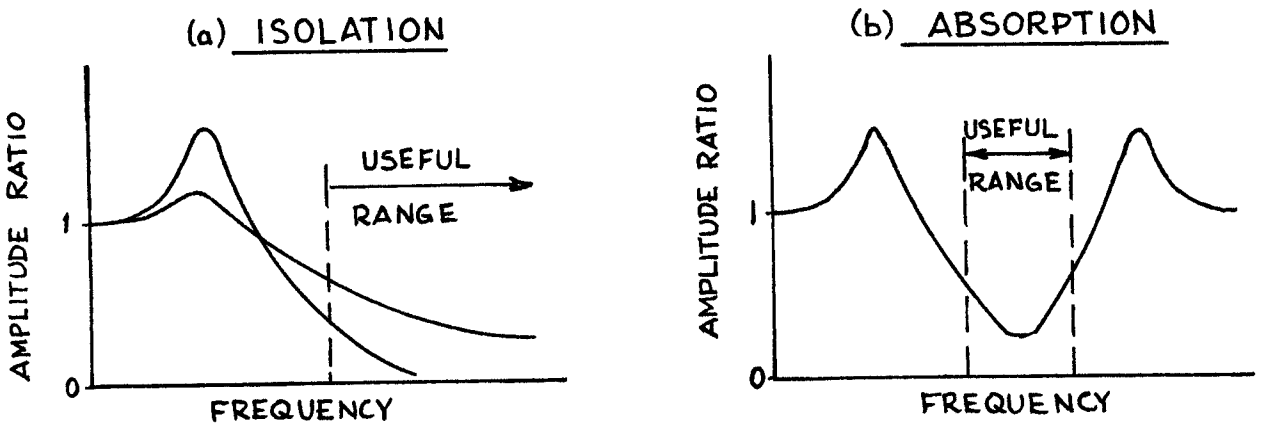

FIG. 1.2.2 PERFORMANCE CHARACTERISTICS

effect is confined to a very narrow frequency band. Also, undesirable resonant peaks occur at two frequencies, corresponding to the separate natural frequencies of the receiver and absorber. Fig. 1.2.2 illustrates the performance of isolators and absorbers.

A passive pneumatic isolator as shown in Fig. 1.2.3(a) has been examined by Cavanaugh[1]. He solved the linearized third order system equations in the frequency domain, and found the optimum critical damping ratio in terms of the tank to cylinder volume ratio. Fig. 1.2.3(b) shows the frequency response of the system, and Fig 1.2.3(c) shows the critical damping ratio function which yields the smallest maximum amplitude ratio.

Another passive isolation system directly applicable to automobile suspensions has been examined by Thompson[2]. He considered a two-dimensional linear system with four degrees of freedom, and developed an optimum performance index based on ride comfort and road-holding ability.

A more general approach to optimizing passive suspensions has been presented by Hedrick for use in the design of high speed tracked vehicles[3]. An optimum passive shock isolator, which uses a variable friction element to dissipate energy has

---

[1] See Ref. (5)
[2] See Refs. (20) and (22)
[3] See Ref. (7)
[4] See Ref. (11)

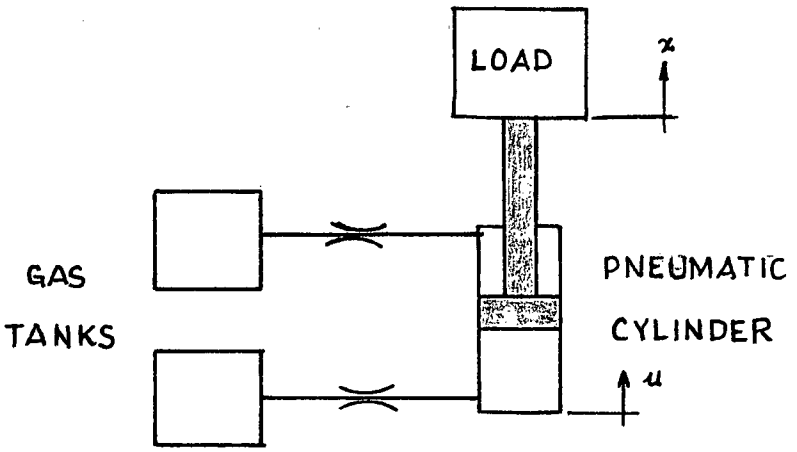

(a) CONFIGURATION

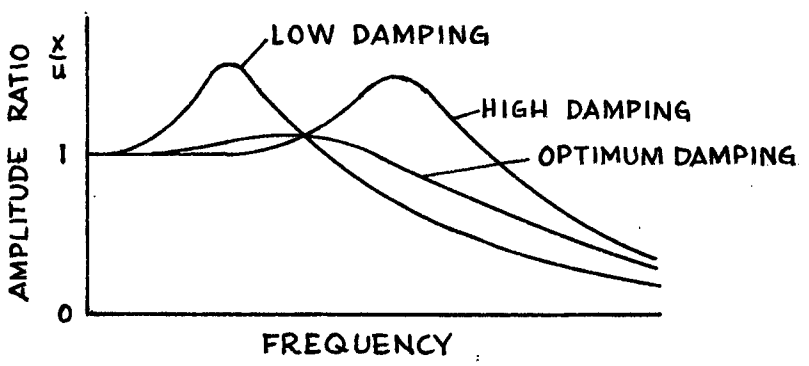

(b) PERFORMANCE

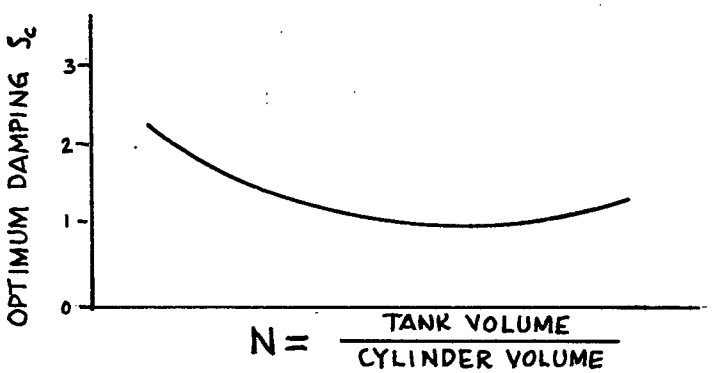

(c) OPTIMUM CRITICAL DAMPING RATIO

FIG. 1.2.3 PASSIVE PNEUMATIC SYSTEM

been proposed by Mercer and Rees[4].

Active systems for shock and vibration isolation have also been examined. Soliman proposed a servovalve controlled pneumatic system using displacement and velocity feedback to control the servovalve[1]. Thompson considered active systems for automobile suspensions[2]. Porter, Athans, and Karnop all presented highly mathematical methods for dealing with linear active systems[3]. Kriebel developed an active system for shock isolation[4].

None of the above-mentioned work is in a form which is readily applicable to the problem of motion compensation in the marine environment. The theoretical solutions relate mostly to linear systems, while the more practical solutions are too specific and require much modification to make them useful for other design purposes.

There are a number of marine motion compensation systems (mostly passive) operational around the world, but little documentation exists to help predict a system's performance before it is built. Most systems consist of a pneumatic spring, as described in Section 1.1, and are classed as vibration isolators. Keefer proposed a simple manner in which an isolator

---

[1] See Refs. (17) and (18)
[2] See Ref. (21)
[3] See Refs. (13), (1) and (8)
[4] See Ref. (10)

can be made into an absorber by making the direction of motion of the compensator mass orthogonal to the input disturbance[1]. Fig. 1.2.4(a) illustrates a ram tensioner in such a configuration. Such a system is tuned so that the anti-resonance occurs at the frequency which contains the dominant amplitude of vibration. Fig 1.2.4(b) shows the typical performance of a tuned system. Note that damping increases bandwidth at the expense of the system's attenuation.

Buck[2] and Sutherland[3] suggested the use of active systems, but neither has developed a complete analysis of such a system, nor suggested a method of predicting the performance of a real, nonlinear system. In addition, they have not recognized the fact that power consumption can be reduced by incorporating a passive system to support the static weight of the load while the active system is used solely for motion compensation.

---

[1] See Ref. (9)
[2] See Ref. (3)
[3] See Ref. (19)

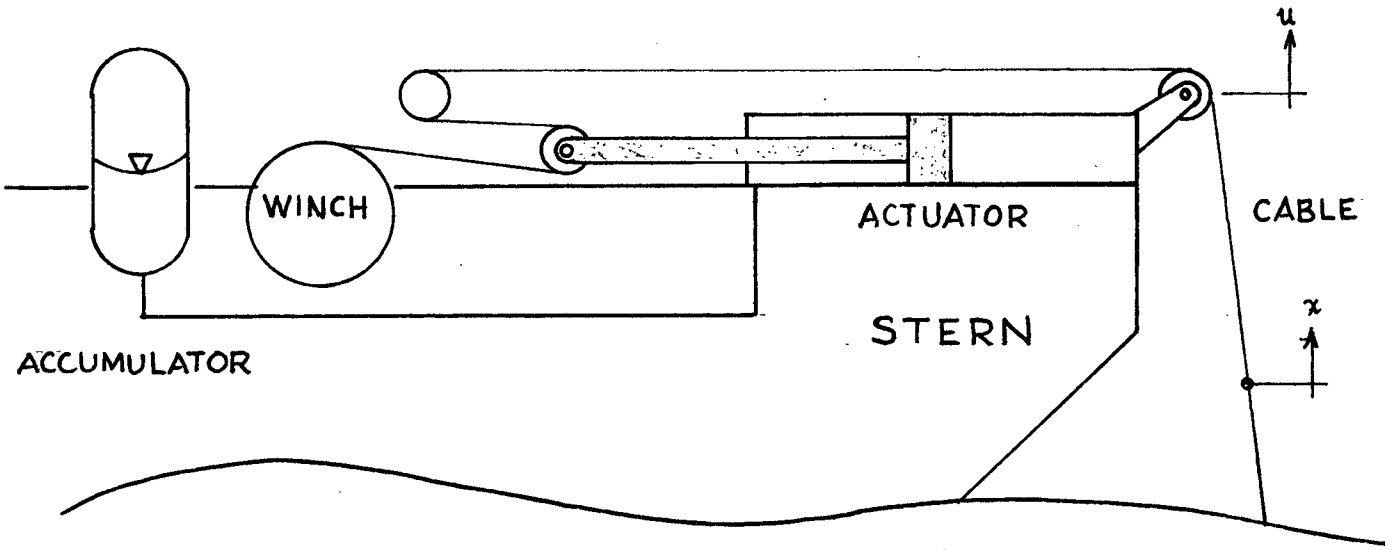

(a) GENERAL ARRANGEMENT

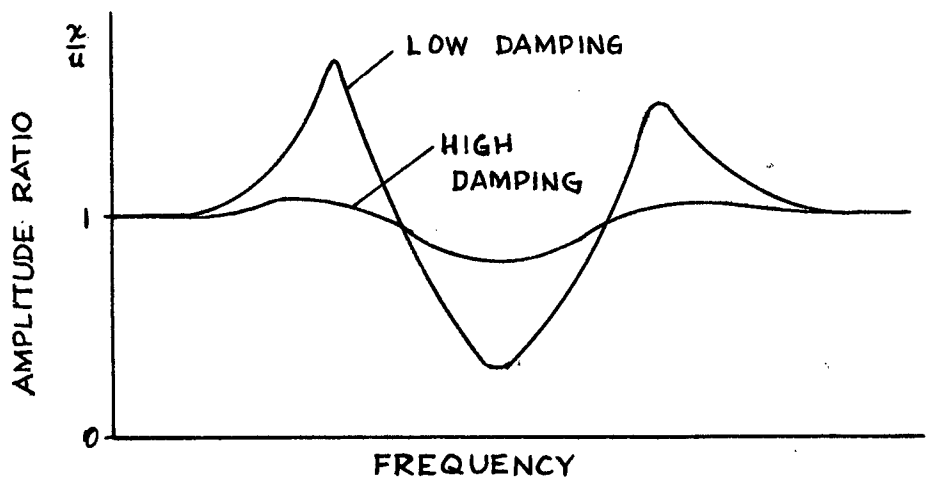

(b) PERFORMANCE

FIG. 1.2.4 TUNED RAM TENSIONER

1.3 Objectives and Scope of Project

The objectives of this project are first, to study the dynamics of an active-passive motion compensation system for marine towing, and second, to use the results of this study to develop guidelines for use in designing real systems. These objectives are accomplished by proceeding in six steps:

1. Representing a typical system in a form which closely approximates reality, yet which lends itself to mathematical analysis and simulation.
2. Developing the mathematical model, including such nonlinearities as hydrodynamic drag and dry friction.
3. Linearizing the mathematical equations and conducting a frequency-domain analysis to obtain a first approximation of the important system parameters.
4. Developing a digital computer simulation program which will validate and optimize the parameters derived in step #3.
5. Constructing a small working model to check the validity of the mathematical and simulation models.
6. Relating the results of the foregoing to the design of real systems.

CHAPTER II

THEORETICAL ANALYSIS

2.1 Typical System

Some of the commonly used passive motion compensation systems were shown in Fig. 1.1.1. It is possible to devise an active-passive system by adding an active actuator parallel to the passive one. In the case of the ram tensioner and boom bobber, this means adding a second cylinder, while for the tensionig winch, adding a second hydraulic motor. The three configurations shown in Fig 1.1.1 are very similar mathematically. The similarity between (a) and (b) is obvious -- only the mechanical advantages of the reeving, in the case of (a), or the boom, in the case of (b), are different. In the case of the winch, the hydraulic motor is equivalent to a number of cylinders connected in parallel, and hence can be modelled as a single cylinder. Thus, for the purpose of this project the ram tensioner is selected as a typical system.

The overall configuration of the typical system is shown in Fig. 2.1.1. The passive subsystem is the same as before, while the active subsystem consists of a hydraulic cylinder controlled by an electrohydraulic servovalve. The control system consists of accelerometers mounted on the towing and ram sheaves, whose signals are processed and fed to the servovalve. The signal processing network is the most vital component of the system,

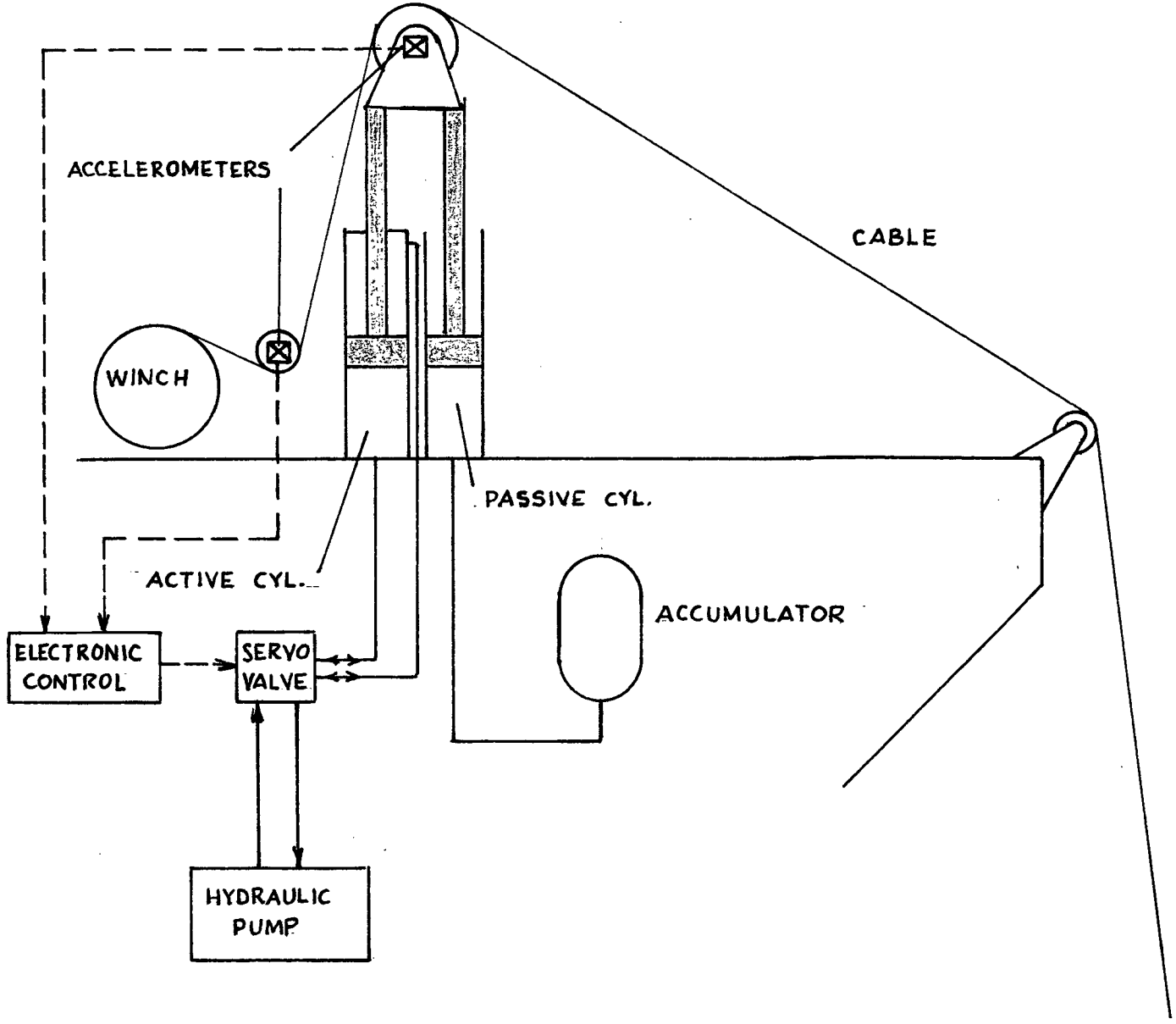

FIG. 2.1.1 ACTIVE/PASSIVE RAM TENSIONER

and will be the subject of thorough analysis.

As pointed out earlier, the load can be a diving bell suspended from a stationary ship, a submerged body towed at high speed (in the order of 10 knots), or a surface vessel such as a barge. For the case of a submersible supported from a ship which is not moving horizontally with respect to the water, the cable can be represented as a one-dimensional elastic link whose longitudinal axis is vertical. In the case of a moving ship towing a barge or submersible, the cable will assume a complex three-dimensional curve. Since this project is concerned primarily with the behaviour of the motion compensation system, the typical system considered will include the one-dimensional cable. Application of the approach to the case of three-dimensional cable, as developed by Walton and Polachek, is discussed in Chapter V.

2.2 The Equivalent Model

To facilitate the analysis of the ram tensioner described in Section 2.1, the following simplifications will be made:

1. The static tension in the cable due to the submersible's weight is not considered. This simplification does not affect the dynamics of the motion compensator.

2. The cable is considered to be a one-dimensional elastic link for the reasons set forth in Section 2.1.

3. The passive subsystem is considered to be purely pneumatic. This restriction actually increases the complexity of the problem, but is included to demonstrate the method of application of the compressible fluid flow equations. In many applications, the passive system would actually be an "air-over-oil", or hydropneumatic system, as shown in Figure 1.1.1.

Using these simplifications, it is possible to model the chosen system as shown in Figure 2.2.1. The form shown in Fig. 2.2.1 was devised to facilitate mathematical analysis and test-model construction. The active and passive motion compensation

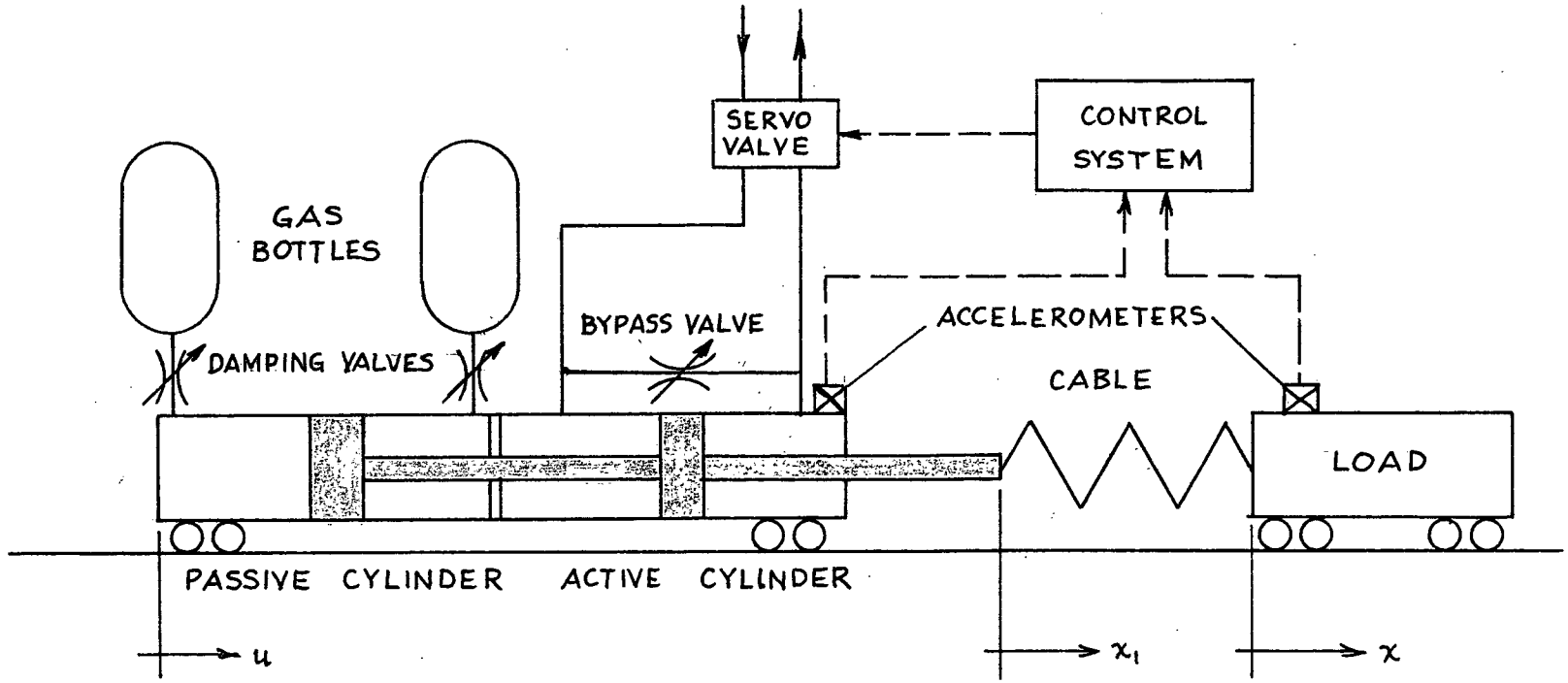

FIG. 2.2.1 EQUIVALENT SYSTEM

cylinders are placed horizontally on a carriage, with their piston rods connected sc as tc function in parallel. The carriage is driven horizontally in a sinusoidal manner, with the desired frequency and amplitude, simulating the vertical motion of the ship. The load is modelled by a second carriage containing the desired mass, connected to the motion compensation piston rod by means of a spring which is assumed to model the cable. The entire system is similar to the real case of Fig. 2.1.1 except that all motion is horizontal instead of vertical. As a result, the static weight of the towed body is not considered. Therefore, in modelling the spring characteristic of the passive system, it is necessary to pressurize both sides of the passive cylinder, such that the net static force at the piston rod is zero.

In general, this equivalent system accurately models the motion compensation system, but does not fully consider the dynamics of the cable and towed body. However, the design method developed here is flexible enough to accomodate these additions if the necessary parameters are available to the designer.

2.3 The Passive System

The passive side of the system under consideration consists of a pneumatic ram, with each end connected via a throttling valve to a receiving tank (Fig. 2.3.1). The throttling valves are used to introduce damping into the system.

The mass flow to and from a tank or cylinder is derived in Appendix A, and is given by

$$\dot{m} = \frac{1}{RT}\left[\frac{V}{\gamma}\dot{P} + P\dot{V}\right] \qquad (2.3.1)$$

where

$\dot{m}$ is the mass flow rate,

R is the gas constant for the particular gas used,

T is the absolute temperature,

V is the tank or cylinder volume,

P is the absolute pressure,

and γ is the ratio of specific heats.

Because the receiving tanks have fixed volumes, and the mass flows are proportional to the negative of the pressure changes, we can write

$$\dot{V}_t = 0 \qquad (2.3.2)$$

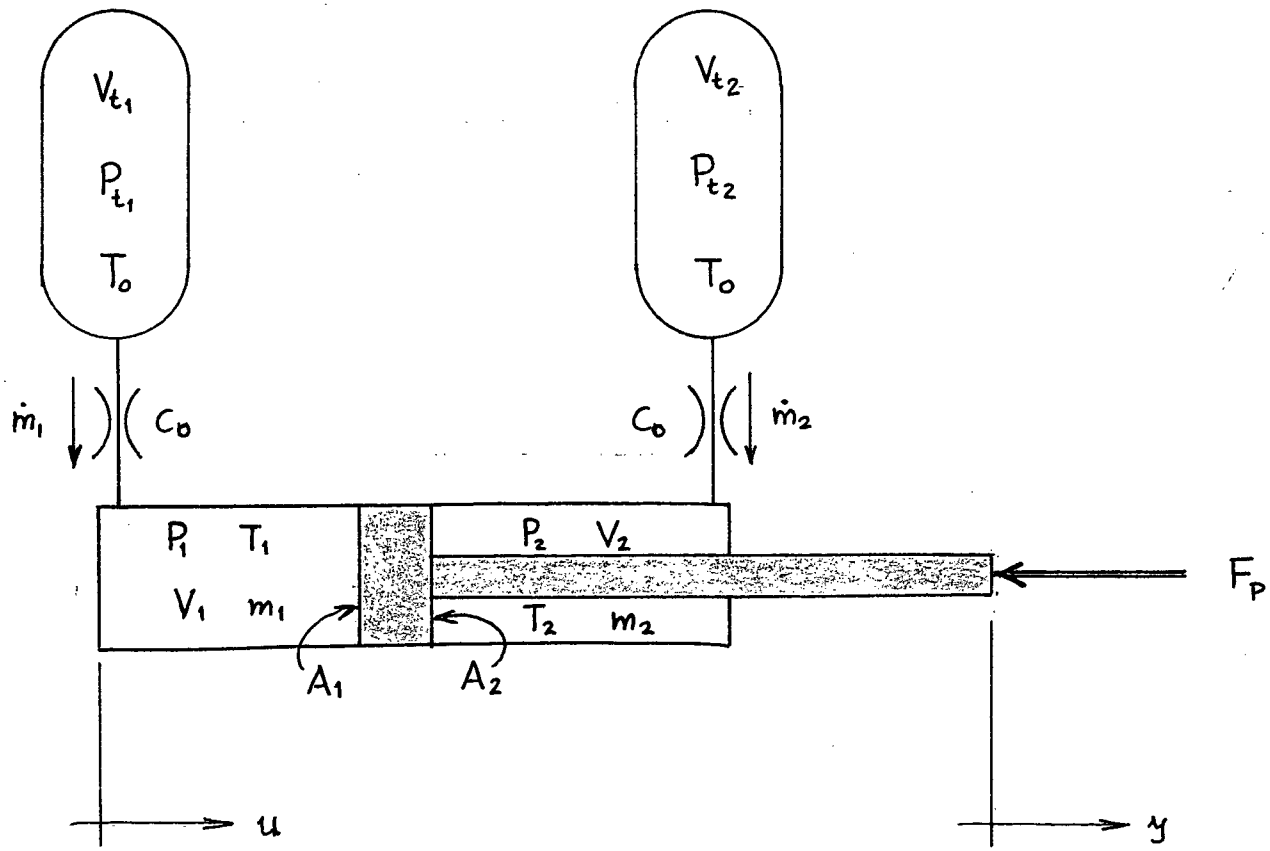

FIG. 2.3.1 PASSIVE SYSTEM

and

$$\dot{m} \propto - \dot{P}_t \tag{2.3.3}$$

where

V_t is the tank volume

and P_t is the tank pressure.

Substituting (2.3.2) and (2.3.3) into (2.3.1) gives

$$\dot{m}_1 = - \frac{V_{t_1}}{\gamma R T_1} \dot{P}_{t_1}$$
$$\dot{m}_2 = - \frac{V_{t_2}}{\gamma R T_2} \dot{P}_{t_2} \tag{2.3.4}$$

where the subscripts 1 and 2 refer tc the left and right hand sides of the passive system, respectively.

In general, the volume of the receiving tanks, and hence the volume of fluid contained, is large compared to the mass flow in and out of the tanks; thus the temperature cf the gas can be considered constant,[1] i.e.

---

[1] For an actual system having an effective piston area of 13.46 square inches, a displacement of five feet as measured at the tow point causes a change in absolute temperature cf cnly 1.9%, assuming adiabatic compression or expansion (worst case).

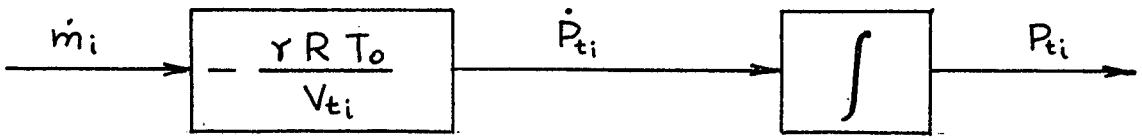

FIG. 2.3.2

BLOCK DIAGRAM of TANK DYNAMICS

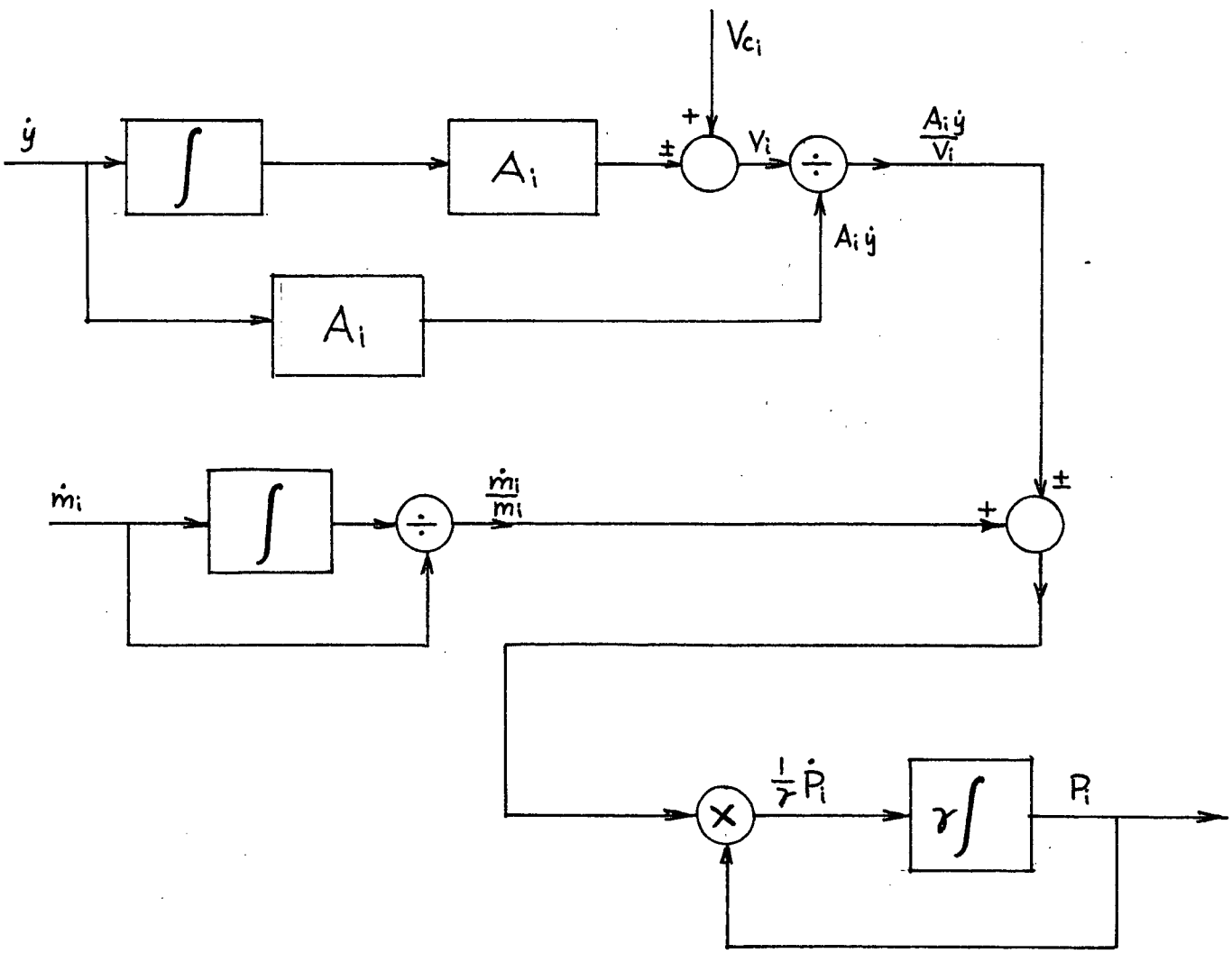

FIG. 2.3.3

BLOCK DIAGRAM of CYLINDER DYNAMICS

$$T_1 = T_2 = T_o \tag{2.3.5}$$

Fig. 2.3.2 is a block diagram of the tank flow equations.

The mass flow to and from the cylinders is also expressed by (2.3.1), except that:

$$\begin{aligned} V_1 &= V_{c_1} + A_1 y \\ V_2 &= V_{c_2} - A_2 y \end{aligned} \tag{2.3.6}$$

$$\begin{aligned} \dot{V}_1 &= A_1 \dot{y} \\ \dot{V}_2 &= -A_2 \dot{y} \end{aligned} \tag{2.3.7}$$

$$\begin{aligned} \dot{m}_1 &\propto \dot{P}_1 \\ \dot{m}_2 &\propto \dot{P}_2 \end{aligned} \tag{2.3.8}$$

where

V_1 and V_2 are the volumes of the left and right sides of the cylinder,

V_{c_1} and V_{c_2} are the initial values of V_1 and V_2,

A_1 and A_2 are the effective piston areas,

and y is the piston displacement.

Substituting (2.3.6), (2.3.7) and (2.3.8) into (2.3.1) gives

$$\dot{m}_1 = \left[\frac{V_1}{\gamma} \dot{P}_1 + P_1 A_1 \dot{y} \right] \frac{1}{RT_1}$$
$$\dot{m}_2 = \left[\frac{V_2}{\gamma} \dot{P}_2 - P_2 A_2 \dot{y} \right] \frac{1}{RT_2} \qquad (2.3.9)$$

Due to the relatively small volume of the cylinder and the large variation in pressure, temperature change is nc longer negligible. Using the equation of state for an ideal gas,

$$T_i = \frac{P_i V_i}{m_i R} \qquad (i = 1,2) \qquad (2.3.10)$$

where

$\dot{m}_i$ is the mass of gas in the i-th side of the cylinder.

Substituting (2.3.10) into (2.3.9) gives

$$\dot{m}_1 = m_1 \left[\frac{1}{\gamma} \frac{\dot{P}_1}{P_1} + \frac{A_1}{V_1} \dot{y} \right]$$
$$\dot{m}_2 = m_2 \left[\frac{1}{\gamma} \frac{\dot{P}_2}{P_2} - \frac{A_2}{V_2} \dot{y} \right] \qquad (2.3.11)$$

Fig. 2.3.3 shows the block diagram of the the cylinder equations.

The mass flow through each throttling valve is derived in

Appendix A , and is given by

$$\dot{m} = C_o P_u \left(\frac{P_d}{P_u}\right)^{1/\gamma} \sqrt{\frac{2\gamma}{RT_u(\gamma-1)} \left\{ 1 - \left(\frac{P_d}{P_u}\right)^{\frac{\gamma-1}{\gamma}} \right\}} \qquad (2.3.12)$$

where

C_o is the valve constant,

P_u is the upstream pressure,

P_d is the downstream pressure,

and T_u is the upstream temperature.

It is observed that the direction of mass flow is from high to low pressure; that is, P_u, the upstream pressure, is the greater of P_u, P_d . By the convention shown in Fig. 2.3.1, if $P_{ti} > P_i$ then $\dot{m}_i > 0$; conversely, when $P_{ti} < P_i$, $\dot{m}_i < 0$. Consequently, in solving (2.3.12) the upstream end must first be determined. Then the correct algebraic sign can be assigned to $\dot{m}_i$. Fig. 2.3.4 shows the block diagram of the valve equations.

The equations (2.3.4), (2.3.9) and (2.3.12) must be solved simultaneously to yield P_1 and P_2 given a piston displacement y. The force generated in the ram can then be found:

$$F_p = P_1 A_1 - P_2 A_2 \qquad (2.3.13)$$

where

F_p is the ram force.

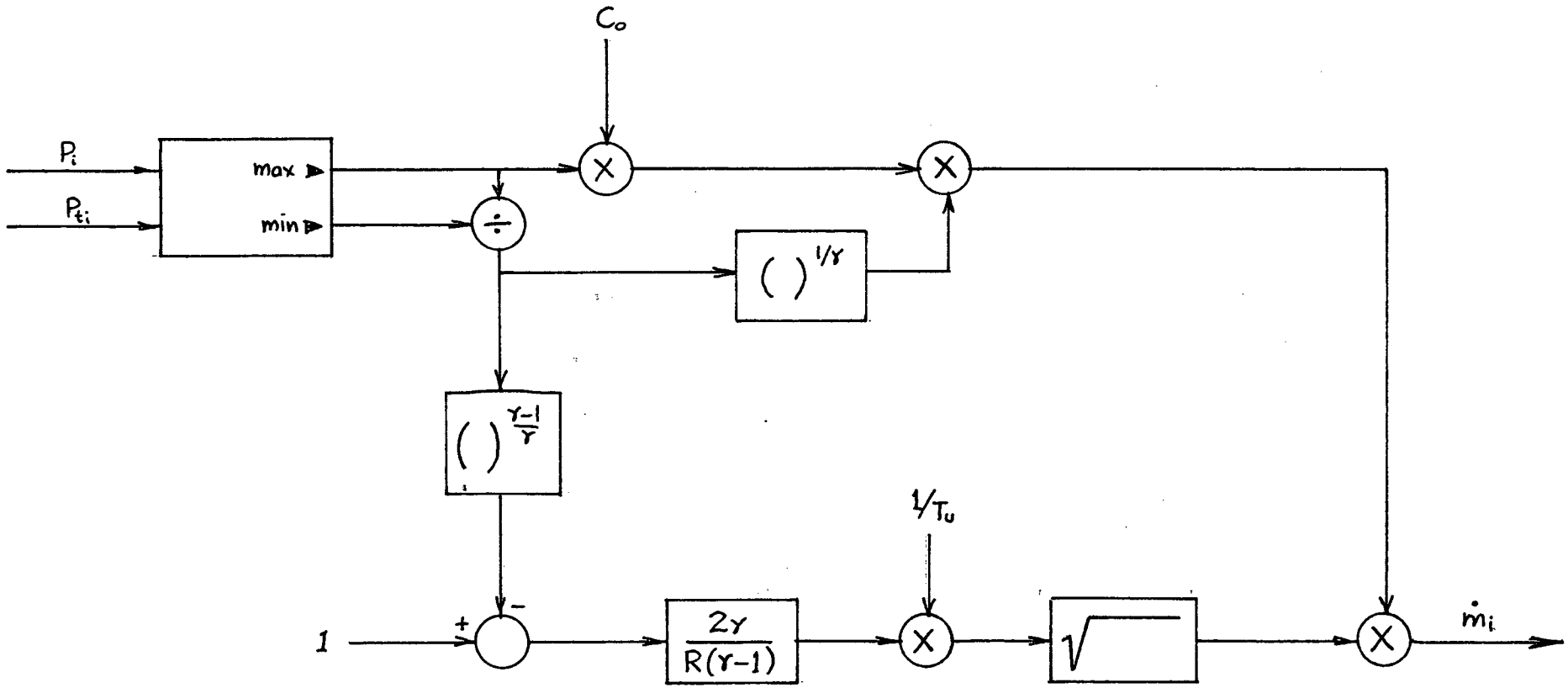

FIG. 2.3.4.

BLOCK DIAGRAM of VALVE DYNAMICS

The block diagram of the passive system dynamics is shown in Fig. 2.3.5. Since it is difficult to solve this system of equations analytically, a numerical solution is now developed. The strategy used in the numerical solution is as follows:

1. Calculate P_{t_i} as shown in Fig. 2.3.2
2. Calculate P_i as shown in Fig. 2.3.3
3. Calculate $\dot{m}_i$ as shown in Fig. 2.3.4.
4. Repeat steps 1 to 3 with the new value of $\dot{m}_i$ until P_{t_i} and P_i no longer change from iteration to iteration.
5. Calculate the ram force from (2.3.13).

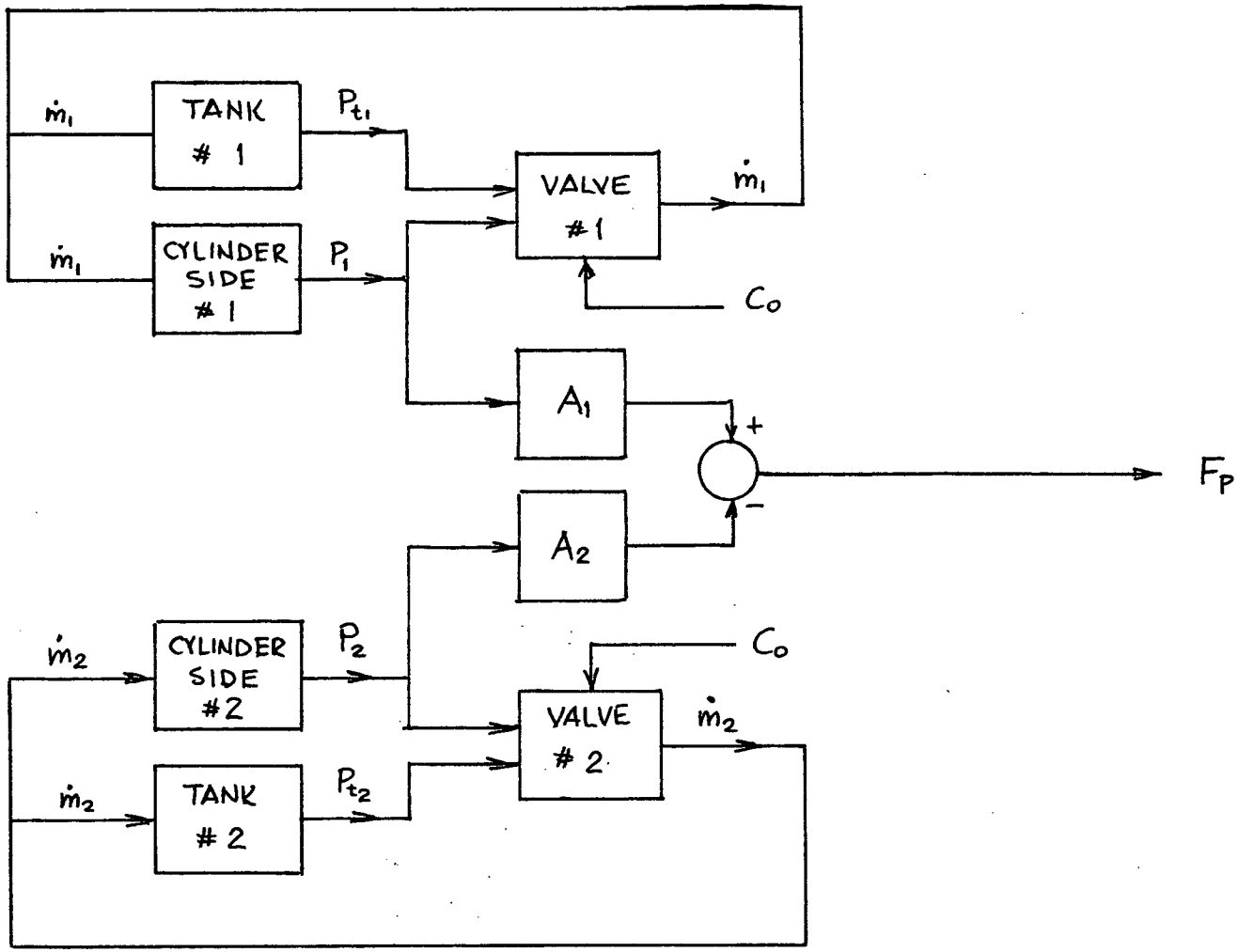

FIG. 2.3.5

BLOCK DIAGRAM of PASSIVE SYSTEM DYNAMICS

2.4 The Active System

The active side of the system under consideration consists of a positive displacement hydraulic pump, relief valve, gas accumulator, servo-valve, and hydraulic cylinder. (Fig. 2.4.1)

It is assumed that the pump discharge flow rate always exceeds the system requirement, hence maintaining the pressure in the accumulator equal to the relief valve setting. In fact, the accumulator pressure will vary slightly with changes in flow rate due to friction losses in the hydraulic lines, but this fluctution is negligible compared to the working pressure. Therefore, the supply pressure is considered constant.

The compressibility effect of the hydraulic fluid is examined in Appendix C, and is found to contribute an error in flow of only 2.6% for a typical full-scale system. Therefore, the compressibility of the fluid is not considered.

The flow-pressure relationship for the servo-valve is given by the manufacturer for selected values of actuating signal, z (Fig. 2.4.2). As shown in Appendix B, this relationship, for a zero-lapped valve[1], can be accurately modelled by

---

[1] See Ref. (6) for the equations of under- and over-lapped servo-valves.

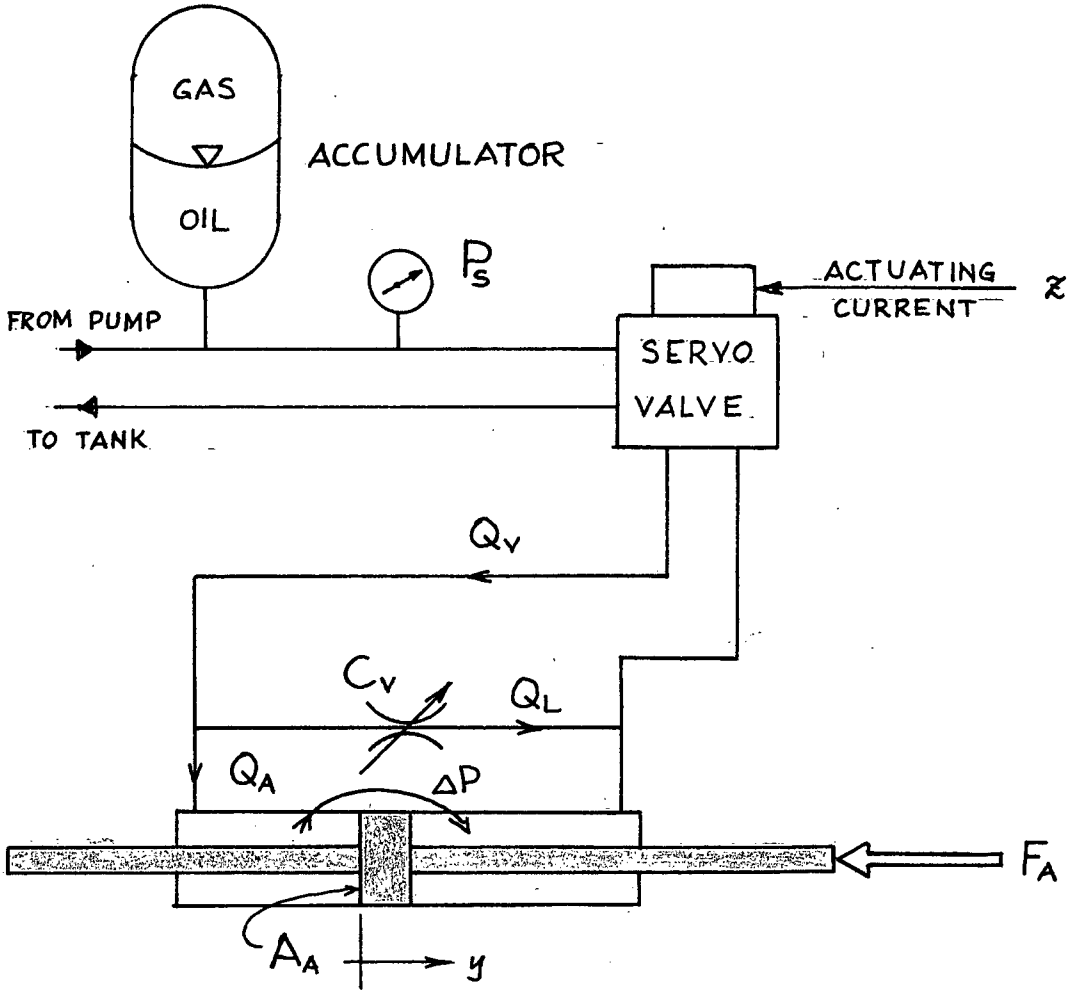

FIG. 2.4.1 ACTIVE SYSTEM

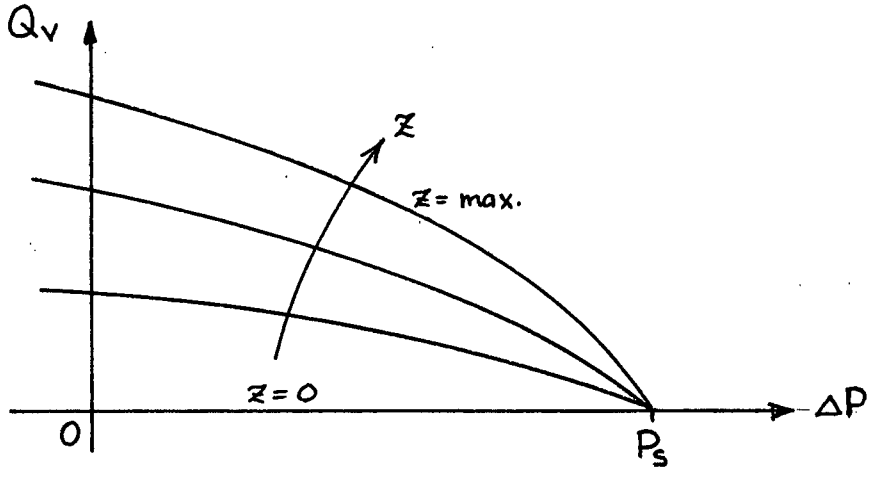

FIG. 2.4.2 SERVOVALVE CHARACTERISTICS

$$Q_V = C_{SV}\, z \sqrt{P_s - \Delta P} \qquad (2.4.1)$$

where

Q_V is the volume flow through the valve,

ΔP is the pressure drop across the load,

C_{SV} is the characteristic constant of the servo-valve,

P_s is the supply pressure, assumed constant,

and z is the actuating signal.

Leakage across the cylinder is often useful in stabilizing a servo-system, and is therefore included in the analysis. Leakage is provided by means of an auxiliary path around the piston, and controlled by means of a valve. The leakage flow, Q_L, is given by

$$Q_L = C_v \sqrt{\Delta P} \qquad (2.4.2)$$

where

C_v is the characteristic constant of the valve.

The total flow into the ram, Q_A, is the difference between the flow through the servo-valve and the leakage flow:

$$Q_A = Q_v - Q_L \tag{2.4.3}$$

The sign convention is such that Q_A is positive when it causes the piston tc move to the right. Substituting (2.4.1) and (2.4.2) into (2.4.3) gives

$$Q_A = C_{sv}\, z \sqrt{P_s - \Delta P} - C_v \sqrt{\Delta P} \tag{2.4.4}$$

The velocity of the piston with respect to the cylinder, $\dot{y}$, can now be expressed as

$$\dot{y} = \frac{Q_A}{A_A} = \frac{C_{sv}}{A_A} z \sqrt{P_s - \Delta P} - \frac{C_v}{A_A} \sqrt{\Delta P} \tag{2.4.5}$$

where

A_A is the effective area of the piston.

The force available to do work at the end of the piston rod, F_A, is given by

$$F_A = A_A \Delta P \tag{2.4.6}$$

Equations (2.4.5) and (2.4.6) can now be combined to yield

$\dot{y}$ directly as a function of F :

$$\dot{y} = \frac{C_{sv}}{A_A} z \sqrt{P_s - F_A/A_A} - \frac{C_v}{A_A} \sqrt{F_A/A_A} \qquad (2.4.7)$$

In computing (2.4.7) it is necessary to introduce an artificial sign assignment to avoid negative values within the surds. This is done by noting that

1. In the case of flow through the servo-valve, P_s must take the sign of z. The surd then becomes

$$\sqrt{|\, \text{sign}(z) P_s - F_A/A_A \,|} \qquad (2.4.8)$$

2. In the case of the leakage flow, the surd takes the sign of F_A, which is actually the direction of pressure drop. The surd thus becomes

$$\text{sign}(F_A) \sqrt{|\, F_A/A_A \,|} \qquad (2.4.9)$$

Substituting the modified expressions (2.4.8) and (2.4.9) into (2.4.7) gives the equation for computing $\dot{y}$ from F_A consistent with the sign convention:

$$\dot{y} = \frac{C_{sv}}{A_A} z \sqrt{\left| \text{sign}(z) P_s - F_A/A_A \right|} - \frac{C_v}{A_A} \text{sign}(F_A) \sqrt{\left| F_A/A_A \right|} \qquad (2.4.10)$$

Fig. 2.4.3 shows the block diagram of the active system.

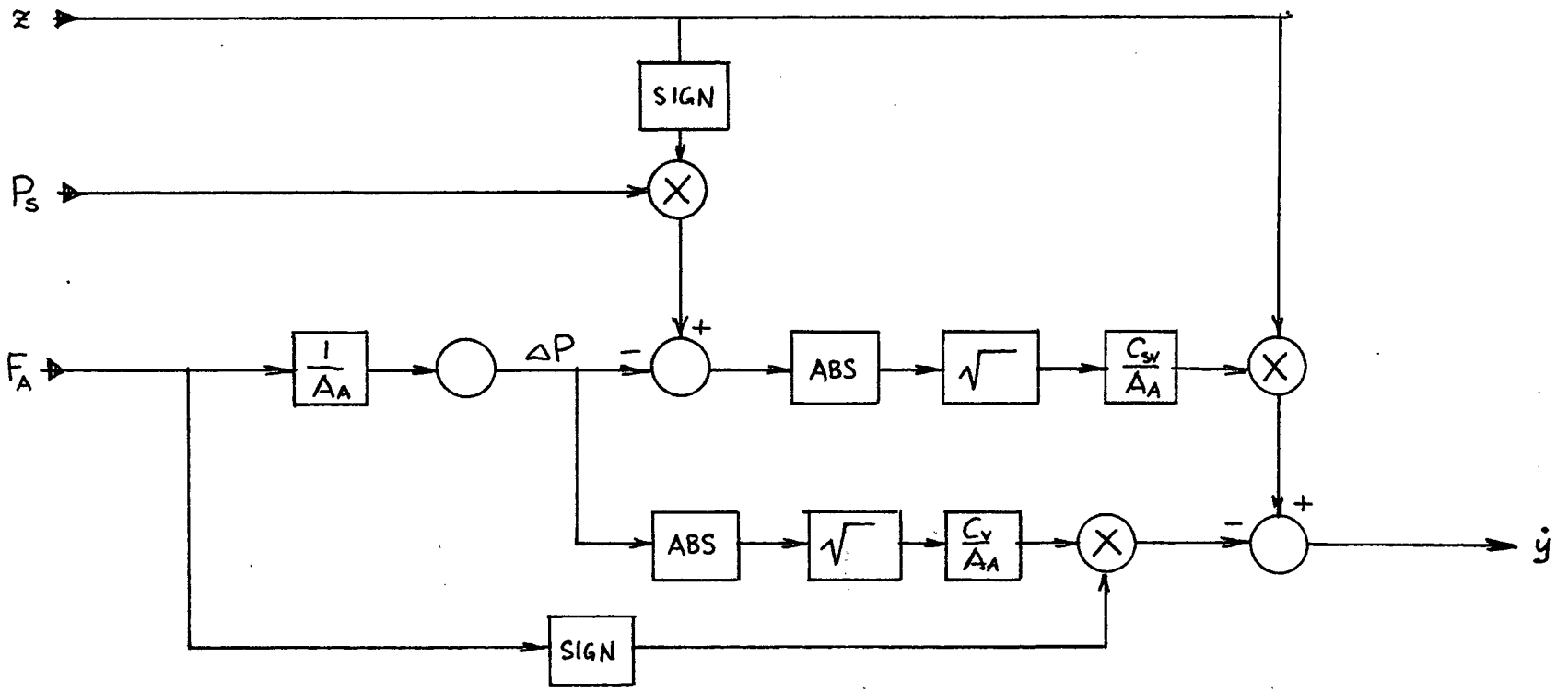

FIG. 2.4.3 BLOCK DIAGRAM of ACTIVE SYSTEM

2.5 Active-Passive System

The total ram force is the sum of the forces exerted by the passive and active cylinders, less friction:

$$F_{RAM} = F_P + F_A - f \qquad (2.5.1)$$

where

F_{RAM} is the ram force,

F_A is the active cylinder force,

F_P is the passive cylinder force,

and f is the friction force, as discussed in Appendix E. The force felt by the cable is directly proportional to F_{RAM}, where the constant of proportionality is the reciprocal of the mechanical advantage of the reeving:

$$F_{NET} = \frac{1}{K_{MA}} F_{RAM} \qquad (2.5.2)$$

where

K_{MA} is the mechanical advantage of the reeving,

and F_{NET} is the force acting on the cable.

The towed body can be represented by a mass M, subjected to hydrodynamic drag and towing cable tension. (Fig. 2.5.1) The cable is assumed to be a massless linear spring.

The compensator force causes an elongation of the cable

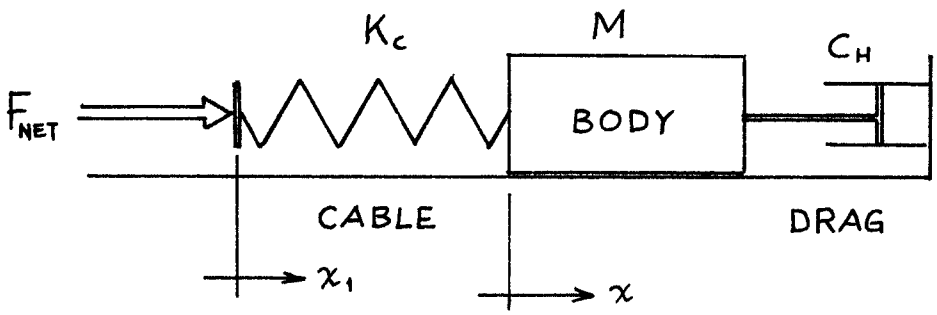

FIG. 2.5.1 CABLE/BODY MODEL

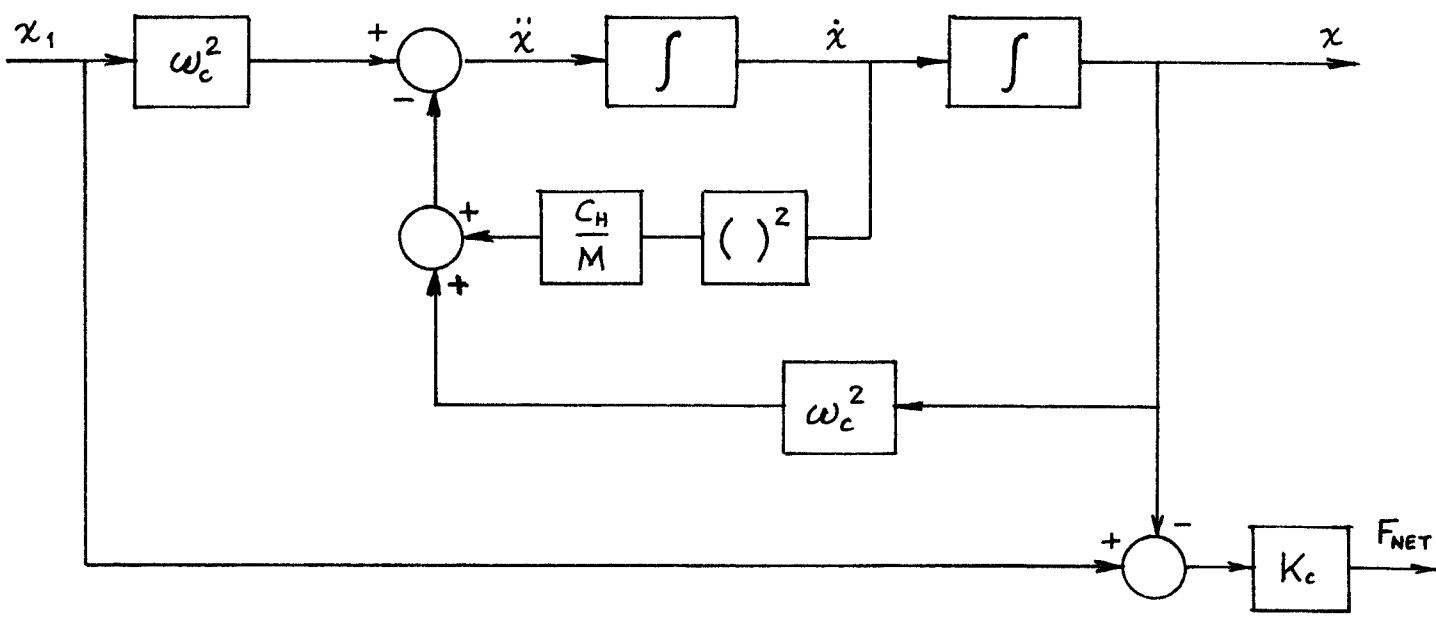

FIG. 2.5.2 BLOCK DIAGRAM of CABLE/BODY DYNAMICS

according to the relation

$$F_{NET} = K_c(x_1 - x) \tag{2.5.3}$$

The cable then applies the same force to the body, whose motion can be described by:

$$F_{NET} = M\ddot{x} + C_H \dot{x}^2 \tag{2.5.4}$$

where

M is the mass of the towed body,

and C_H is the hydrodynamic drag factor.

Equating (2.5.3) and (2.5.4) and rearranging, gives the nonlinear differential equation of motion of the body:

$$\ddot{x} + \frac{C_H}{M}\dot{x}^2 + \omega_c^2 x = \omega_c^2 x_1 \tag{2.5.5}$$

where

ω_c is the cable-mass natural frequency, $\sqrt{K_c/M}$.

Once (2.5.5) is solved, it is possible to find F_{NET} by direct application of (2.5.4) or (2.5.3). The block diagram of the towed body and cable system is shown in Fig. 2.5.2.

The absolute displacement of the shipboard end of the

cable, x_1, is the sum of the input, u, and the displacement of the end of the cable with respect to the input, y_c:

$$x_1 = u + y_c \tag{2.5.6}$$

For the case where the actuator acts on the cable through a mechanical advantage (e.g., the ram tensioner of Fig. 2.1.1), the motion of the cable with respect to the ship's stern can be expressed as:

$$y_c = K_{MA}\, y \tag{2.5.7}$$

where

y is the extension of the actuator.

Equations (2.5.6) and (2.5.7) are combined with the block diagrams of the passive, active, and cable-mass systems (Figs. 2.3.5, 2.4.3, and 2.5.2) to give the block diagram of the entire system, as shown in Fig. 2.5.3.

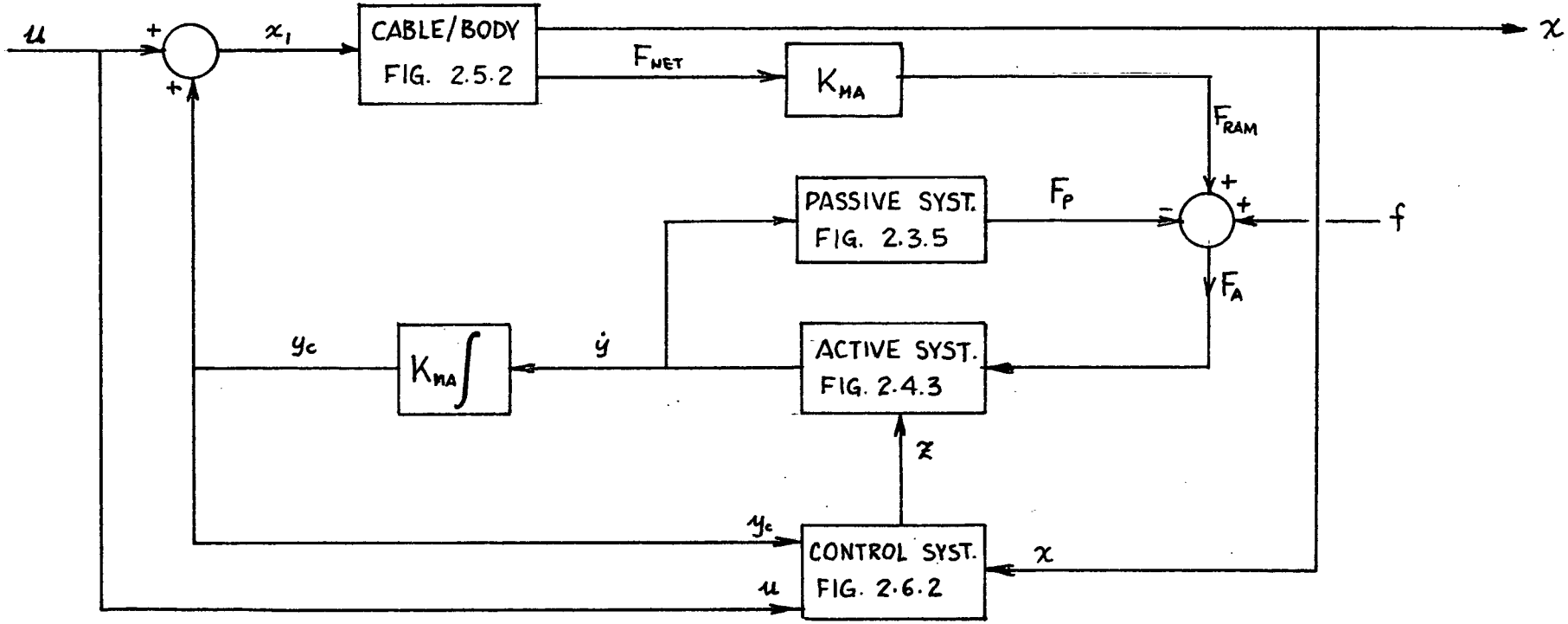

FIG. 2.5.3 BLOCK DIAGRAM of ACTIVE-PASSIVE SYSTEM

2.6 The Control System

The control system generates the signal to operate the active actuator by means of monitoring and processing certain variables. The controlled variable can be considered as either x or F_{NET}, and Figure 2.5.2 suggests that both can be controlled simultaneously because they are linearly dependent. This means that the index of performance, as discussed in Chapter I, can be either F_{NET}/u or x/u, and both must be made to fall below certain specified limits for acceptable operation. In addition, the control system must ensure that the long term average motion of the actuator piston does not drift from the centre of the cylinder.

The controlled variable (F_{NET} or x) can be used to generate the primary actuating signal for the servovalve. This constitutes a simple feedback control system where the reference input is zero, as shown in Fig. 2.6.1. (The passive system is omitted from Fig. 2.6.1 for clarity.) The "Control Elements" block may contain filters, integrators, etc., as required for best operation.

In addition to feedback, it may be desirable to include a portion of the disturbance input, u(t), as indicated by the feedforward loop in Fig. 2.6.1.

The piston centering control is a minor loop used to restore the piston to the centre of the actuator slowly with

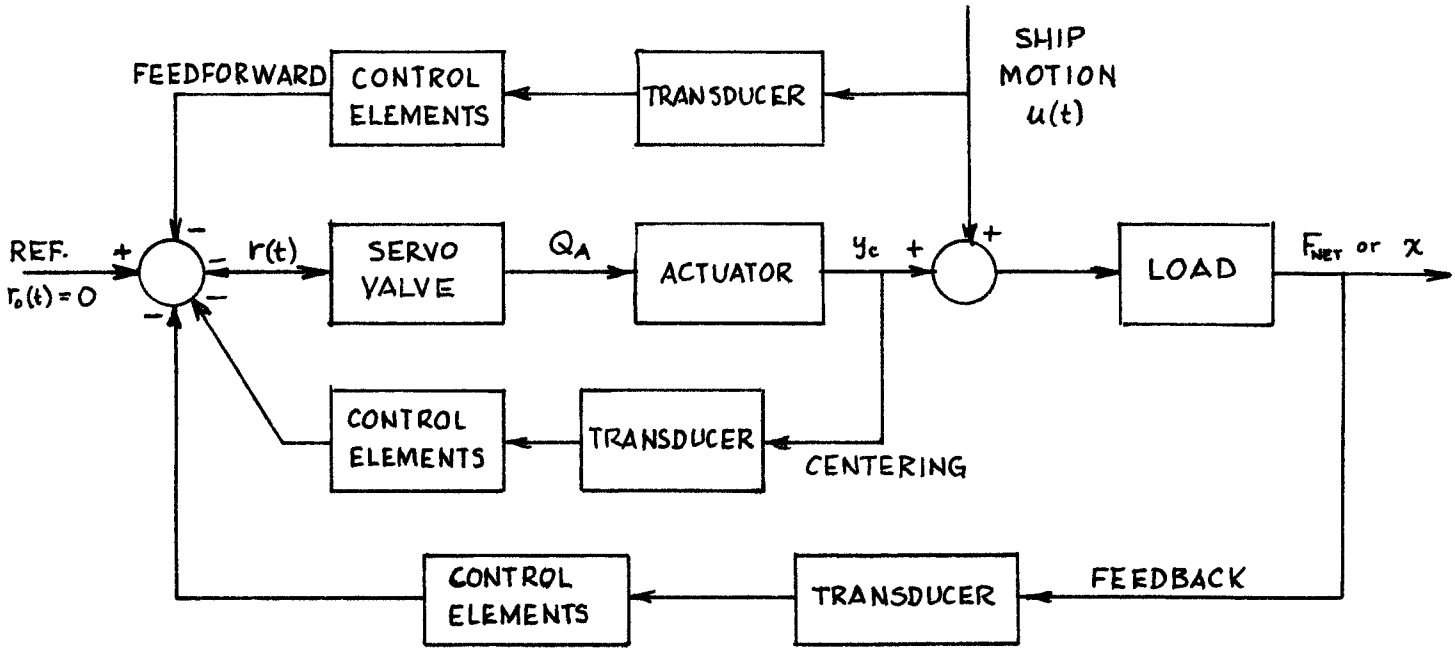

FIG. 2.6.1 ACTIVE SYSTEM WITH CONTROL BLOCKS

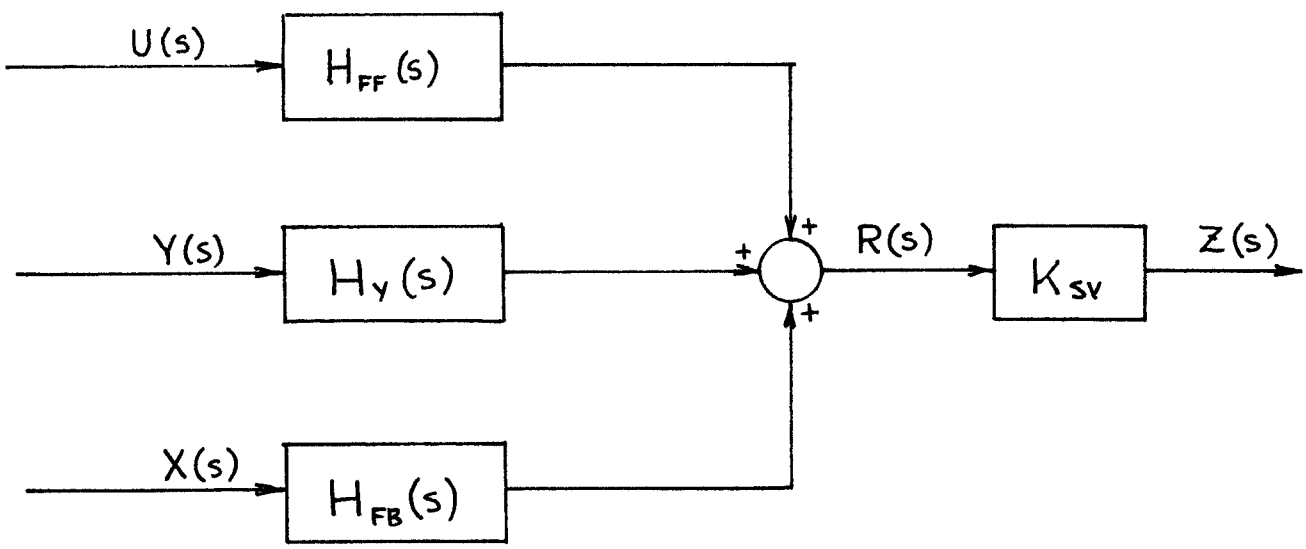

FIG. 2.6.2 BLOCK DIAGRAM of CONTROL SYSTEM

respect to the forcing frequency. That is, the time constant of the loop is at least one order of magnitude greater than the reciprocal of the input frequency. The choice between using F_{NET} and x as the controlled variable is made based on the availability and suitability of transducers. In either case, however, it is necessary to provide a physical path in the towing cable for the feedback signal to reach the surface vessel. If this is not possible, then the absolute motion of the shipboard end of the cable, x_1, can be used as the feedback signal. Such a strategy is easily feasible in the case of the ram tensioner and boom-bobber (Fig. 1.1.1(a),(b)), but not so for the constant tension winch (Fig. 1.1.1(c)). For demonstration purposes, it is assumed that x is the feedback variable.

The control system elements are now lumped into three blocks, as shown in Fig. 2.6.2. The total control voltage, R(s) is given by (in Laplace notation):

$$R(s) = H_{FB}(s)X(s) + H_{FF}(s)U(s) + H_y(s)Y(s) \qquad (2.6.1)$$

where

$H_{FB}(s)$ represents the feedback element,

$H_{FF}(s)$ represents the feedforward element,

and $H_y(s)$ represents the piston centering element.

The servovalve actuating current is obtained by passing the

control voltage through a power amplifier:

$$Z(s) = K_{sv} R(s) \tag{2.6.2}$$

where

$Z(s)$ is the actuator current,

and K_{sv} is the amplifier gain.

2.7 Computer Simulation

The active-passive system as depicted in Fig. 2.5.3 has been modelled by means of a "Continuous Systems Modelling Program" (CSMP), an IBM product for use on their System/370. The programming language consists of a number of functional blocks such as integration, differentiation, etc., in addition to all the usual mathematical functions available in Fortran. These blocks are assembled in much the same manner as an analogue computer network, but without the inconvenience of scaling variables. Integration can be performed using any of five different built-in routines; the one employed in this project is fourth order Runge-Kutta with fixed integration interval. This method was selected because it is found to be the least expensive for the degree of accuracy required.

The logic flow of the program is exactly as depicted in Fig. 2.5.3. The listing is shown in Appendix F.1.

CHAPTER III

LINEAR ANALYSIS

The equations of the active/passive motion compensation system developed in Chapter II are difficult to handle without extensive use of computers. In order that the designer can quickly gain a feel for the problem and thereby establish first approximations for important parameters, I have simplified the equations to permit a fast approximate solution. The simplified approach uses linearized equations and a frequency-domain solution.

3.1 Linearized Passive System

In linearizing the passive pneumatic system, I have assumed that the changes in pressure within the cylinder and tanks are linear with respect to the piston displacement, y, and that y is too small to affect the temperature in the system. This leads to the following:

1. $\delta = \Delta y$: i.e., the perturbation in piston displacement is small, and denoted by δ.
2. $P_1 + P_2 = 2P_o$; i.e., the average pressure in the cylinder is constant, and equal to the quiescent pressure P_o .
3. $\dot{P}_1 = -\dot{P}_2$; i.e., the rate of increase of pressure on one side of the cylinder is equal to the rate of

decrease on the other.

4. The temperature throughout the passive system is constant and equal to T_o.

Furthermore, the geometry of the system is assumed to be symmetric, which leads to the following:

5. $A_1+A_2=2A_p$; i.e., the effective piston areas are averaged to a constant A_p.
6. $V_{c_1}+V_{c_2}=2V_c$; i.e., the tank volumes are averaged to a constant V_c.

The gas flow equations are linearized by first considering the mass flow through the throttling valve as given in (2.2.12), and restated here:

$$\dot{m} = C_o P_u \left(\frac{P_d}{P_u}\right)^{1/\gamma} \sqrt{\frac{2\gamma}{RT_o(1-\gamma)}\left\{1-\left(\frac{P_d}{P_u}\right)^{\frac{\gamma-1}{\gamma}}\right\}}$$

$$= C_o' \left(\frac{P_d}{P_u}\right)^{1/\gamma} \sqrt{1-\left(\frac{P_d}{P_u}\right)^{\frac{\gamma-1}{\gamma}}} \qquad (3.1.1)$$

where

$$C_o' = C_o P_u \sqrt{\frac{2\gamma}{RT_o(\gamma-1)}}$$

Considering the upstream pressure, P_u, as constant and equal to the quiescent pressure P_o, and small variations in pressure drop (P_o-P_d), equation (3.1.1) can be linearized into

the form:

$$\Delta \dot{m} = C_r \Delta (P_o - P_d) \tag{3.1.2}$$

where

$$C_r = \frac{\partial \dot{m}}{\partial (P_o - P_d)} = \frac{\partial \dot{m}}{\partial (P_d/P_o)} \cdot \frac{\partial (P_d/P_o)}{\partial (P_o - P_d)}$$

$$= \frac{C_o'}{\gamma P_o} \left[\frac{\gamma - 1}{2\sqrt{1-(P_d/P_o)^{\frac{\gamma-1}{\gamma}}}} - \left(\frac{P_d}{P_o}\right)^{\frac{1-\gamma}{\gamma}} \sqrt{1-\left(\frac{P_d}{P_o}\right)^{\frac{\gamma-1}{\gamma}}} \right] \tag{3.1.3}$$

The flow through the valve will be positive for the half cycle when the piston moves one way, and negative for the other half. Therefore, $(P_o - P_d)$ can assume positive or negative values. It is thus necessary to select $\dot{m}_o = (P_o - P_d) = 0$ as the equilibrium point about which perturbations are considered. However, this will yield infinite value for C_r, since the slope of the $\dot{m}$ vs $(P_o - P_d)$ curve, as shown in Fig. 3.1.1, is vertical at $P_o - P_d = 0$. It is therefore more reasonable to select values of P_o, P_d which coincide with some average operating condition, for example the root-mean-square value. The equilibrium point, however, is still the origin. Renaming P_o and P_d to correspond to the tank and cylinder pressures, the linearized mass flow equations are:

$$\dot{m}_1 = C_r (P_{t_1} - P_1)$$
$$\dot{m}_2 = C_r (P_{t_2} - P_2) \qquad (3.1.4)$$

Equation (3.1.4.) is plotted together with its nonlinear form in Fig. 3.1.1.

The cylinder flow equations are considered next. Incorporating the simplifications of geometry as discussed above, equation (2.2.9) becomes:

$$\dot{m}_1 = \frac{1}{RT_0}\left[\frac{V_c + A_p\delta}{\gamma}\dot{P}_1 + P_1 A_1 \dot{\delta}\right]$$
$$\dot{m}_2 = \frac{1}{RT_0}\left[\frac{V_c - A_p\delta}{\gamma}\dot{P}_2 - P_2 A_2 \dot{\delta}\right] \qquad (3.1.5)$$

The net mass flow into the cylinder is given by

$$(\dot{m}_1 - \dot{m}_2) = \frac{1}{RT_0}\left[\frac{V_c}{\gamma}(\dot{P}_1 - \dot{P}_2) + \frac{A_p\delta}{\gamma}(\dot{P}_1 + \dot{P}_2) + A_p\dot{\delta}(P_1 + P_2)\right] \qquad (3.1.6)$$

Incorporating the approximations of pressure as described above, and introducing the differential operator $D = \frac{d}{dt}$, equation (3.1.6) can be rewritten as:

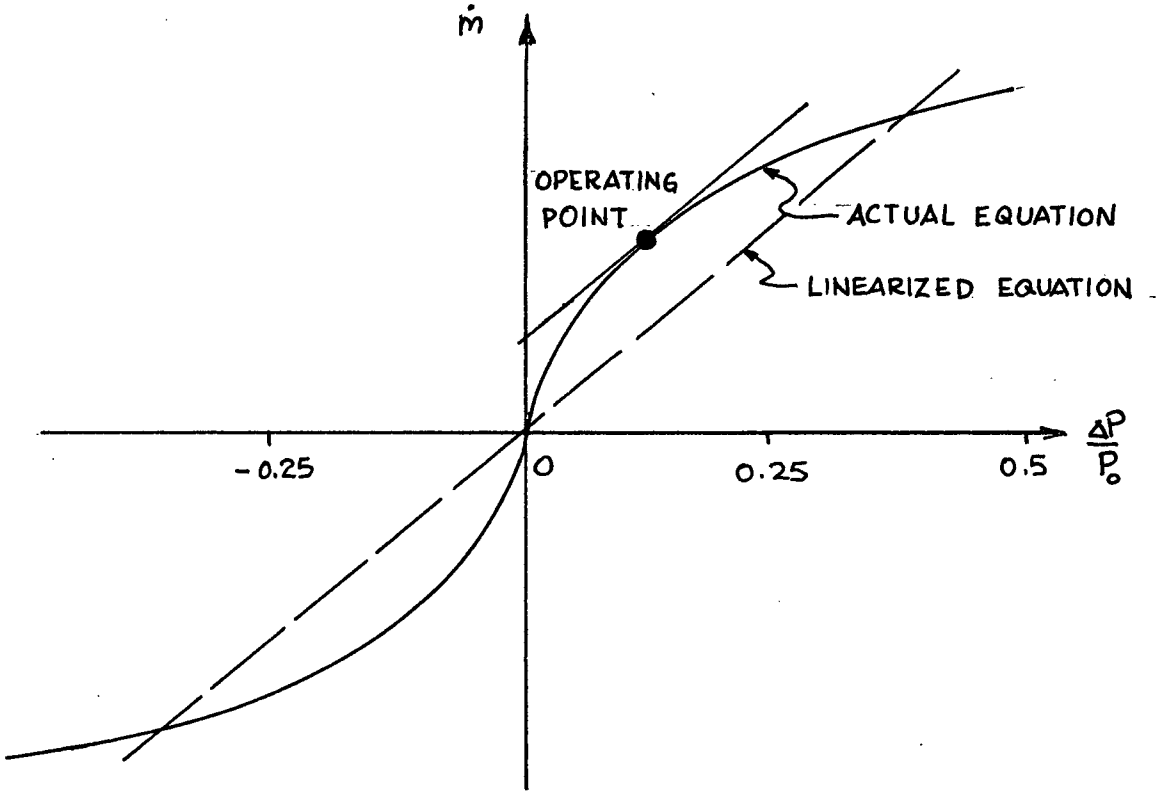

FIG 3.1.1
PRESSURE - FLOW CURVE
for THROTTLING VALVES

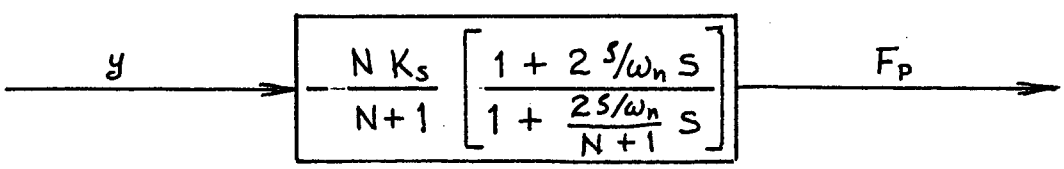

FIG. 3.1.2
LINEARIZED PASSIVE SYSTEM TRANSFER FUNCTION

$$(\dot{m}_1-\dot{m}_2)=\frac{1}{RT_o}\left[\frac{V_c}{\gamma}D(P_1-P_2)+2A_pP_o\,D\delta\right] \tag{3.1.7}$$

Finally, the flow out of the receiving tanks is considered. Equation (2.2.4) can be rewritten, in differential operator notation, as:

$$\dot{m}_1 = -\frac{V_t}{\gamma RT_o}DP_{t_1}$$
$$\dot{m}_2 = -\frac{V_t}{\gamma RT_o}DP_{t_2} \tag{3.1.8}$$

Solving (3.1.4.) for P_{t_1} and P_{t_2} and substituting into equation (3.1.8), the net flow into the cylinder can be expressed as:

$$(\dot{m}_1-\dot{m}_2)=-\frac{V_t}{\gamma RT_o}\left[\frac{D(P_1-P_2)}{1+\frac{V_t}{1+\gamma RC_rT_o}D}\right] \tag{3.1.9}$$

Equating (3.1.9) and (3.1.6) and solving for P-P gives

$$P_1-P_2 = -\frac{2\gamma A_pP_o}{V_c\left[1+\frac{V_t/V_c}{1+\frac{V_t}{\gamma RC_rT_o}D}\right]} \tag{3.1.10}$$

The force exerted by the ram is then given by

$$F_p = A_p (P_1 - P_2) \tag{3.1.11}$$

and the overall transfer function of ram force to piston displacement is

$$\frac{F_p}{\delta} = - \frac{2 \gamma P_o A_p^2}{V_c \left[1 + \frac{V_t / V_c}{1 + \frac{V_t}{\gamma C_r R T_o} D} \right]} \tag{3.1.12}$$

Lumping parameters and introducing the Laplace operator, s, in place of the differential operator, D, the overall transfer function becomes

$$G_p(s) = - \frac{N K_s}{N+1} \left[\frac{1 + 2 \zeta / \omega_n s}{1 + \frac{2}{N+1} \zeta / \omega_n s} \right] \tag{3.1.13}$$

where

$K_s = \frac{2 \gamma P_o A_p^2}{V_t}$ = Static stiffness,

$N = V_c / V_t$ = tank to cylinder volume ratio,

and $2 \zeta / \omega_n = \frac{V_t}{\gamma C_r R T_o}$

The parameters ω_n and ζ are the natural frequency and critical damping ratio, respectively, and are ultimately a function of the mass which the system must control. In particular,

$$\omega_n = \sqrt{\frac{K_s}{M}} \quad , \qquad \zeta = \frac{\omega_n V_c}{2\gamma C_r R T_o} \tag{3.1.14}$$

The linearized transfer function $G_p(s)$ is now extended to cover the full range of piston displacement, y, such that

$$F_p = G_p(s)\, y \tag{3.1.15}$$

The transfer function is shown in block diagram form in Fig. 3.1.2.

Introducing the time constants

$$\tau_1 = 2\zeta/\omega_n \quad , \qquad \tau_2 = \frac{\tau_1}{N+1} \tag{3.1.16}$$

the transfer function may be restated as

$$G_p(s) = -\frac{NK_s}{N+1} \; \frac{1+\tau_1 s}{1+\tau_2 s} \tag{3.1.17}$$

3.2 Linearized Active System

The equation of the active system, as presented in Section 2.3, is restated here:

$$\dot{y} = \frac{C_{sv}}{A_A} z \sqrt{P_s - F_A/A_A} - \frac{C_v}{A_A} \sqrt{F_A/A_A} \qquad (3.2.1)$$

Equation (3.2.1) is to be linearized about some operating point $(\dot{y}_o, z_o, F_{A_o})$. Perturbations about that point can be represented, by Δ-notation, as

$$\Delta\dot{y} = \left(\lambda_1 \Delta z + \lambda_2 \Delta F_A\right) + \lambda_3 \Delta F_A \qquad (3.2.2)$$

where

$$\lambda_1 = \frac{\partial \dot{y}}{\partial z} = \frac{C_{sv}}{A_A} \sqrt{P_s - F_{A_o}/A_A} \qquad (3.2.3)$$

$$\lambda_2 = \left(\frac{\partial \dot{y}}{\partial F_A}\right)_{\substack{\text{SERVO} \\ \text{VALVE}}} = - \frac{C_{sv}\, z_o}{2A_A^2 \sqrt{P_s - F_{A_o}/A_A}} \qquad (3.2.4)$$

$$\lambda_3 = \left(\frac{\partial \dot{y}}{\partial F_A}\right)_{\text{LEAKAGE}} = - \frac{C_v}{2A_A^2 \sqrt{F_{A_o}/A_A}} \qquad (3.2.5)$$

The constants λ_1 and λ_2 are termed the "flcw gain" and "flow-presure coefficient" of the servovalve, respectively, and

λ_3 the "flow coefficient" of the bypass valve. Friction is not considered in the linear analysis because of the discontinuity at $\dot{y}=0$.

Equation (3.2.2) is valid only for perturbations about the operating point $(\dot{y}_o, z_o, F_{A_o})$. However, during normal operation of the valve the operating point can travel in a band spanning both the negative and positive regions of $\dot{y}$, z, and F_A. The linearized equation then becomes inappropriate in its present form.

It is proposed that the perturbations $\dot{y}$, z, and F_A be centred about the origin, i.e., $\dot{y}_o = z_o = F_{A_o} = 0$, but that λ_1, λ_2, λ_3 be calculated about a root-mean-square point using equations (3.2.3) to (3.2.5.). Equation (3.2.2) can thus be rewritten as

$$\dot{y} = \lambda_1 z + (\lambda_2 + \lambda_3) F_A \qquad (3.2.6)$$

and $(\dot{y}_o, z_o, F_{A_o})$ can be considered as the RMS operating point.

The effect of linearizing the servovalve equation is to change the family of parabolae to one of straight lines, as indicated in Fig. 3.2.1. The linear system thus developed is found to model the active system adequately over the entire operating range.

The transfer function is shown in block diagram form in Fig. 3.2.2.

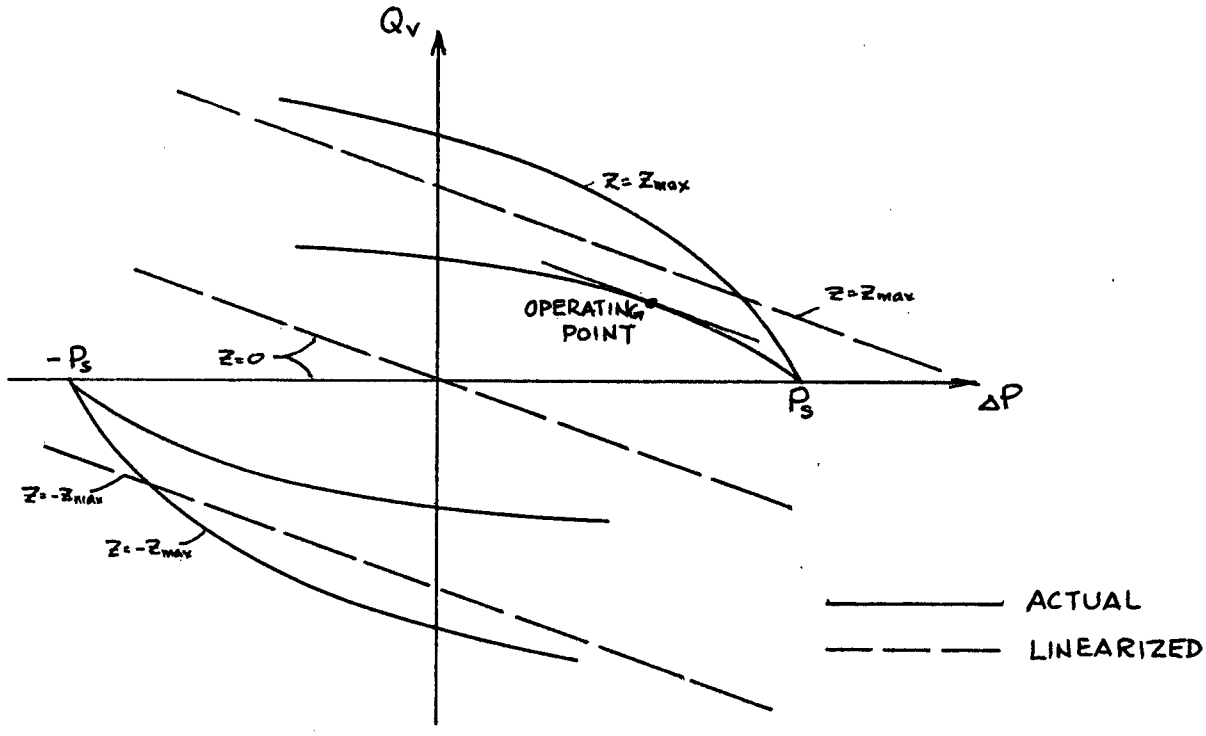

FIG. 3.2.1

LINEARIZED SERVOVALVE CHARACTERISTICS

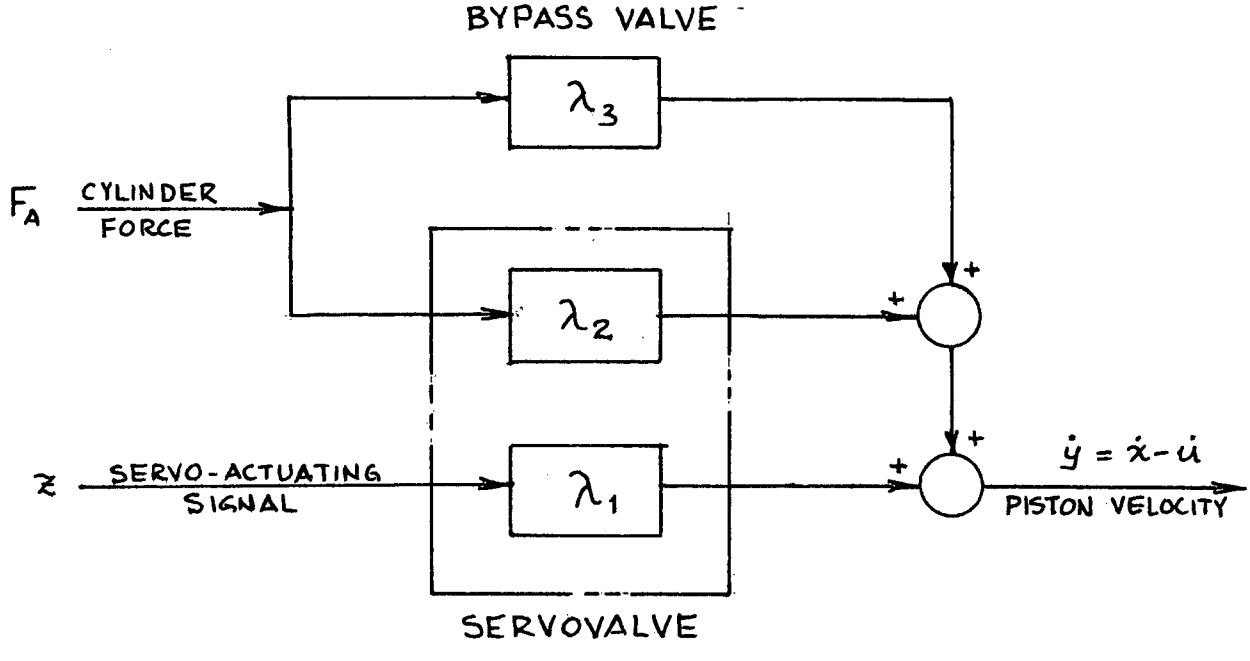

FIG. 3.2.2 LINEARIZED ACTIVE SYSTEM TRANSFER FUNCTION

3.3 Linearized Active-Passive System

The linear transfer functions of the active and passive systems are combined in the same manner as in Section 2.4. It will be necessary, however, to first linearize the body dynamics transfer function. Recalling equation (2.5.4)

$$F_{NET} = M\ddot{x} + C_H \dot{x}^2 \tag{3.3.1}$$

it is seen that only the damping term is nonlinear. This can be linearized about $\dot{x}=0$, giving

$$F_{NET} = M\ddot{x} + C_L \dot{x} \tag{3.3.2}$$

where

$$C_L = C_H \frac{\partial \dot{x}^2}{\partial \dot{x}} = 2 C_H \dot{x}_o$$

and $\dot{x}_o$ is taken as the root-mean-square velocity.
C_L is then the linearized drag coefficient.

The differential equation of (2.6.4.) can now be linearized to give

$$\ddot{x} + \frac{C_L}{M}\dot{x} + \omega_c^2 x = \omega_c^2 x_1 \tag{3.3.3}$$

The transfer function of the compensator motion x_1, to body motion x can then be expressed, in Laplace notation, as

$$F_c(s) = \frac{x}{x_1} = \frac{1}{1 + 2\zeta/\omega_c\, s + s^2/\omega_c^2} \qquad (3.3.4)$$

where

$$\zeta_c = \frac{C_L}{2M\omega_c}$$

and $F_c(s)$ is the cable transfer function.

The transfer function of body displacement, x, to cable tension, F_{NET}, is derived from (3.3.2)

$$F_B(s) = \frac{F_{NET}}{x} = Ms^2 + C_L s \qquad (3.3.5)$$

The block diagram of the linearized cable and body dynamics is shown in Fig. 3.3.1. The block diagram of the linearized motion compensation system is shown in Fig 3.3.2.

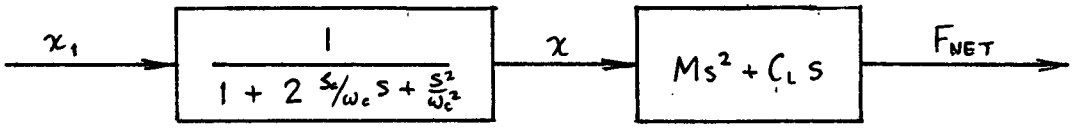

FIG. 3.3.1

LINEARIZED CABLE/BODY TRANSFER FUNCTION

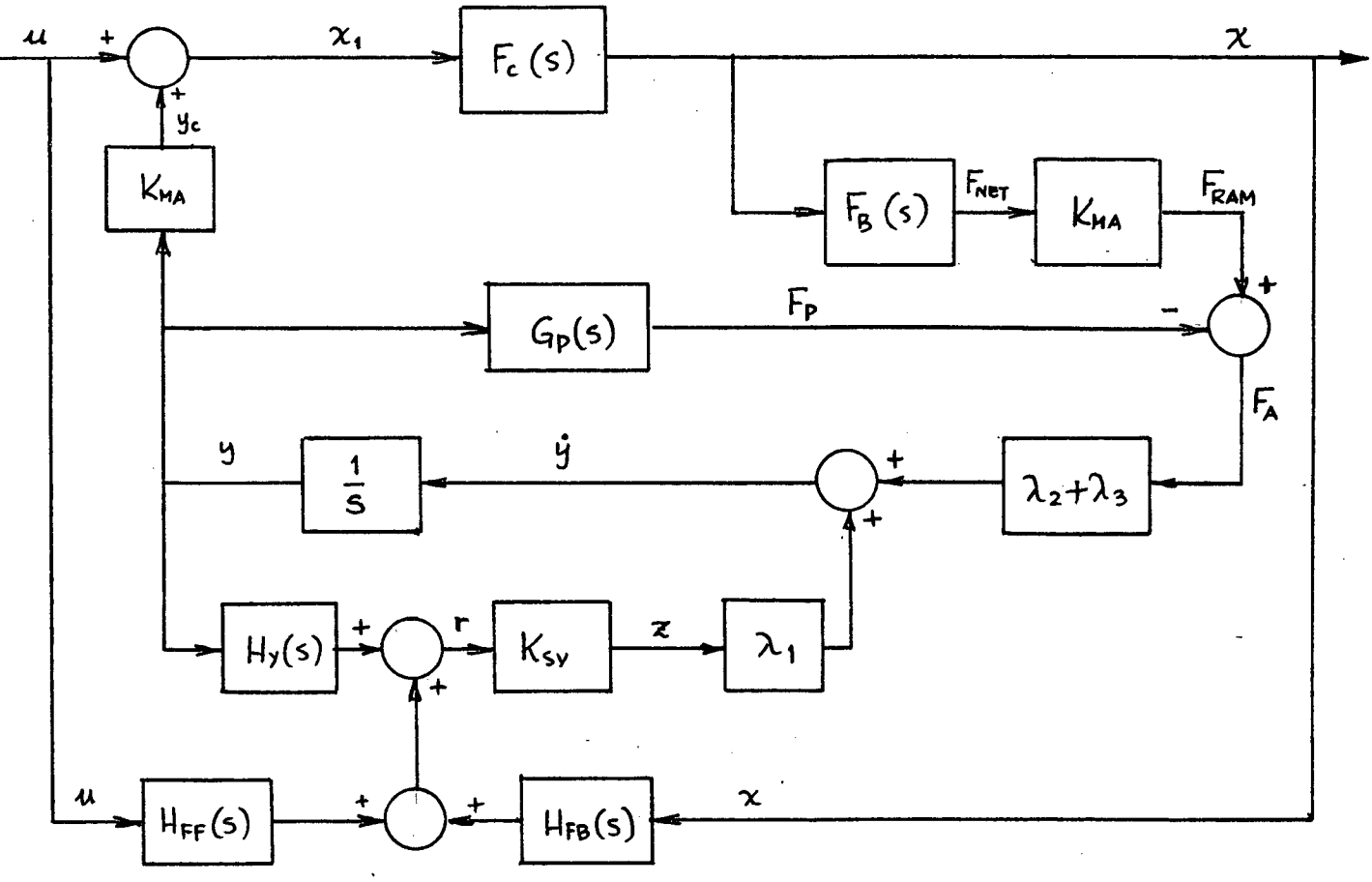

FIG. 3.3.2 BLOCK DIAGRAM of

LINEARIZED ACTIVE-PASSIVE SYSTEM

3.4 Performance Analysis and Optimization

As a first approximation to system performance, the linear model derived in Section 3.3 will be examined in the frequency domain. It will be most convenient to use the ratio of body to surface ship displacement, x/u, as the criterion of performance. Due to the linearity of the system, a minimum x/u is equivalent to minimum variation in F_{NET}/u.

Solving the block diagram of Fig 3.3.2 yields the overall transfer function:

$$\frac{X(s)}{U(s)} = \frac{F_c(s)}{1 + H(s)} \tag{3.4.1}$$

where H(s) is the open-loop transfer function, given by:

$$H(s) = -\frac{Y_c(s)}{X_1(s)}$$

$$= -\frac{K_{HA}\left[(\lambda_2+\lambda_3)K_{HA}F_B(s)F_c(s) + \lambda_1 K_{SV}F_c(s)H_{FB}(s) + \lambda_1 K_{HA}K_{SV}H_{FF}(s)\right]}{s + (\lambda_2+\lambda_3)G_p(s) + \lambda_1 H_y(s) + \lambda_1 K_{HA}K_{SV}H_{FF}(s)} \tag{3.4.2}$$

In designing an active-passive system, the absolute value of the closed loop transfer function, $\left|\frac{X}{U}(s)\right|$, is to be minimized within the range of operating frequencies. This in turn yields H(s), the closed loop transfer function, a maximum.

In general, the designer has no control over the cable and body dynamics, which are represented by $F_c(s)$ and $F_B(s)$. Furthermore, he has very little control over the passive system,

$G_p(s)$, since the primary design criterion for that system is to be able to carry the static weight of the towed body.[1] Thus, in maximizing $H(s)$, it is necessary to design $H_{FB}(s)$, $H_{FF}(s)$, $H_y(s)$, and to select a suitable servo-valve and hydraulic cylinder as represented by λ_1 and λ_2.

3.3.1 The Feedforward Element

The first step in maximizing $H(s)$ is to minimize its denominator. Ideally, it is set to zero, which yields

$$H_{FF}(s) = -\frac{1}{\lambda_1 K_{MA} K_{SV}} \left[s + (\lambda_2+\lambda_3) G_p(s) + \lambda_1 K_{SV} H_y(s) \right] \qquad (3.4.3)$$

As pointed out earlier, $H_y(s)$ is the ram centering network. Because it is relatively slow-acting it has little or no effect at operating frequencies. Thus, it can be deleted from (3.4.3). The feedforward compensator can now be given as

$$H_{FF}(s) = -\frac{1}{\lambda_1 K_{MA} K_{SV}} \left[s + (\lambda_2+\lambda_3) G_p(s) \right] \qquad (3.4.4)$$

---

[1] The stiffness of the passive system is usually specified in order that the active-passive system be capable of operating in a purely passive mode when working in a low sea state, or in case of a power failure in the active system.

3.4.2 The Feedback Element

The second step in maximizing H(s) is tc maximize the numerator. An examination of (3.4.2) reveals that this can be done by setting the gain cf $H_{FB}(s)$ as large as possible; however, the servovalve saturates when the actuating current, z, exceeds a critical value, z_o. Therefore, $H_{FB}(s)$ must be optimized with respect tc the above constraint.

As is customary in position servos, the feedback element $H_{FB}(s)$ is assumed to be a combination of displacement, velccity, and acceleration feedback. Thus,

$$H_{FB}(s) = K_1 + K_2 s + K_3 s^2 \qquad (3.4.5)$$

where

K_1, K_2 and K_3 are ccnstants.

This yields a servo-actuating current z, given by

$$Z(s) = K_{sv}\left[H_{FF}(s)U(s) + H_{FB}(s)X(s)\right] \qquad (3.4.6)$$

(The ram centering network, $H_y(s)$, is again ignored because it has negligible effect at operating frequencies).

The amplitude of the actuating current, $|Z(s)|$, is now constrained to be less than or equal to the critical value, z_o:

$$|Z(s)| = K_{sv}\left| H_{FF}(s)U(s) + H_{FB}(s)X(s)\right| \leq Z_o \qquad (3.4.7)$$

For convenience, (3.4.7) is rewritten in terms of ratios:

$$\left| \frac{Z(s)}{U(s)} \right| = K_{sv}\left| H_{FF}(s) + H_{FB}(s)\frac{X(s)}{U(s)} \right| \leq \frac{Z_o}{u_o} \qquad (3.4.8)$$

where

u_o is the amplitude of the input, $|U(s)|$,

and $\frac{X}{U}(s)$ is the closed loop transfer function as given by (3.4.1).

The optimum values of K_1, K_2 and K_3 are found using a digital computer program listed in Appendix F.3. The optimization process is carried out at one frequency only, that being the "design frequency" which contains the greatest energy.

3.4.3 Ram Centering

The ram centering network is required to maintain the long term average ram displacement zero. Under static conditions, this is equivalent to returning the ram to centre position in a given (long) time after receiving a step input.

Considering the centering loop as shown in Fig 3.4.1, the active ram force F_A can be set to zero under static conditions.

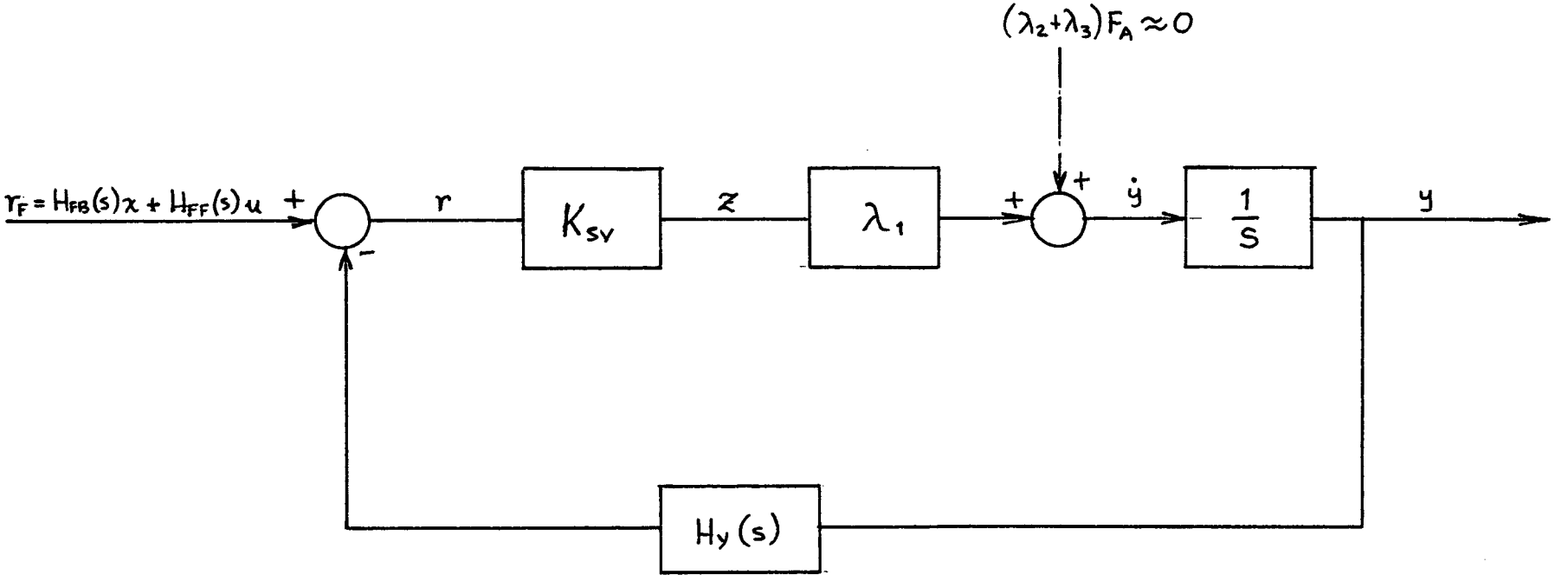

FIG. 3.4.1

RAM CENTERING NETWORK

This gives a closed loop transfer function of

$$\frac{Y(s)}{R_F(s)} = \frac{1}{H_y(s)} \frac{1}{1 + \frac{s}{\lambda_1 K_{sv} H_y(s)}} \tag{3.4.9}$$

Letting $H_y(s) = K_y$ = constant gives

$$\frac{Y(s)}{R_F(s)} = \frac{1/K_y}{1 + \tau_y s} \tag{3.4.10}$$

where

$$\tau_y = \frac{1}{\lambda_1 K_{sv} K_y}$$

It now remains to select K_y such that

$$\tau_y > \frac{10}{\omega_o}$$

where ω_o is the design frequency.

3.4.4 System Stability

The stability of the system is determined by solving the characteristic equation

$$1 + H(s) = 0 \tag{3.4.11}$$

and examining the root locus as the feedback gains K_1, K_2 and K_3 are varied. In general, the characteristic function is cumbersome to deal with, and the following simplifications are therefore assumed:

1. Let $G_p(s) = -K_p$ -- i.e., assume the passive system behaves as a simple spring (where Hooke's law applies).
2. Let $F_c(s) = 1$ -- i.e., neglect the cable dynamics. This is reasonable because the effect of the cable on the motion compensation system is relatively small, except at the natural frequency of the towed system. This frequency should lie outside the range of operation.
3. Neglect $H_y(s)$ as explained earlier.

With the above assumptions, (3.4.11) can be expressed as:

$$s - (\lambda_2+\lambda_3) K_p + (1-K_{MA}) \lambda_1 K_{MA} K_{SV} H_{FF}(s) - K_{MA} (\lambda_2+\lambda_3) F_B(s) - \lambda K_{MA} K_{SV} H_{FB}(s) = 0 \qquad (3.4.12)$$

The application of (3.4.12) to the laboratory model is discussed in Chapter IV.

3.4.5 Power Consumption

The power consumed by the active system is the sum of the power dissipated in the servovalve and the power required to drive the load. This is equal to the product of the volume rate of oil flow into the valve and the supply pressure:

$$\dot{W} = A_A P_s |\dot{y}| \tag{3.4.13}$$

where

$\dot{W}$ is the instantaneous power consumption.

Note that although $\dot{y}$ changes in direction, $\dot{W}$ is always positive. This is due to the fact that the direction switching occurs in the valve itself, but the oil flow to the valve is unidirectional. Thus, the average power consumed is the root-mean-square of the amplitude of $\dot{W}$:

$$\overline{\dot{W}} = 0.707\ A_A P_s |\dot{Y}(s)| \tag{3.4.14}$$

where

0.707 is the rms factor for a sine wave,

P_s is the supply pressure,

A_A is the ram area,

and $\overline{\dot{W}}$ is the average power consumption. It is convenient to express $\overline{\dot{W}}$ in the frequency domain as a ratio to input displacement U(s):

$$\left|\frac{\overline{\dot{W}}}{U}(s)\right| = \frac{0.707\ A_A P_s}{K_{MA}} \left[\frac{1}{F_c(s)} \frac{X(s)}{U(s)} - 1\right] \tag{3.4.15}$$

where

$\frac{X}{U}(s)$ is the closed loop transfer function given in (3.4.1.)

The reason for the inclusion of an accumulator in the active system now becomes obvious: the hydraulic power supply needs only to provide power at the steady rate $\bar{\dot{W}}$, while the accumulator supplies (or absorbs) the difference between the average and instantaneous values. To avoid wasting power when the accumulator is fully charged, it is necessary to use either an unloading valve or a pressure compensated pump. This way, the pump does not discharge through the relief valve (at high pressure) when there is no flow demand.

CHAPTER IV

THE LABORATORY MODEL

4.1 General Description

A laboratory model, closely resembling the equivalent system discussed in Chapter II was constructed to validate the mathematical and simulation models developed, and as a prototype small scale mechanical simulator for designing and evaluating full scale systems. The apparatus consists of a hydraulic power supply, active and passive cylinders, a variable frequency displacement generator, and various pieces of electronic monitoring, processing, and display equipment. See Figures 4.1.1 and 4.1.2.

The power supply consists of a variable displacement pump of five gallons per minute capacity driven by a 5 HP electric motor. A pressure relief valve is provided on the discharge of the pump, which can be set to between 100 and 2000 psi. The entire unit is mounted on top of a 15 gallon oil reservoir.

The motion compensator consists of a pair of cylinders mounted in tandem on a carriage, Fig. 4.1.3. The carriage is given an approximate sinusoidal displacement of variable frequency and amplitude by means of a crank mechanism driven by a 1-1/2 HP DC motor. The piston rods of the two cylinders are pinned together, so that they act in parallel, rather than in

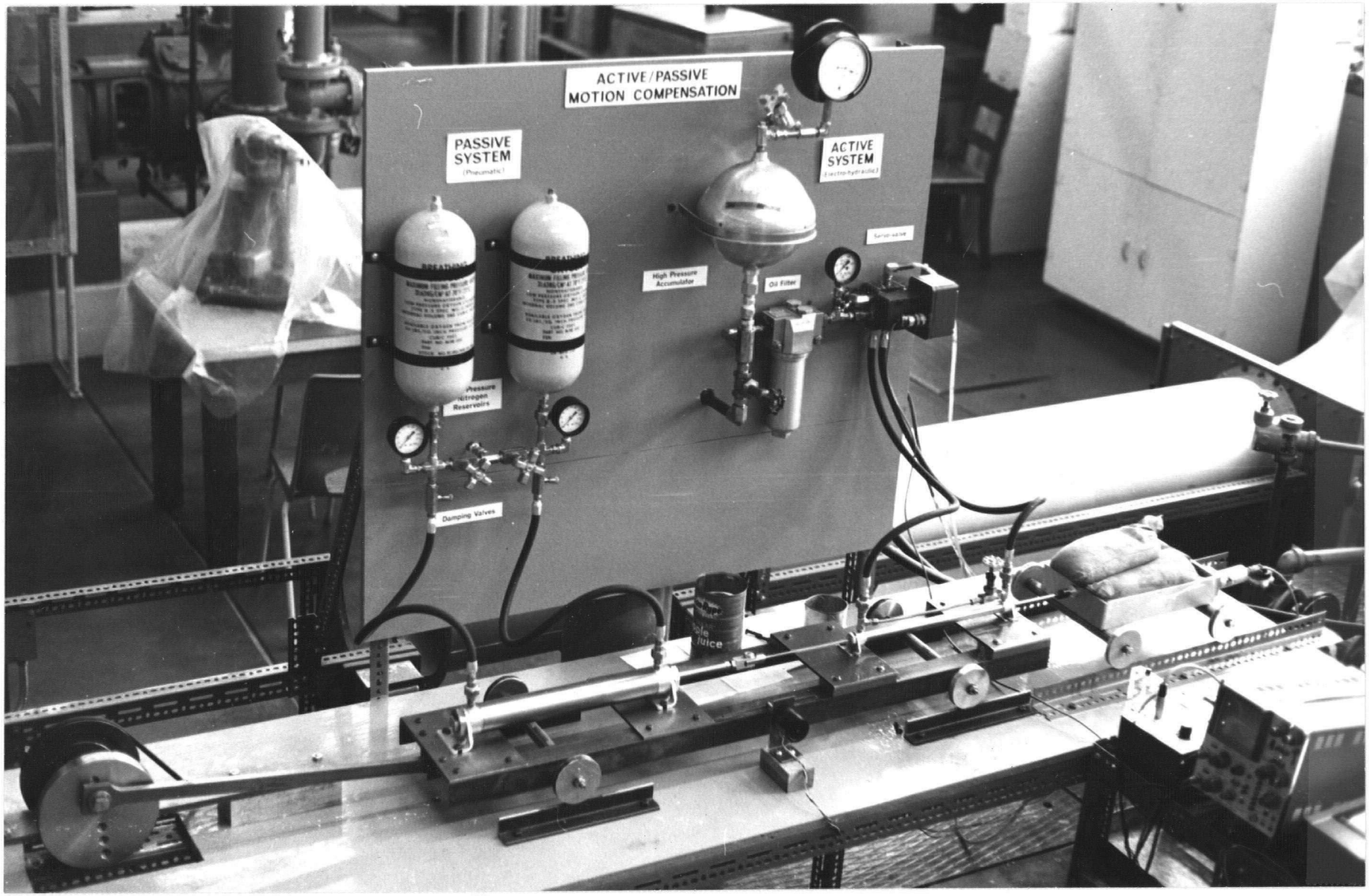

FIG. 4.1.1: THE LABORATORY APPARATUS.

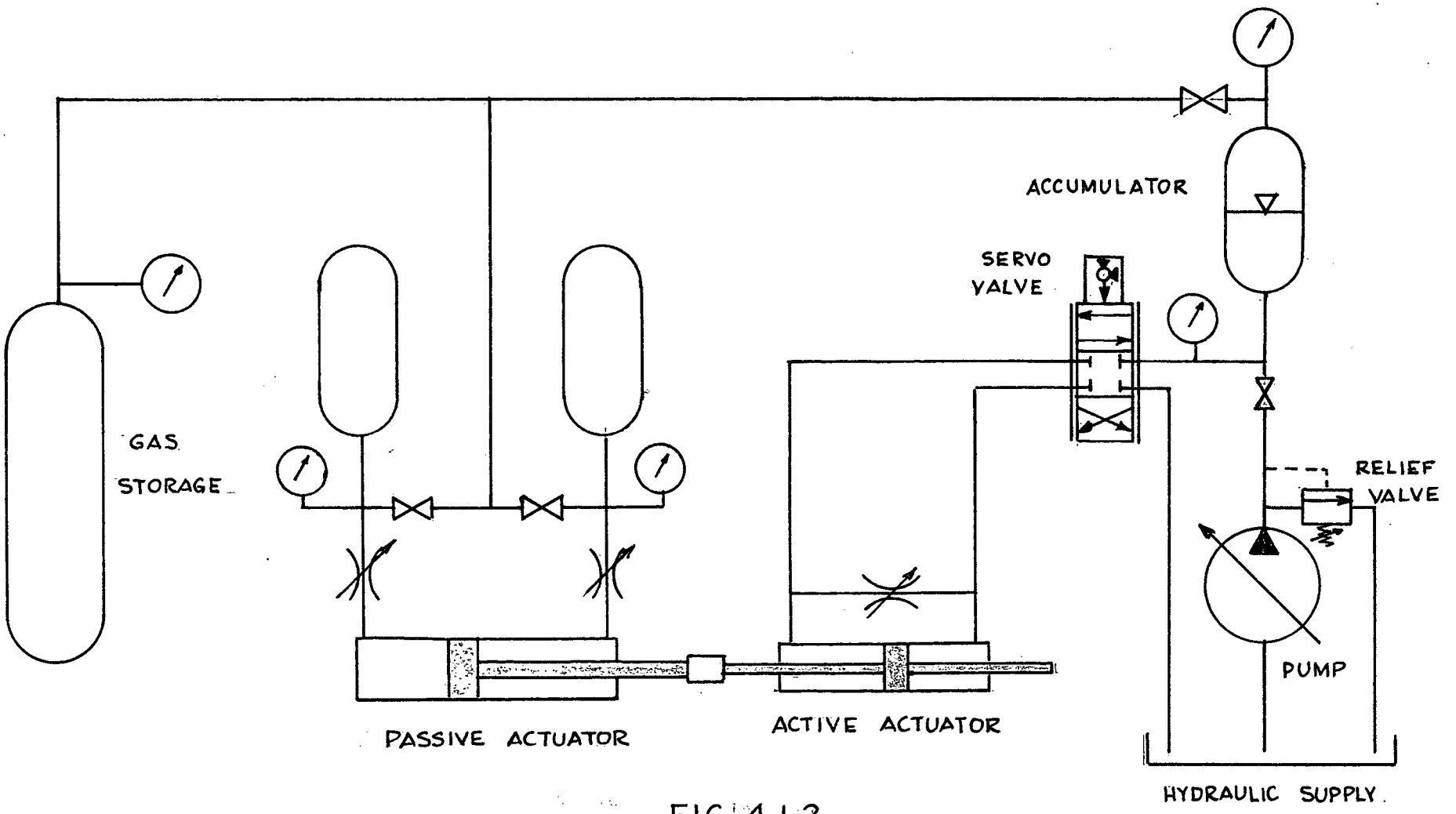

FIG. 4.1.2

LABORATORY APPARATUS - SCHEMATIC

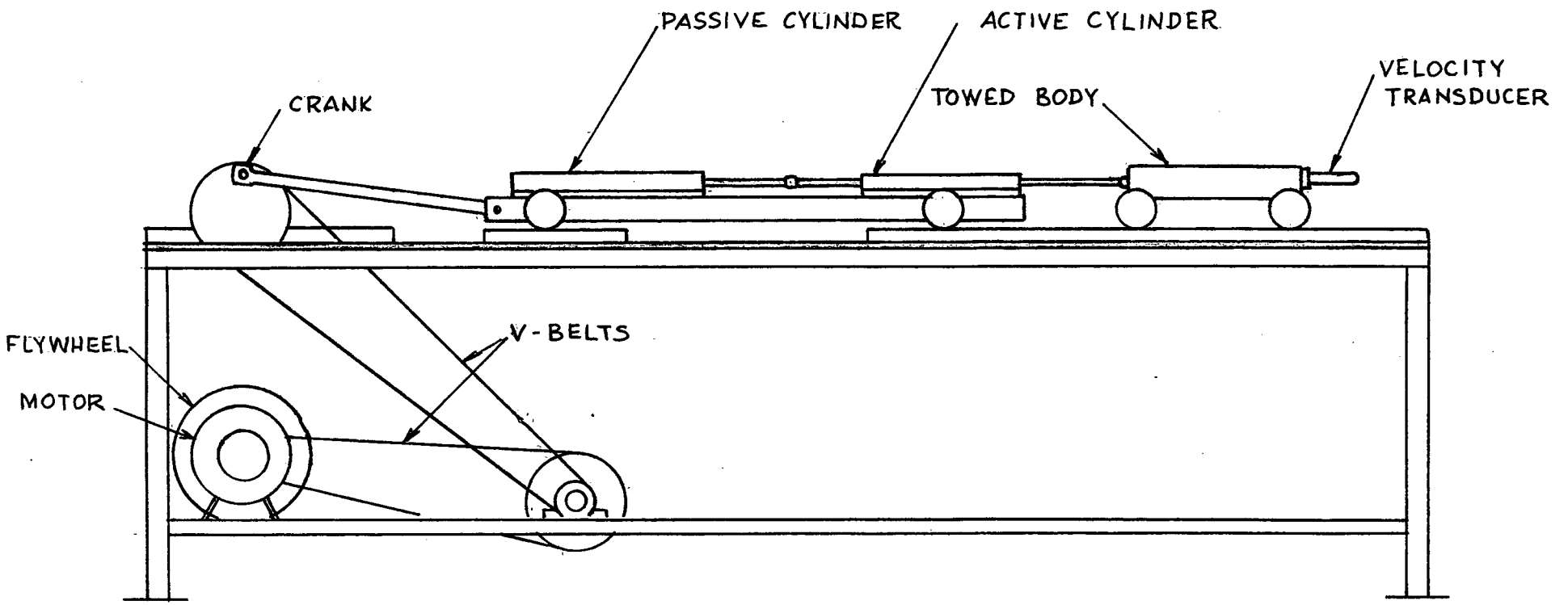

FIG. 4.1.3 MOTION GENERATOR ARRANGEMENT

series as the arrangement might first suggest. The other end of the double-ended piston rod is pinned to a second carriage which contains weights to represent the mass whose motion is to be isolated.

The passive system is purely pneumatic, consisting of a pair of gas bottles, one connected to each end of the larger of the two cylinders described above. A flow control valve on each gas bottle is used to adjust the damping of the passive system.

The active system consists of a gas/oil accumulator which feeds oil to a servovalve through a filter. The servovalve controls the flow of oil into the two ports of the smaller of the two cylinders mounted on the carriage. A gas line to the top of the accumulator controls the charge pressure of the system.

The control system monitors body and ram motions by a seismic velocity transducer mounted on the mass carriage, and a displacement potentiometer on the ram carriage. The signal processing function is achieved by an analogue computer which integrates, amplifies, and sums the two signals. A filter is also included to remove high frequency noise, such as the type generated by the wheels of the carriage. The processed signal is fed to a power amplifier which drives the servovalve. An oscilloscope and chart recorder are used to monitor any two of mass velocity,mass displacement, input displacement, or low level servo-actuating voltage. (Fig. 4.1.4)

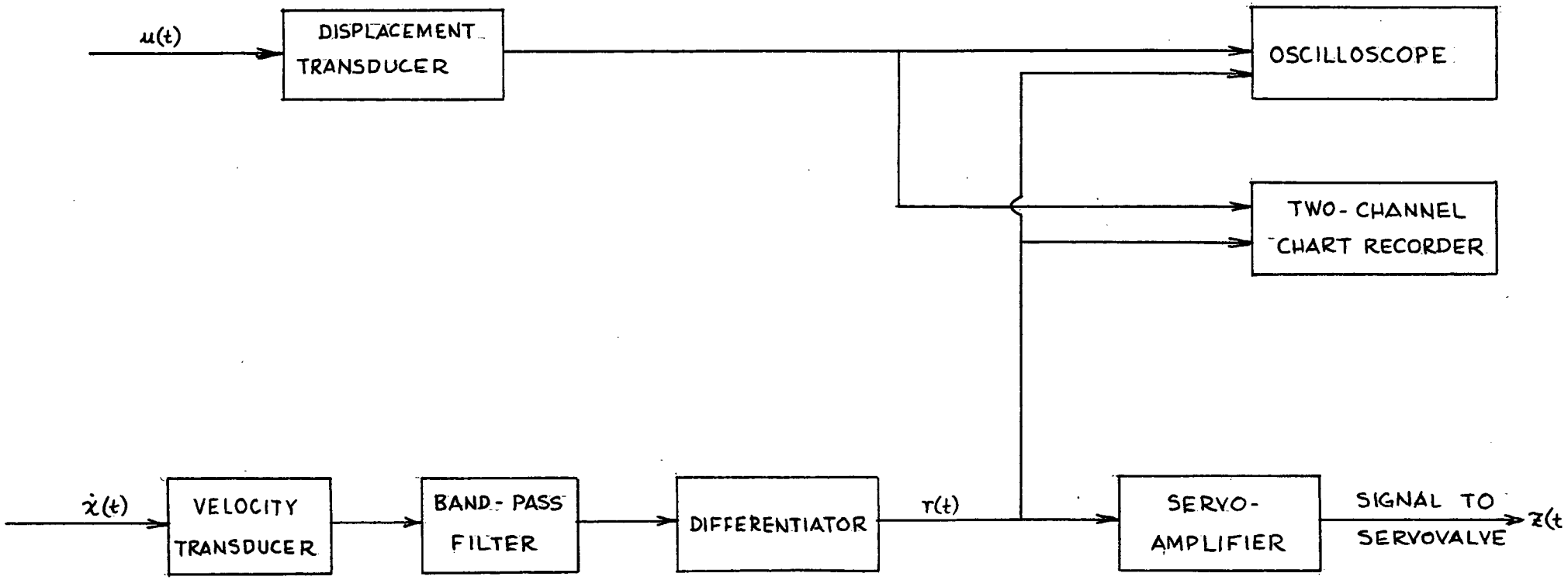

FIG. 4.1.4 CONTROL SYSTEM

The apparatus as constructed does not model the spring (i.e. cable) nor the hydrodynamic drag of the body. All other aspects of the equivalent system are included. The exclusion of these two parameters does not affect the model of the motion compensation system because they are both properties of the towed system.

4.2 Performance Prediction and Evaluation

The physical properties of the laboratory model are given in Appendix D. The design is not based on any particular requirement, but employs hardware which was readily available. The input amplitude was set to 1.5 inches, and the design frequency to 1 Hz.

The velocity transducer used to measure the motion of the body was quite unsuitable at the low frequencies at which the system could operate, and as a result some electronic signal processing was necessary to obtain a useable signal. As a result of this, only acceleration feedback was available for use in the control system. The stability equation (3.4.12) can now be expressed using acceleration feedback:

$$As^2 + Bs + C = 0 \qquad (4.2.1)$$

where

$$A = (\lambda_2 + \lambda_3)M + K_{sv} K_3 \lambda_1$$
$$B = (\lambda_2 + \lambda_3)C_L - 1$$
$$C = (\lambda_2 + \lambda_3)K_p$$

By making the acceleration feedback K_3 negative, the coefficients A, B and C are always negative (note that λ_2 and λ_3 are negative, while K_p is positive). Therefore, the system is

stable for all negative values of K_3.

A point to note is that the feedback constant, K_3, has the effect of increasing the apparent mass of the system, as shown in (4.2.1).

Because only one feedback variable is considered, it is not necessary to use the optimization technique outlined in Section 3.4. A feedback constant of

$$K_{sv} K_3 = -5 \text{ ma}/(\text{ft}/\text{sec}^2)$$

was used in the experiment.

The experiment was conducted at three frequencies: 0.5, 1.0, and 2.0 Hz. In each case, the system was first run in the passive mode ($K_3=0$), then with $K_{sv} K_3=-5$. The computer simulation was then conducted under the same conditions, and the results of both are shown in Appendix G.

The time-domain records are then transformed to the frequency domain, and plotted as distinct points on a Bode plot in Fig. 4.2.1. The linear model response is also plotted on the same graph for comparison, over a frequency range of 0.1 to 10 Hz.

There appears to be good agreement between the mathematical models and the real system. Any discrepancies are due to the uncertainties involved in estimating hydraulic and pneumatic throttling coefficients and mechanical friction. However, by

designing a real system with variable throttling valves, the former uncertainty can be removed since the real system can then be matched to the model. Friction, on the other hand, can neither be easily predicted nor altered once the system is operational.

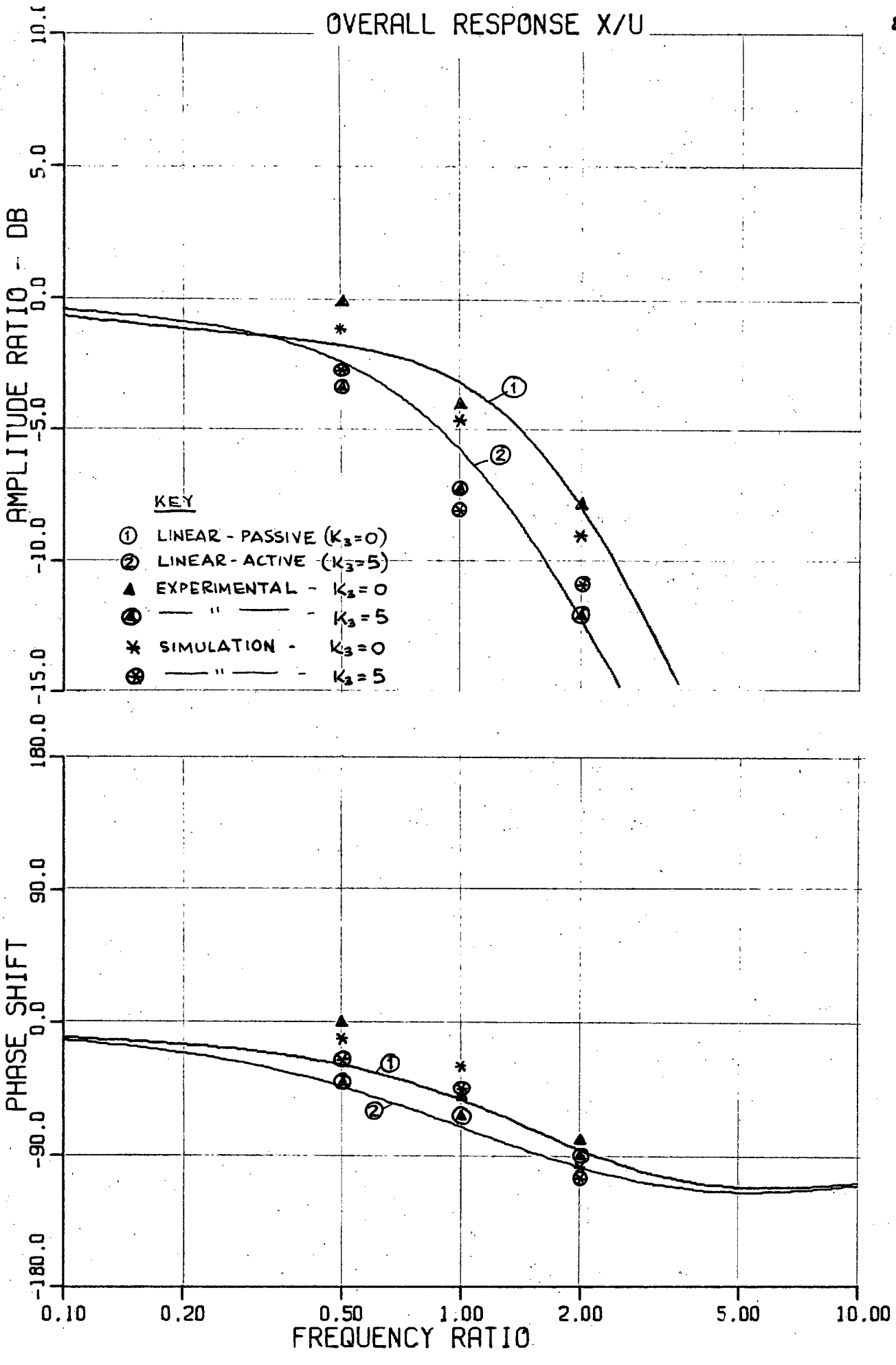

FIG. 4.2.1 THEORETICAL & EXPERIMENTAL RESULTS

CHAPTER V

APPLICATION

This chapter is intended as a guide to the application of the mathematical and computer simulation models to the design of real systems.

5.1 Input Conditions

The input, as stated in Chapter I, can be approximated by a Fourier series representing the vertical displacement of the surface of the water at a given point. The Bretschneider equation[1] can be used to obtain an estimate of the spectral energy density from the average height and period of the seaway for a given Sea State:

$$S(T) = \frac{2.7\bar{h}^2}{\bar{T}^4} T^3 \exp\left[-\frac{0.675}{\bar{T}^4} T^4\right] \qquad (5.1.1)$$

where

$S(T)$ is the spectral energy density in ft^2/sec,

T is the wave period in seconds,

$\bar{T}$ is the average wave period in seconds,

and $\bar{h}$ is the average peak-to-trough wave height in feet.

---

[1] See Ref. (12)

Values for $\bar{h}$ and $\bar{T}$ can be readily found in most nautical handbooks. Figure 5.1.1 shows a typical plot of the spectral density function for Sea State 4, having mean wave height and period of 4.9 feet and 5.4 seconds, respectively.

A ship subjected to a multi-frequency displacement input will behave as a low pass filter, and will not respond significantly to waves whose length is less than one-half the ship's length. A typical response curve is shown in Fig. 5.1.2. The motion of the ship is then the product of the sea state spectral density function and ship response, as shown in Fig. 5.1.3. The wave component which contains the most energy is found to have a period T_o, and $\omega_o = 2\pi/T_o$ is used as the primary design frequency.

Figure 5.1.3 can now be used to obtain the coefficients A_i of the Fourier Series

$$u(t) = \sum_{i=1}^{n} A_i \sin \omega_i t \qquad (5.1.2)$$

which can represent the motion of the ship in the time domain. This is done by dividing the Ship Motion Spectral Density Function into n cells spanning the entire range of period, and calculating the energy associated with each cell:

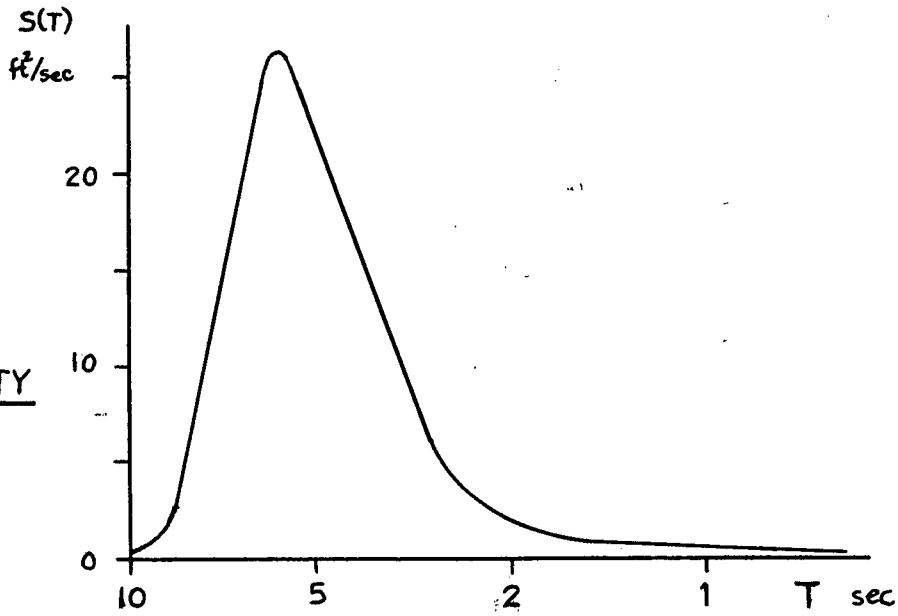

FIG. 5.1.1
SEA STATE "4"
SPECTRAL DENSITY
FUNCTION

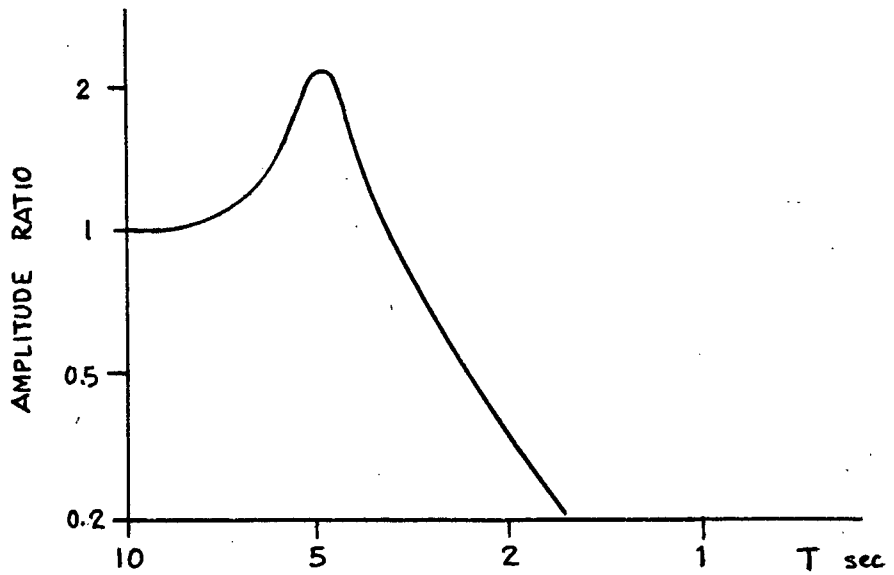

FIG. 5.1.2
SHIP HEAVE
RESPONSE

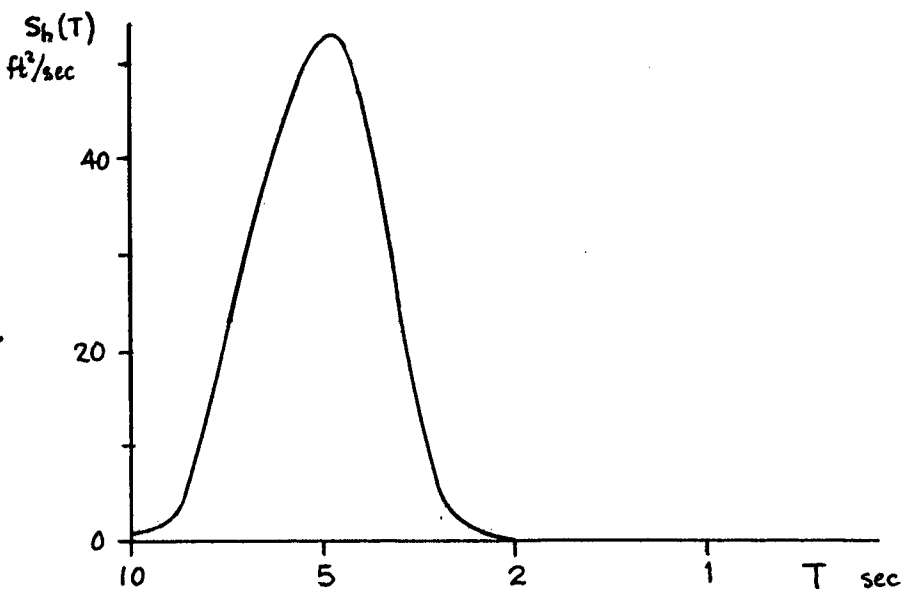

FIG. 5.1.3
SHIP HEAVE
SPECTRAL DENSITY
FUNCTION

$$\Delta S_i = \int_{T_i - \frac{\Delta T}{2}}^{T_i + \frac{\Delta T}{2}} S(T)\, dT \qquad (5.1.3)$$

where

ΔS_i is the energy asscciated with the i-th cell,

T is the central period of the i-th cell,

and ΔT is the cell width.

The coefficients A_i can be expressed as

$$A_i = \frac{1}{2}\sqrt{\Delta S_i} \qquad (5.1.4)$$

The approximate ship displacement as given by (5.1.2) can then be used in the simulation model to give a realistic input condition. It is not necessary to use more than three to five terms in the series to give a good wave profile.

5.2 Two-Dimensional Cable Model

When dealing with long cable lengths (over 2000 feet) or horizontal motion with respect to the water, the cable assumes a catenary shape which can no longer be assumed one-dimensional.

Walton and Polachek[1] developed a program to compute the shape and tension of a cable subject to a displacement boundary condition at one end and hydrodynamic drag along its entire length. In essence, the continuous cable is modelled as a number of elastic links pinned together end-to-end. Each link has masses concentrated at its two ends, as well as longitudinal and transverse drag coefficients. (Fig. 5.2.1) The towed body is represented as the last link of the cable, given the appropriate values for mass and drag coefficient.

The program uses a displacement input at the top (i.e. surface) end of the cable, and calculates the displacements and axial elongations of all the links. This in turn yields the cable tension in each link. The model of the motion compensation system developed here can use this cable/body model by supplying the variable x_1 as the boundary condition, and receiving F_{NET}, the cable tension at the surface tow point. If desired, the compensator motion can be resolved into horizontal and vertical components to increase the model's realism.

---

[1] See Ref. (23)

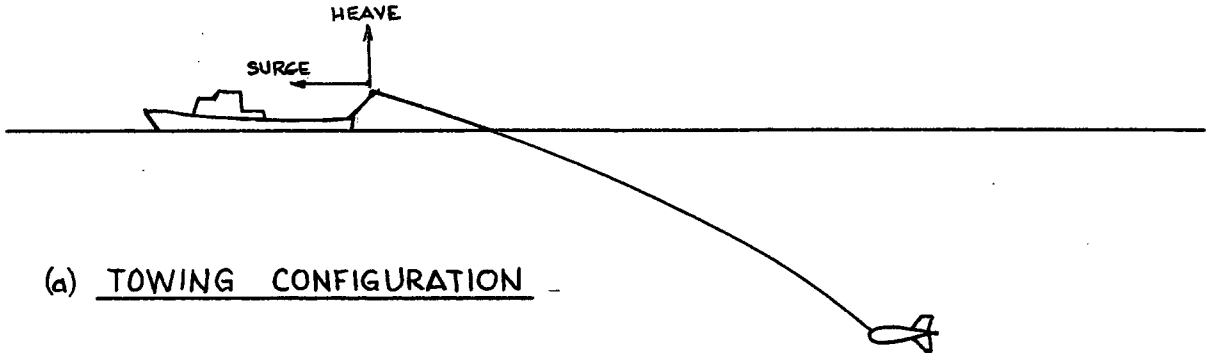

(a) TOWING CONFIGURATION

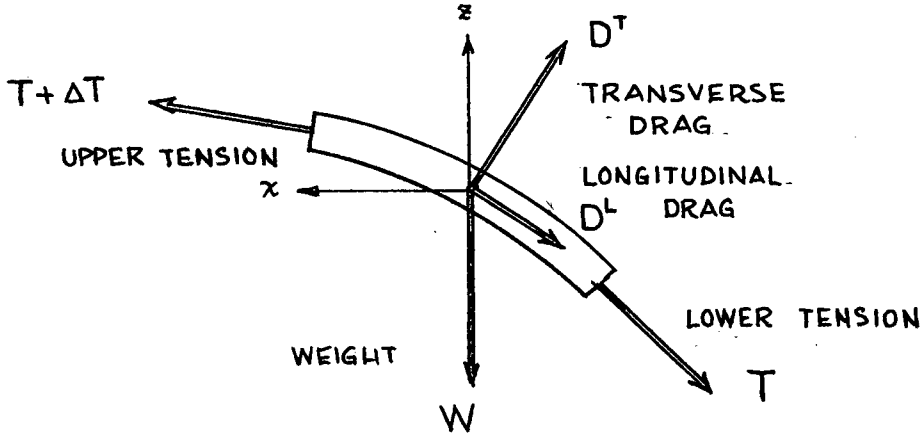

(b) CABLE SEGMENT

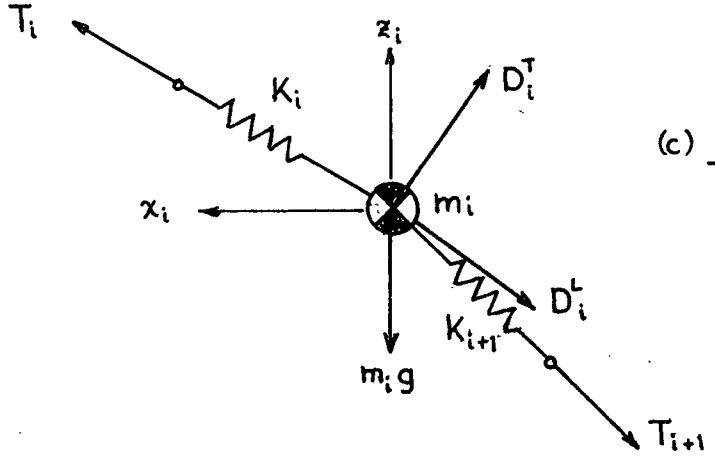

(c) MATHEMATICAL MODEL

FIG. 5.2.1 TWO-DIMENSIONAL CABLE

5.3 Servo-valve Model Extension

The servo-valve considered here is assumed to operate instantly upon application of a control signal. However, in the case of large valves which are usually multi-stage, there is considerable time lag even at low frequencies. The dynamic response of such valves can be considered as a first or second order system, depending on the accuracy desired. The valve equation then becomes

$$Q_v = H_{sv}(s)\, z \sqrt{P_s - \Delta P} \tag{5.3.1}$$

where $H_{sv}(s)$ is the dynamic characteristic of the valve.
In the case of a first-order valve,

$$H_{sv}(s) = \frac{C_{sv}}{1 + \tau_{sv} s} \tag{5.3.2}$$

and for a second-order,

$$H_{sv}(s) = \frac{C_{sv}}{1 + 2\frac{\zeta_{sv}}{\omega_{sv}} s + \frac{s^2}{\omega_{sv}^2}} \tag{5.3.3}$$

where

C_{sv} is the valve constant (as before),

τ_{sv} is the first-order time constant,

ω_{sv} is the second-order natural frequency,

and ζ_{sv} is the second-order damping ratio.

The parameters τ_{sv}, ω_{sv} and ζ_{sv} are estimated from the response curve supplied by the valve manufacturer, Fig. 5.3.1. They are chosen such that the phase lags of the real valve and the model coincide over the frequency range of interest. When operating near the resonance of the valve (which is generally not recommended since servo-valves are usually underdamped) a higher order model may be necessary.

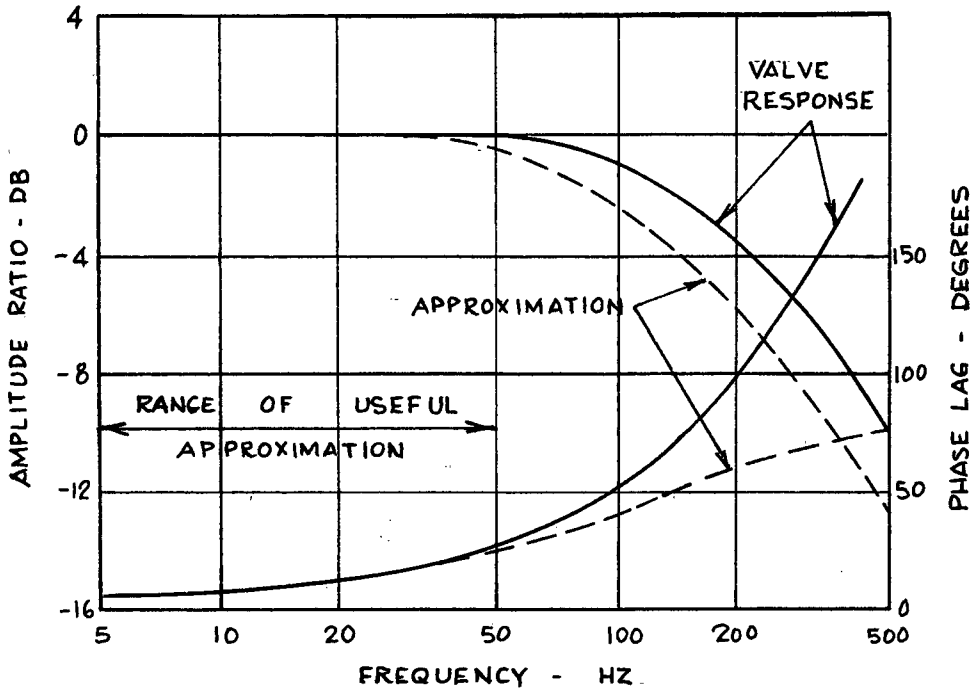

(a) RESPONSE WITH FIRST-ORDER APPROXIMATION

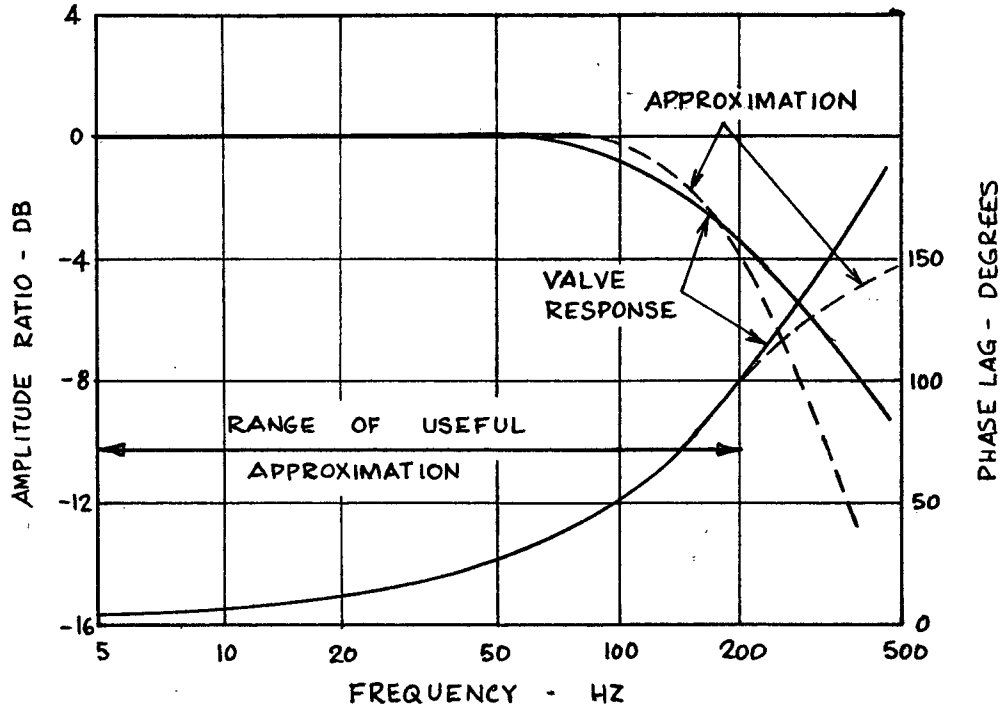

(b) RESPONSE WITH SECOND-ORDER APPROXIMATION

FIG. 5.3.1 SERVOVALVE RESPONSE

5.4 Control System Considerations

In setting down the performance requirements of a real system, the frequency response must be carefully considered. In particular, long period waves generally have larger amplitudes than short waves, hence it is not always possible to compensate for them as effectively due to the limited travel of the compensator. Therefore, it is desirable to design for zero compensation at high wave periods (in the order of 20 to 50 seconds), increasing to maximum compensation at the design frequency. An acceleration feedback system will inherently behave in this manner.

At frequencies above the ship's natural frequency it is desirable to decrease compensation since the ship does not respond to such waves. Furthermore, shipboard vibrations due to the engine and propellors may be significant above one Hz. A typical frequency response which would give acceptable performance is shown in Fig. 5.4.1. The low frequency cut-off can be moved to the left by either decreasing the stiffness of the passive system, increasing amplifier gain, or increasing the time constant of the ram centering loop.

The point of maximum compensation is set by introducing a second-order low-pass filter, Fig. 5.4.2. The corner frequency coincides with the design frequency, where motion compensation is maximum. The critical damping ratio determines the bandwidth

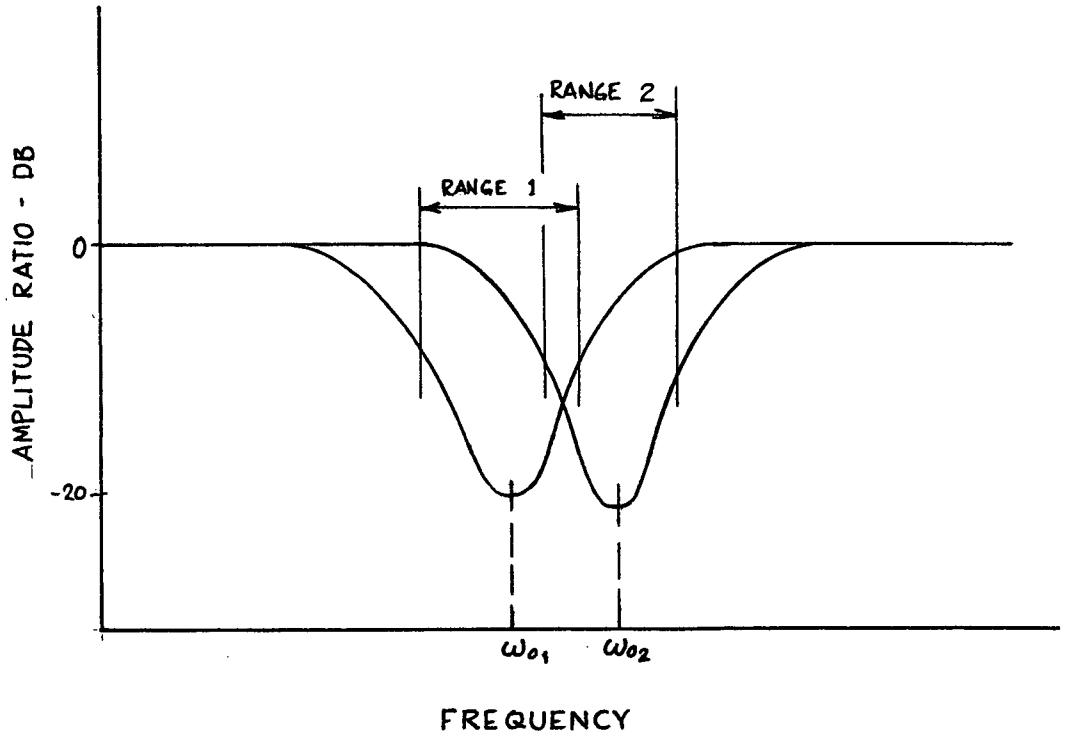

FIG. 5.4.1

MOTION COMPENSATION TRANSFER FUNCTION

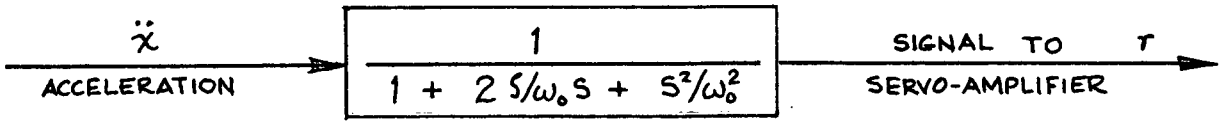

ω_o SETS DESIGN FREQUENCY
ζ CONTROLS BANDWIDTH

FIG. 5.4.2 TYPICAL FEEDBACK NETWORK

of the response curve. Such a filter can be used tc tune the system to virtually any sea state condition, provided that the system is designed to handle the corresponding amplitudes. This feature can be used to improve an existing passive system by adding on an active one.

CHAPTER VI

CONCLUSIONS

The dynamic behaviour of an active-passive motion compensation system has been analysed and a mathematical model developed. Experiments performed on a laboratory apparatus indicate that the system is adequately described by the equations derived.

The mathematical model has been simplified by linearizing the equations, and computer programs have been developed which can assist in the initial design of real systems. In addition, a program which solves the nonlinear equations by simulation has been written, and can be used to refine the initial design. The programs are flexible enough to accomodate a variety of system configurations.

This project, in essence, has provided a design tool, based on mathematical analysis, to an area which has traditionally relied on seat-of-the-pants engineering.

REFERENCES

1. Athans, M.: On the Design of a Digital Computer Program for the Design of Feedback Compensators in Transfer Function Form NTIS Acc. #AD-700-431
2. Blackburn, J. F.: Fluid Power Control MIT Press, Cambridge, Mass., 1960.
3. Buck, J. R. & Stoll, H. W.: Investigation of a Method to Provide Motion Synchronization During Submersible Retrieval Naval Eng. J., Dec. 1969.
4. Burrows, C. R.: Fluid Power Servomechanisms Van Nostrand Reinhold Company, London, 1972.
5. Cavanaugh, R. D.: Air Suspension and Servo Controlled Isolation Systems Shock & Vibration Handbook, Ch. 33, McGraw Hill, 1961.
6. Guillon, M.: Hydraulic Servosystems Analysis and Design Butterworth and Company, 1969.
7. Hedrick, J. K.: A Summary of The Optimization Techniques that Can Be Applied to Suspension Systems Design Ariz. State. U. Report #PB-220553.
8. Karnop, D.: Vibration Control Using Semi-Active Force Generators ASME Paper # 73-DET-122.
9. Keefer, B. G.: Improved Hydropneumatic Tensioning Systems for Marine Applications B. C. Research Council Report, 1972.
10. Kriebel, H.: A Study of the Feasibility of Active Shock Isolation Inginieur Archiv Berlin, Vol. 36 #6, 1968.
11. Mercer, C. A. & Rees, P. L.: An Optimum Shock Isolator J. Sound & Vibr., 18(4) 1971.
12. Myers, J. J.: Handbook of Ocean and Underwater Engineering McGraw Hill, 1969.
13. Porter, B. & Bradshaw, A.: Synthesis of Active Controllers for Vibratory Systems J. of M. E. Sci., V. 14 #5, 1972.
14. Raven, F. H. Automatic Control Engineering McGraw Hill, 1968.
15. Ruzicka, J. E.: Fundamental Concepts of Vibration Control Tech. Inf. Service, AIAA Doc. #A72-29555.
16. Shinners, S. M.: Modern Control Systems Theory and Application Addison Wesley, 1972.
17. Soliman, J. I. & Tajer-Ardabili: Active Isolation Systems Using a Nozzle Flapper Valve Inst. M. E. Proc., V. 182 #30, 1967.
18. Soliman, J. I., & Tajer-Ardabili: Servovalve Controlled Isolation Systems Inst. M. E. Proc., V. 185 #10, 1970.
19. Sutherland, A.: Mechanical Systems for Ocean Engineering Naval Eng. J., Oct. 1970.
20. Thompson, A. G.: Quadratic Performance Indices and Optimum Suspension Design Inst. M. E. Proc., V. 187, 1973.
21. Thompson, A. G.: Design of Active Suspensions Inst. M. E. Proc., V. 185, 1970.

22. Thompson, A. G.: Optimum Damping in a Randomly Excited Nonlinear Suspension Inst. M. E. Proc., V. 184, 1969.
23. Walton & Polachek: Calculation of Transient Motion of Submerged Cables Math. Tables & Aids to Computation, V. 14, 1960.
24. Yeaple, F. D.: Hydraulic and Pneumatic Power and Control McGraw Hill, 1966.

APPENDIX A

GAS FLOW EQUATIONS

1. FLOW INTO A CLOSED VOLUME

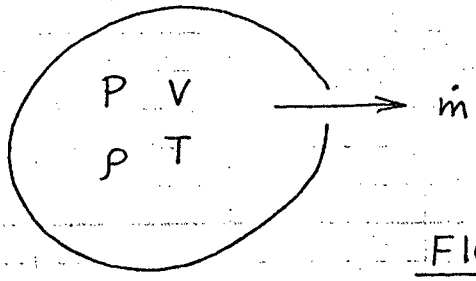

FIG. A-1

RATE OF CHANGE OF ENTHALPY WITHIN CONTROL VOLUME OF FIG. A-1:

$$\frac{dH}{dt} = \frac{dU}{dt} + \frac{dE}{dt} = \dot{m}\, C_p T \qquad (A.1)$$

THE RATE OF CHANGE OF INTERNAL ENERGY IS THE FLOW RATE OF GAS MULTIPLIED BY ITS UNIT INTERNAL ENERGY:

$$\frac{dU}{dt} = \dot{m}\, C_v T = \frac{C_v}{R}\,\frac{d}{dt}(PV) \qquad (A.2)$$

THE RATE OF CHANGE OF ENERGY IS THE WORK DONE ON THE GAS BY EXPANSION OR COMPRESSION OF THE CONTROL VOLUME:

$$\frac{dE}{dt} = P\,\frac{dV}{dt} \qquad (A.3)$$

SUBSTITUTING (A.2) AND (A.3) INTO (A.1) GIVES:

$$\dot{m}\, C_p T = \frac{C_v}{R}\,\frac{d}{dt}(PV) + P\,\frac{dV}{dt} \qquad (A.4)$$

SOLVING FOR $\dot{m}$ AND SUBSTITUTING

$$\frac{1}{C_p} + \frac{1}{\gamma R} = \frac{1}{R} \qquad (A.5)$$

INTO (A.4), GIVES:

$$\dot{m} = \frac{1}{RT}\left[\frac{V}{\gamma}\,\frac{dP}{dt} + P\,\frac{dV}{dt}\right] \qquad (A.6)$$

2. FLOW THROUGH A NEEDLE VALVE

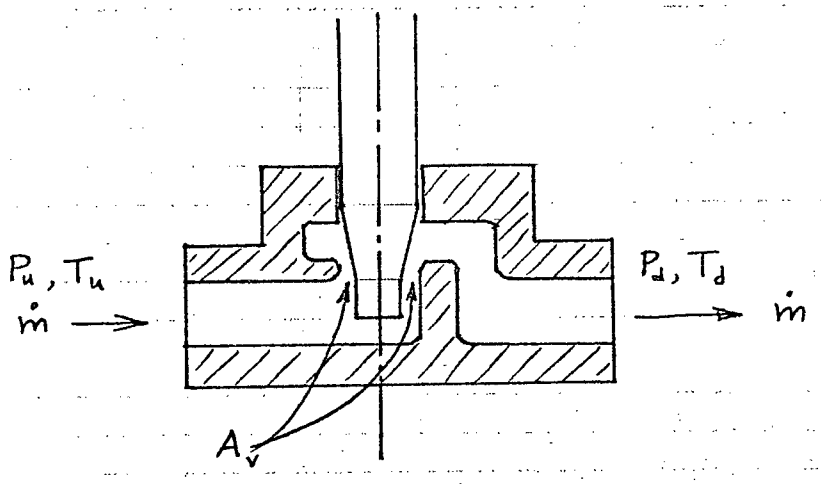

FIG. A-2

THE NEEDLE VALVE, FIG. A-2, CONSISTS OF A VARIABLE AREA ANNULUS, A_v, WHICH IS CONTROLLED BY RAISING OR LOWERING A TAPERED NEEDLE. THIS CAN BE MODELLED BY A CONVERGENT NOZZLE.

APPLYING THE ENERGY EQUATION:

$$H_u = H_d + \frac{\bar{v}^2}{2} \qquad (A\text{-}7)$$

WHERE $\bar{v}$ IS THE AVERAGE VELOCITY ACROSS A_v.

ASSUMING THE FLUID IS A PERFECT GAS

$$C_p T_u = C_p T_d + \frac{1}{2}\bar{v}^2 \qquad (A\text{-}8)$$

ASSUMING ISENTROPIC FLOW

$$\frac{P_d}{P_u} = \left(\frac{\rho_d}{\rho_u}\right)^{\gamma} = \left(\frac{T_d}{T_u}\right)^{\gamma/\gamma-1} \qquad (A\text{-}9)$$

THE MASS FLOW RATE IS GIVEN BY

$$\dot{m} = \rho A_v \bar{v} \qquad (A\text{-}10)$$

SUBSTITUTING (A·8), (A·9) INTO (A·10) GIVES:

$$\dot{m} = \rho_u \left(\frac{P_d}{P_u}\right)^{\gamma} A_v \sqrt{\left(\frac{2\gamma}{\gamma-1}\ \frac{P_u}{\rho_u}\right)\left\{1-\left(\frac{P_d}{P_u}\right)^{\frac{\gamma-1}{\gamma}}\right\}} \qquad (A\cdot11)$$

SUBSTITUTING THE EQUATION OF STATE (OF A PERFECT GAS)

$$\rho_u = \frac{P_u}{RT_u} \qquad (A\cdot12)$$

INTO (A·11) GIVES:

$$\dot{m} = P_u A_v \left(\frac{P_d}{P_u}\right)^{1/\gamma} \sqrt{\frac{2\gamma}{RT_u(\gamma-1)}\left\{1-\left(\frac{P_d}{P_u}\right)^{\frac{\gamma-1}{\gamma}}\right\}} \qquad (A\cdot13)$$

SINCE THE VALVE IS NOT AN IDEAL CONVERGING NOZZLE, IT IS THEREFORE NECESSARY TO INTRODUCE AN EMPIRICAL DISCHARGE COEFFICIENT, C_D INTO EQUATION (A·13). THIS COEFFICIENT CAN THEN BE COMBINED WITH A_v, SUCH THAT

$$C_o = C_D A_v \qquad (A\cdot14)$$

WHERE C_o IS A FUNCTION OF NEEDLE POSITION. C_o IS DETERMINED EXPERIMENTALLY, AND USUALLY PUBLISHED BY MANUFACTURERS FOR THEIR VALVES.

EQUATION (A·13) CAN THUS BE EXPRESSED AS:

$$\dot{m} = C_o P_u \left(\frac{P_d}{P_u}\right)^{1/\gamma} \sqrt{\frac{2\gamma}{RT_u(\gamma-1)}\left\{1-\left(\frac{P_d}{P_u}\right)^{\frac{\gamma-1}{\gamma}}\right\}} \qquad (A\cdot15)$$

NOTE THAT (A·15) IS ONLY VALID FOR

$$P_c < P_d < P_u \qquad (A\cdot16)$$

I.E., FOR DOWNSTREAM PRESSURE GREATER THAN THAT REQUIRED FOR CHOKED FLOW. FOR NITROGEN AND AIR,

$$P_c = 0.528\, P_u$$

APPENDIX B

HYDRAULIC SERVO-VALVES

1. TYPES OF VALVES:

VALVES CONSIDERED HERE ARE "FOUR-WAY SPOOL VALVES", CONSISTING OF 4 METERING ORIFICES, FIG B.1.

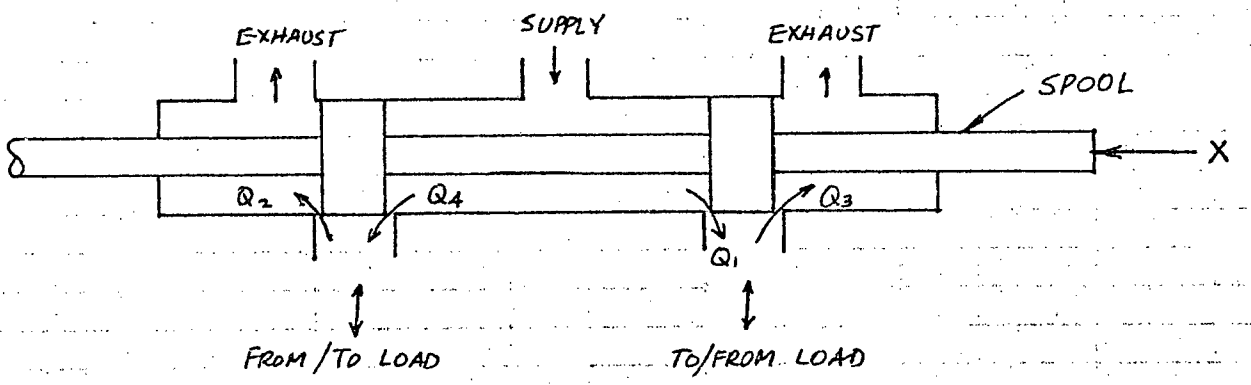

FIG. B.1

SPOOL VALVE

THIS ARRANGEMENT CAN BE MODELLED BY A HYDRAULIC WHEATSTONE BRIDGE, FIG. B.2.

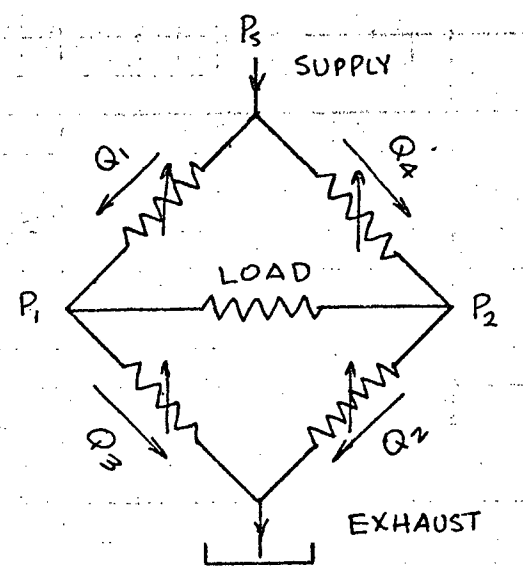

FIG. B.2 WHEATSTONE BRIDGE

THE HYDRAULIC RESISTANCES ARE, OF COURSE, NONLINEAR.

SERVOVALVES MAY BE UNDERLAPPED, OVERLAPPED, OR ZERO-LAPPED AS SHOWN IN FIG. B.3.

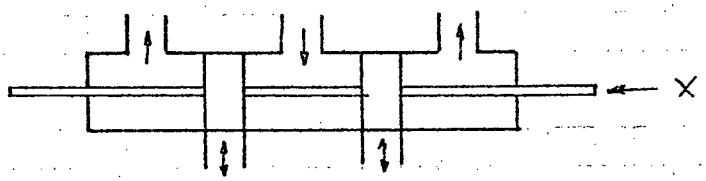

ZERO-LAPPED

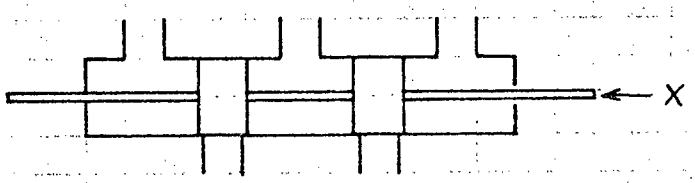

OVER-LAPPED

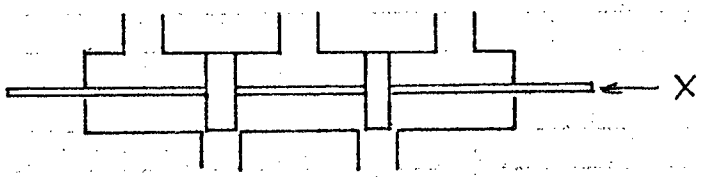

UNDER-LAPPED

FIG. B.3 VALVE SPOOL DESIGNS

OVERLAPPED VALVES EXHIBIT A DEAD ZONE ABOUT THEIR CENTRE POSITION, $X=0$, WHEREAS UNDERLAPPED VALVES ARE FAIRLY LINEAR IN THAT REGION. UNDER-LAPPING TENDS TO ENHANCE STABILITY OF THE SERVO SYSTEM AT THE EXPENSE OF POWER LOSS AT $X=0$.

IN THIS ANALYSIS, ZERO-LAPPED VALVES ARE CONSIDERED. HENCE, $Q_3 = Q_4 = 0$.

LEAF 101 OMITTED

IN PAGE NUMBERING.

2. DERIVATION OF PRESSURE-FLOW EQUATIONS

A ZERO-LAPPED VALVE MAY BE MODELLED BY THE SIMPLIFIED CIRCUIT OF FIG. B·4.

FIG. B·4 ZERO-LAPPED VALVE

IF COMPRESSIBILITY WITHIN THE SYSTEM IS NEGLECTED, THEN

$$Q_1 = Q_2 = Q_L \qquad (B.1)$$

ASSUMING THAT ORIFICE AREA IS PROPORTIONAL TO DISPLACEMENT, X, WE HAVE THE FAMILIAR ORIFICE FLOW EQUATIONS:

$$Q_1 = KX\sqrt{P_S - P_1} = Q_L$$
$$\& \quad Q_2 = KX\sqrt{P_2} = Q_L \qquad (B.2)$$

WHERE

P_S = SUPPLY PRESSURE
K = A CONSTANT
& Q_L = LOAD FLOW.

COMBINING THE TWO EQUATIONS OF (B.2) AND REARRANGING, YIELDS:

$$Q_L = \frac{K}{2} X \sqrt{P_S - \Delta P} \qquad (B.3)$$

WHERE

$$\Delta P = P_1 - P_2$$

FOR NEGATIVE SPOOL DISPLACEMENT ($X < 0$), NOTE THAT

$$Q_1 = Q_2 = 0 \qquad (B.4)$$
$$\& \quad Q_3 = Q_4 = Q_L$$

THIS YIELDS

$$Q_L = \frac{K}{2} \times \sqrt{P_s + \Delta P} \qquad (B.5)$$

COMBINING (B.3) AND (B.5), AND LETTING

$$C_{sv} = K/2$$

WE GET:

$$Q_L = C_{sv} \times \sqrt{P_s - \text{sign}(z)\,\Delta P} \qquad (B.6)$$

WHICH IS THE GENERAL SERVOVALVE EQUATION.

APPENDIX C

COMPRESSIBILITY EFFECT OF HYDRAULIC FLUID

CONSIDER THE CYLINDER SHOWN IN FIG. C.1 :

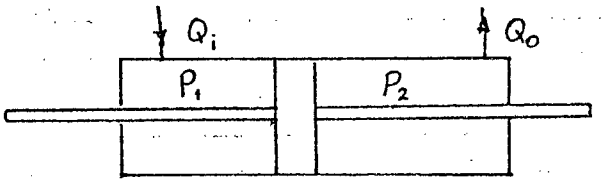

FIG. C.1

THE FLOW OUT, Q_o, IS EQUAL TO THE FLOW IN, Q_i, LESS THE RATE OF FLUID COMPRESSION INSIDE, THE "COMPRESSIBILITY FLOW", Q_c.

$$Q_o = Q_i - Q_c$$

$$\text{&} \quad Q_c = \frac{V}{B}\frac{dP}{dt}$$

WHERE

V IS THE VOLUME OF THE CYLINDER,
B IS THE BULK MODULUS OF THE FLUID,
& dP/dt IS THE RATE OF CHANGE OF PRESSURE IN THE CYLINDER.

FOR THE EQUIVALENT MODEL DISCUSSED IN THE TEXT,

$$V = 4.70 \text{ in}^3$$
$$B = 95000 \text{ psi}$$

$$\text{&} \quad P \simeq 300(1 + \sin \omega t)$$

WHERE $\omega_{max} \simeq 4 \text{Hz.} \simeq 25 \text{ rad/sec.}$

THIS GIVES $\frac{dP}{dt} = 300\,\omega \cos \omega t$

OR $\left(\frac{dP}{dt}\right)_{max} = 300\omega = 7500 \text{ psi/sec.}$

THIS GIVES $(Q_c)_{max} = \frac{4.70}{95000} \times 7500 = 0.371 \text{ in}^3/\text{sec}$

FOR MAXIMUM INLET FLOW CONDITION,

$$Q_i = A\dot{y}$$

WHERE A = PISTON AREA = 0.393 in^2
& $\dot{y}$ = PISTON VELOCITY.

CONSIDERING FULL 12-INCH STROKE:

$$y = 6 \sin \omega t$$

$$\dot{y} = 6\omega \cos \omega t$$

$$(\dot{y})_{max} = 6\omega = 150 \text{ in/sec}$$

THIS GIVES $Q_i = 0.393 \times 150$

$= 59 \text{ in}^3/\text{sec}.$

THIS GIVES THE RATIO

$$\frac{Q_c}{Q_i} = \frac{0.371}{59} = 0.6\%$$

THE COMPRESSIBILITY FLOW IS THUS NEGLIGIBLE.

CONSIDER NOW A FULL-SCALE SYSTEM. TYPICALLY,

$V = 5000 \text{ in}^3$ (8" DIA. x 8 FT. LONG (96 INCHES))

$P = 1000(1 + \sin \omega t)$

WHERE $\omega_{max} = 0.25 \text{ Hz} = 1.57 \text{ rad/sec}.$

THIS GIVES $\left(\frac{dP}{dt}\right)_{max} = 1000 \times 1.57 = 1570 \text{ psi/sec}$

HENCE $Q_c = \frac{5000}{95000} \times 1570 = 83 \text{ in}^3/\text{sec}$

THE INLET FLOW RATE IS NOW

$$Q_i = A\dot{y}_{max} = 50 \times 48 \times 1.57 \quad (in^3/sec)$$

$$= 3770 \quad in^3/sec.$$

THIS GIVES THE RATIO

$$\frac{Q_c}{Q_i} = \frac{83}{3770} = 2.2\%$$

THIS IS ALSO NEGLIGIBLE.

APPENDIX D

LABORATORY MODEL SPECIFICATIONS

1. INPUT:

$u_o = \pm 1\frac{1}{2}" = \pm 0.125$ ft.

$\omega_o = 1$ Hz (DESIGN FREQUENCY)

2. LOAD

$M = 3.0$ slugs $\simeq$ 97 lb-mass.

$K_c = \infty$

$C_H \simeq 0$

3. PASSIVE SYSTEM

$P_o = 0$ psig $= 15$ psia

$A_1 = 3.14$ in^2

$A_2 = 2.95$ in^2

AV. AREA: $A_p = 3.04$ in^2

$V_c = 20$ in^3

$V_t = 280$ in^3

$$N = \frac{V_t}{V_c} = 14$$

STIFFNESS: $$K_p = \frac{N}{N+1}\,\frac{2\gamma P_o A_p^2}{V_t} = 1.1 \text{ lb/in} = 13 \text{ lb/ft.}$$

4. ACTIVE SYSTEM

SERVOVALVE: VICKERS SC4-03
3 USGPM @ 500 psi drop

$C_{sv} = 0.0118$ (in^3/sec)/(ma $\sqrt{\text{psi}}$)

$A_A = 0.393\ in^2$

$C_v = 3.75\ (in^3/sec)/\sqrt{psi}$

$P_s = 500\ psi$

LINEAR APPROXIMATION:

LET $F_{A_o} = 10^{\#}$

$\frac{F_{A_o}}{A_A} \simeq 25\ psi$

$\dot{y}_{max} = y_o \omega_o \simeq u_o \omega_o = 1.5 \times 6.28 = 9.42\ in/sec$

$\therefore \dot{y}_o = \dot{y}_{rms} = 0.707 \times 9.42 = 6.66\ in/sec$

$\therefore \dot{y}_o = \frac{C_{sv}}{A_A} z_o \sqrt{P_s - F_{A_o}/A_A}$

$\therefore z_o = \frac{\dot{y}_o A_A}{C_{sv}\sqrt{P_s - F_{A_o}/A_A}} = \frac{6.66 \times 0.393}{0.0118\ \sqrt{475}}$

$\simeq 10\ ma$

$\therefore \lambda_1 = \frac{C_{sv}}{A_A}\sqrt{P_s - \frac{F_{A_o}}{A_A}} = \frac{0.0118}{0.393}\sqrt{475}$

$= 0.66\ (in/sec)/ma$

$= 0.055\ (ft/sec)/ma.$

$\lambda_2 = -\frac{C_{sv} z_o}{2 A_A^2 \sqrt{P_s - F_{A_o}/A_A}} = -\frac{0.0118 \times 10}{2 \times (0.393)^2 \sqrt{475}}$

$= -0.017\ (in/sec)/lb$

$= -0.0014\ (ft/sec)/lb$

$\lambda_3 = -\frac{C_v}{2 A_A^2 \sqrt{F_{A_o}/A_A}}$

$= -\frac{3.75}{2 \times (0.393)^2 \sqrt{25}} = -2.4\ (in/sec)/lb$

$= -0.2\ (ft/sec)/lb$

APPENDIX E

FRICTION PARAMETER

FRICTION IS CONSIDERED AS AN EXTERNAL FORCE ON THE SYSTEM, AS SHOWN IN FIG. E.1 :

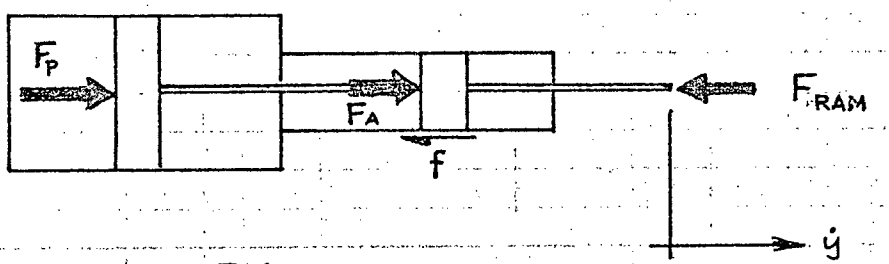

FIG. E.1

THE NET FORCE IS GIVEN BY

$$F_{RAM} = F_A + F_P - f$$

WHERE f IS THE FRICTION FORCE.

f IS A FUNCTION OF $\dot{y}$:

(a) $\dot{y} = 0$: f IS EQUAL AND OPPOSITE TO $(F_A + F_P)$ UNTIL MOTION BEGINS

(b) $\dot{y} \neq 0$: f IS CONSTANT AND OPPOSITE IN SENSE TO $\dot{y}$

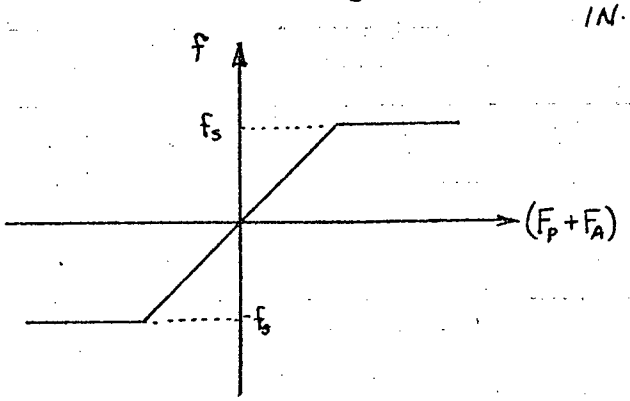

$\dot{y} = 0$

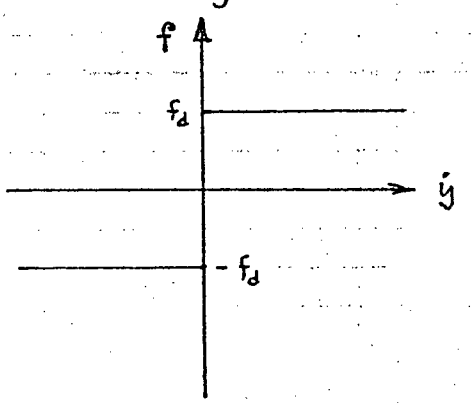

$\dot{y} \neq 0$

APPENDIX F.1

```
NONLIN
    1      ************** REMC:NONLIN ******************
    2      *
    3      ***** NONLINEAR MODEL SIMULATION PROGRAM ***
    4      *
    5      INITIAL
    6         CONSTANT CSV=0.0118, U0=0.125, AA=0.393, AP=3.0, ...
    7                  V0=20., VT=280., M=3.0, GAM=1.2, PS=500.,...
    8                  W0=6.28
    9         PARAMETER  K2=0., K3=0.0, KSV=1.0, P0=15.0,...
   10                  ZETA=1.00, CV=3.75, FF0=1., YDCR=0.0000001, CX=1.
10.25         PARAMETER K1=(0.,5.)
   11         PARAMETER RW= 1.0, TCV=0.025
   12                  N=VT/V0
   13                  KS=2.*GAM*P0*AP**2/VT*12.
   14                  WN=SQRT(KS/M)
   15                  TC1=2.*ZETA/WN
   16                  TC2=TC1/(N+1.)
   17                  KP=N*KS/(N+1.)
   18                  W=RW*W0
   19      DYNAMIC
   20                  U1=U0*SINE(0.,W,0.)
   21                  U2=RAMP(0.0)-RAMP(1.0)
   22                  U=U1*U2
   23                   UD=DERIV(0.,U)
   24                   UDD=DERIV(0.,UD)
   25                  X=U+Y
25.25                  X1=CMPXPL(0.,0.,0.5,W,XD)
25.5                   XOUT=W*X1
   26                  F1=LEDLAG(TC1,TC2,Y)
   27                  FP=-KP*F1
   28                  YD=IMPL(0.,0.05,FYD)
   31                  XD=UD+YD
   32                  YDD=DERIV(0.,YD)
   33                  XDD=UDD+YDD
   34                  FNET=M*XDD+CX*XD
   35      PROCEDURE FFR=FRIC(YD,FF0,FNET,YDCR)
   36             IF(ABS(YD)-YDCR)10,10,11
   37      11      IF(YD)1,1,3
   38      1        FFR=-FF0
   39               GO TO 4
   40      3        FFR=FF0
   41               GO TO 4
   42      10       FFR=LIMIT(-FF0,FF0,FNET)
42.25      4        CONTINUE
43.25      ENDPROCEDURE
   44                FA=FNET-(FP-FFR)
   45                XDDD=-W**2*XD
   46                R1=-K1*XDDD*W
   47                R=CMPXPL(0.,0.,0.5,W,R1)
   48                Z1=KSV*R
   49                Z=LIMIT(-40.,40.,Z1)
   50                SGN=FCNSW(Z,-1.0,0.0,1.0)
   51                SGN2=FCNSW(FA,-1.0,0.0,1.0)
   52                YD1=CSV*Z*SQRT(PS-LIMIT(-PS,PS,SGN*FA/AA))
   53                YD2=SGN2*CV*SQRT(ABS(FA/AA))
```

```
   54              FYD=(YD1-YD2)/12./AA
   55              Y=INTGRL(0.,YD)
   55.25  NOSORT
   55.5   *       GO TO 30
   55.6   51      IF(KEEP.NE.1) GO TO 30
   55.7           TX=TIME+0.001
   55.8           IF(AMOD(TX,.05).GT.0.002) GO TO 30
   55.81          WRITE(8,31) TIME,XCUT,U
   55.82  31      FORMAT(3E14.6)
   55.83  30      CONTINUE
   56          PRINT U, X, Y, XCUT, R, FNET, FP, FA
   57          TITLE ACTIVE/PASSIVE MOTION COMPENSATION SYSTEM
   58          TIMER PRDEL=0.05, FINTIM=10., DELT=0.05
   59          METHOD  RKSFX
   60       END
   60.7        PARAMETER RW=0.5
   60.8        TIMER DELT=0.1
   60.81    END
   61       STOP
   62       ENDJOB
END OF FILE


$C *SKIP
```

APPENDIX F.2

```
LINSYS
  1      C********************* REMC:LINSYS ****************************
  2      C
  3      C          LINEARIZED MODEL OF MOTION COMPENSATION SYSTEM
  4      C
  5      C*************************************************************
  6            COMPLEX G,F,T1,T2,HFF,HFB,Z1,S,H,PWR
  7            REAL KS,K1,K2,K3,KP,M,N,LOGRW,KFF
  8            READ(5,1,END=99)AA,A,PO,VC,VT,GAM,M,Z,CV1,CV2,CX,DELAY
  9            KS=2.*GAM*PO*A**2/VT*12.
 10            WN=SQRT(KS/M)
 11            N=VT/VC
 12            IF(Z.EQ.0.) Z=SQRT((N+1.)*(N+2.)/(8.*N))
 13            TC1=2.*Z/WN
 14            TC2=TC1/(N+1.)
 15            KP=N*KS/(N+1.)
 18      100   READ(5,1,END=99) W0,K1,K2,K3,KFF,CBP
18.1           HCV1=1./(CV2+CBP)
18.2           HCV2=CV1*HCV1
18.25          RWN=WN/W0
 19            IF(KFF.EQ.0.) KFF=KP*(CV2+CBP)/CV1
 20            WRITE(7,4) PO,VC,VT,N,KS,Z,WN,CX
 21            WRITE(7,5) CV1,CV2,CBP,K1,K2,K3,KFF
21.25          WRITE(7,6) W0,RWN
 22            LOGRW=-1.
22.25          TCV=TAN(DELAY/180.*3.14159)/W0
22.5           ALPH=SQRT(1.+(TCV*W0)**2)
 23            DO 20 I=1,81
 24            RW=10.0**LOGRW
 25            W=RW*W0
 26            S=CMPLX(0.,W)
 27            G=-KP*(1.+TC1*S)/(1.+TC2*S)
 28            F=M*S**2+CX*S
 29            HFB=(K1+K2*S+K3*S**2)*ALPH/(1.+TCV*S)*W*S/(W**2+W*S+S**2)
 30            HFF=KFF
 31            H=-(F/HCV1+CV1*(HFB+HFF))/(G/HCV1+CV1*HFF+1)
 32            T1=1./(1.+H)
 33            PHIH=ATAN2(AIMAG(H),REAL(H))*180./3.14159
 34            Z1=HFB*T1+HFF
 35            T2=T1-CMPLX(1.,0.)
 36            T1A=CABS(T1)
 37            T2A=CABS(T2)
 38            HA=CABS(H)
 39            PHI1=(ATAN2(AIMAG(T1),REAL(T1)))*180./3.14159
 40            PHI2=(ATAN2(AIMAG(T2),REAL(T2)))*180./3.14159
 41            DB1=20.*ALOG10(T1A)
 42            DB2=20.*ALOG10(T2A)
 43            DBH=20.*ALOG10(HA)
 44            Z2=CABS(Z1)
44.25          PWR=500.*AA*S*T2
44.5           PWRA=CABS(PWR)
 45            IF(MOD(I,2).EQ.1) WRITE(7,3) RW,DB1,PHI1,DB2,PHI2,
 46           * DBH,PHIH,Z2,PWRA
46.25          DBZ=20.*ALOG10(Z2)
46.5           PHIZ=(ATAN2(AIMAG(Z1),REAL(Z1)))*180./3.14159
 47            WRITE(8,3) LOGRW,DB1,DB2,PHI1,PHI2
```

```
48      20      LOGRW=LOGRW+0.025
49              GO TO 100
50      1       FORMAT(12E12.0)
51      3       FORMAT(10F13.4)
52      4       FORMAT('1PASSIVE SIDE'/'0PRESS. =',F6.0,5X,'CYL.VOL. =',
53             *F6.0,5X,'TANK VOL. =',F6.0,5X,'VOL RATIO =',F6.3/
54             *' STAT.STIFFNESS =',F8.2,5X,'CRIT.DAMP.RATIO =',F7.3,
55             *5X,'NAT.FREQ. =',F6.2/' BODY DRAG COEFF. =',F6.0)
56      5       FORMAT('0ACTIVE SIDE'/'0LINEAR VALVE COEFFS.  CV1 =',
57             *F9.5,5X,'CV2 =',F9.5,5X,'CBP=',F9.5/' FEEDBACK CONSTS.  K1 ='
57.25          *F6.0,
58             *3X,'K2 =',F6.0,3X,'K3 =',F6.1/' FEEDFWD CONST.  KFF =',F6.3/)
58.25   6       FORMAT('0OPERATING FREQUENCY=',F7.2/
58.5           * 5X,'NAT.FREQ./OP.FREQ.=',F6.2/'0')
59      99      STOP
60              END
OF FILE


SKIP
```

APPENDIX F.3

```
PTIM
 1      C     ******************** REMC:OPTIM ****************************
 2      C
 3      C     **** PROGRAM TO OPTIMIZE PARAMETERS OF CONTROL SYSTEM ***
 4      C
 4.5    C     ************************************************************
 5            DIMENSION VAR(3,6)
 6            EXTERNAL TRANSF,FLO,FHI,FMPL
 7            COMPLEX S,HFF,F,G
 8            REAL M,N,KP,KS
 9            COMMON/PARAM/S,HFF,F,G,HCV1,HCV2
10            READ(5,1) AA, A,PO,VC,VT,GAM,M,Z,CV1,CV2,CBP
10.25         READ(5,1)W
11      1     FORMAT(12E10.0)
13            KS=2.0*GAM*PO*A**2/VT*12.0
14            WN=SQRT(KS/M)
15            N=VT/VC
16            IF(Z.EQ.0.) Z=SQRT((N+1.)*(N+2.)/(8.*N))
17            KP=N*KS/(N+1.)
18            S=CMPLX(0.,W)
18.25         TC1=2.*Z/WN
18.5          TC2=TC1/(N+1.)
18.6          G=KP*(1.+TC1*S)/(1.+TC2*S)
18.7          F=M*S**2
18.8          HCV1=1./(CV2+CBP)
18.81         HCV2=CV1*HCV1
18.82         KFF=0.
18.83         HFF=KFF
19            VAR(1,1)=0.0
20            VAR(2,1)=0.
21            VAR(3,1)=0.
22            CALL COMPLX(X,VAR,3,3,6,4,9.9,50,150,250,10,0.001,TRANSF,FLO,
23           *FHI,FMPL,&999,&777)
24            STOP
25      999   STOP 9
26      777   STOP 7
27            END
28            FUNCTION TRANSF(T,NN)
29            DIMENSION T(1)
30            COMPLEX S,G,F,HFB,T1,HFF
31            REAL K1,K2,K3
32            COMMON/PARAM/S,HFF,F,G,HCV1,HCV2
34            K1=T(1)
35            K2=T(2)
36            K3=T(3)
41            HFB=K1+K2*S+K3*S**2
42            T1=(G-HCV2*HFF-HCV1*S)/(F+G+HCV2*HFB-HCV1*S)
43            TRANSF=CABS(T1)
44            RETURN
45            END
46            FUNCTION FLO(T,N,J)
47            DIMENSION T(1)
48            GO TO (1,2,3,4),J
49      1     FLO=0.
50            RETURN
51      2     FLO=0.
```

```
52              RETURN
53      3       FLO=-10.
54              RETURN
54.25   4       FLO=0.
54.5            RETURN
55              END
56              FUNCTION FHI(T,N,J)
57              DIMENSION T(1)
58              GO TO (1,2,3,4),J
59      1       FHI=0.
60              RETURN
61      2       FHI=0.
62              RETURN
63      3        FHI=10.
64              RETURN
64.25   4       FHI=128.
64.5            RETURN
65              END
66              FUNCTION FMPL(T,N,J)
67              DIMENSION T(1)
68              COMPLEX S,T1,HFF,HFB,F,G
69              COMMON/PARAM/S,HFF,F,G,HCV1,HCV2
69.25           K1=T(1)
69.5            K2=T(2)
69.6            K3=T(3)
69.7            HFB=K1+K2*S+K3*S**2
69.8            T1=(G-HCV2*HFF-HCV1*S)/(F+G+HCV2*HFB-HCV1*S)
69.81           FMPL=CABS(HFB*T1+HFF)
71              RETURN
72              END
OF FILE

*SKIP
```

APPENDIX G

EXPERIMENTAL & SIMULATION RESULTS

FREQ. Hz.	K_3	AMPL. RATIO		PHASE LAG		FIGURE
		EXP'T	SIMUL.	EXP'T	SIMUL.	
0.5	0	0 db	-1.4 db	0°	18°	G.1
0.5	5	-3 db	-2.7 db	41°	27°	G.2
1.0	0	-4 db	-4.75 db	54°	36°	G.3
1.0	5	-7.3 db	-7.8 db	72°	54°	G.4
2.0	0	-7.5 db	-8.5 db	77°	100°	—
2.0	5	-11.7 db	-10.3 db	90°	108°	—

THE ABOVE ARE PLOTTED ON A BODE DIAGRAM IN FIG. 4.2.1.

NOTES ON FIGURES G.1 – G.4 :

- LOWER 2 CURVES WERE GENERATED BY THE COMPUTER USING THE SIMULATION PROGRAM OF APPENDIX F.1.
- UPPER 2 CURVES ARE FROM CHART RECORDER. FULL SCALE DEFLECTION IS ± 1.5 INCHES.
- AMPLITUDE RATIOS AND PHASE SHIFTS WERE ESTIMATED FROM THESE CURVES.

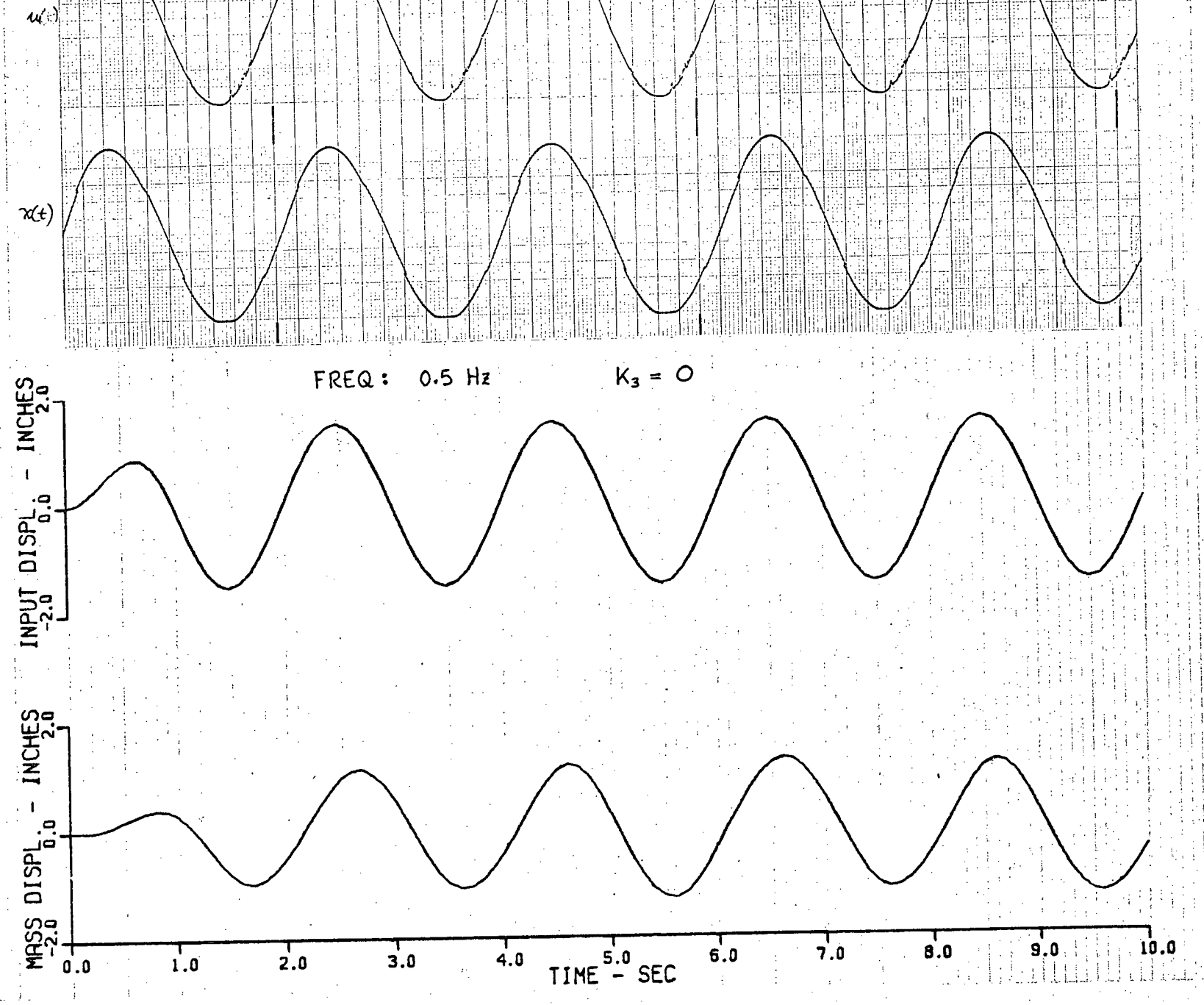
w(t)
x(t)
FREQ: 0.5 Hz
$K_3 = 0$
INPUT DISPL. - INCHES
2.0
0.0
-2.0
MASS DISPL. - INCHES
2.0
0.0
-2.0
0.0
1.0
2.0
3.0
4.0
5.0
6.0
7.0
8.0
9.0
10.0
TIME - SEC

FIG. G.1

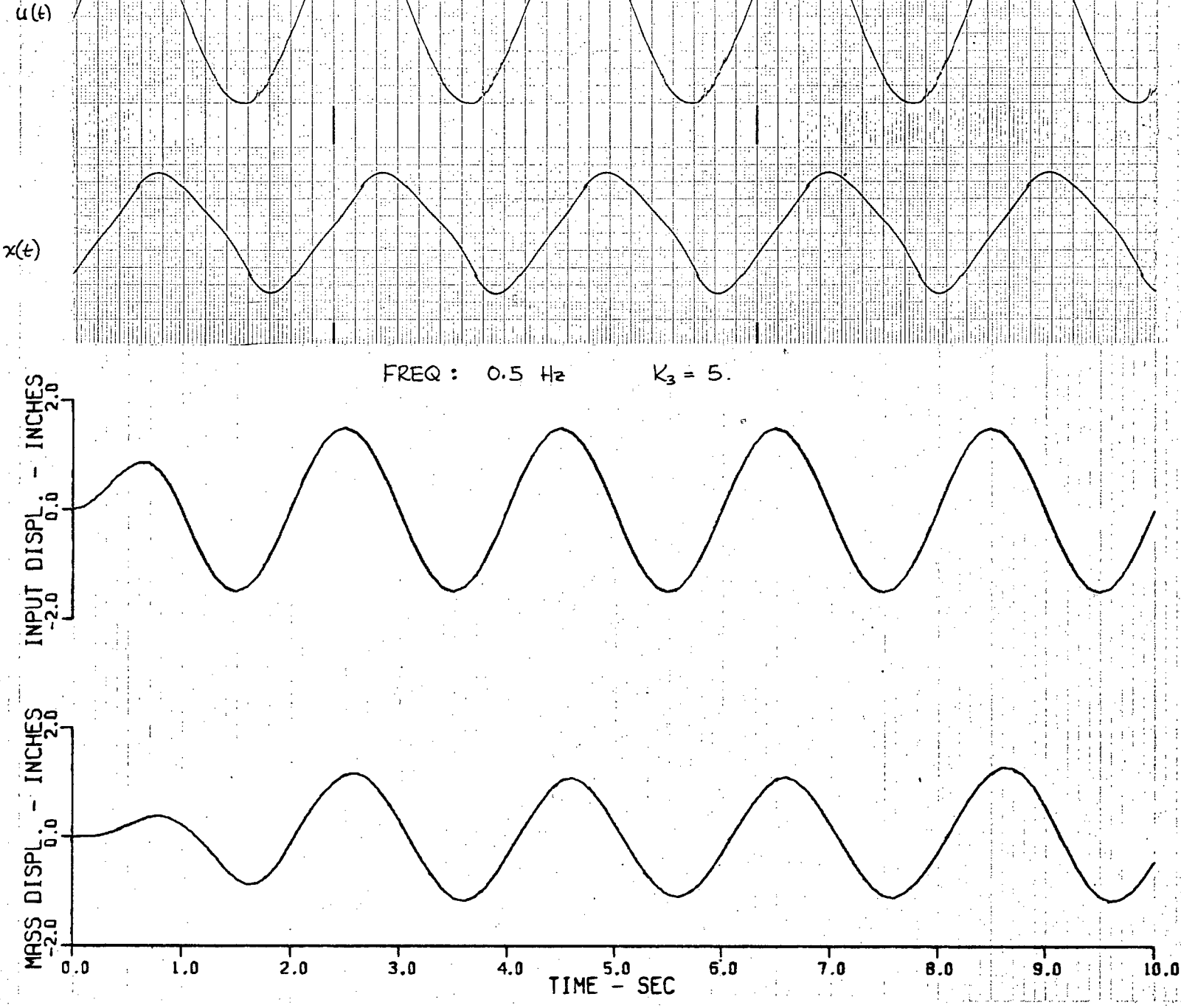
u(t)
x(t)
FREQ : 0.5 Hz
K_3 = 5.
INPUT DISPL. - INCHES
2.0
0.0
-2.0
MASS DISPL. - INCHES
2.0
0.0
-2.0
0.0
1.0
2.0
3.0
4.0
5.0
6.0
7.0
8.0
9.0
10.0
TIME - SEC

FIG. G.2

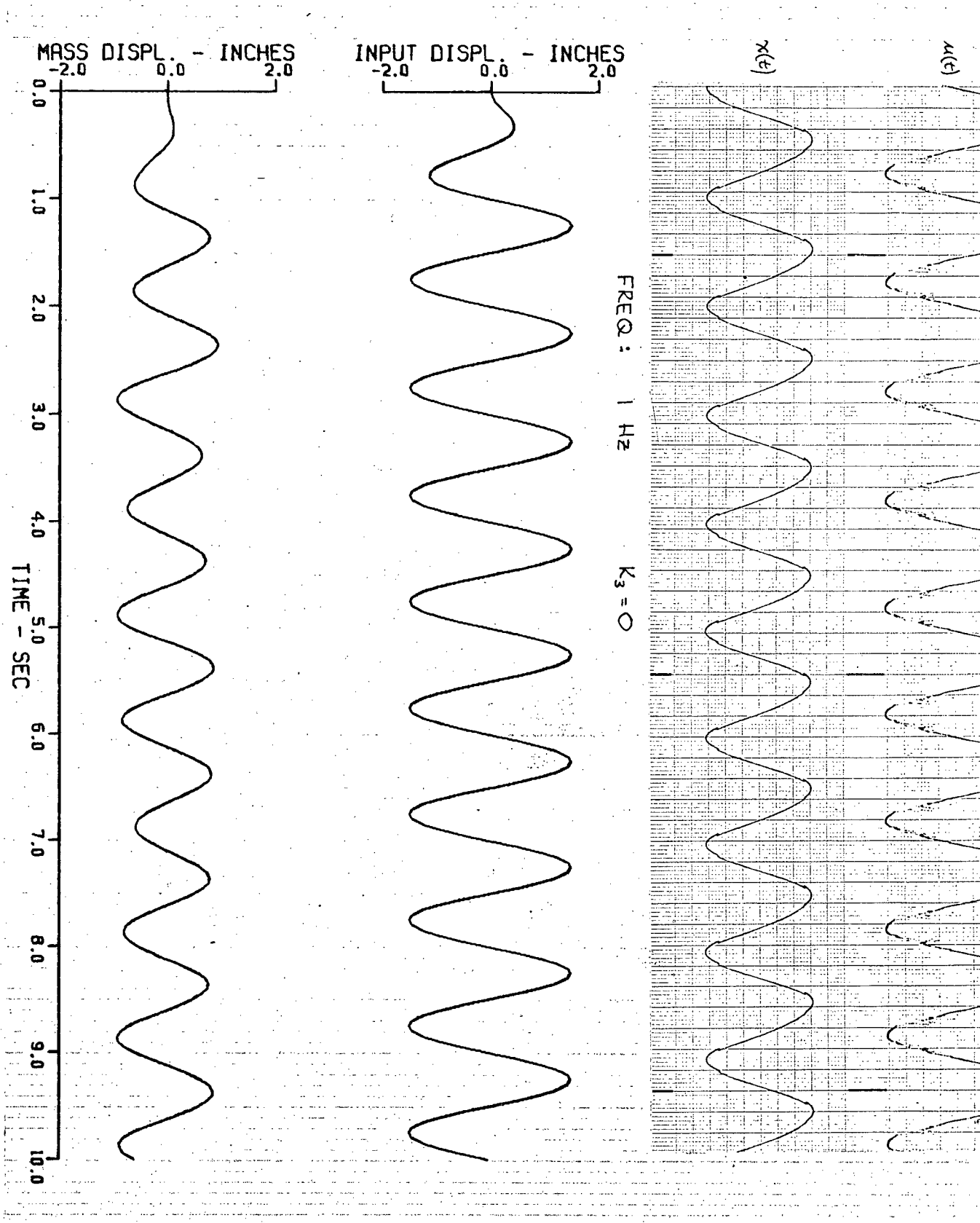
REMC PLOT# 00720098.
MASS DISPL. - INCHES
-2.0
0.0
2.0
INPUT DISPL. - INCHES
-2.0
0.0
2.0
x(t)
u(t)
FREQ: 1 Hz
K3 = 0
0.0
1.0
2.0
3.0
4.0
5.0
6.0
7.0
8.0
9.0
10.0
TIME - SEC

FIG. 6.3

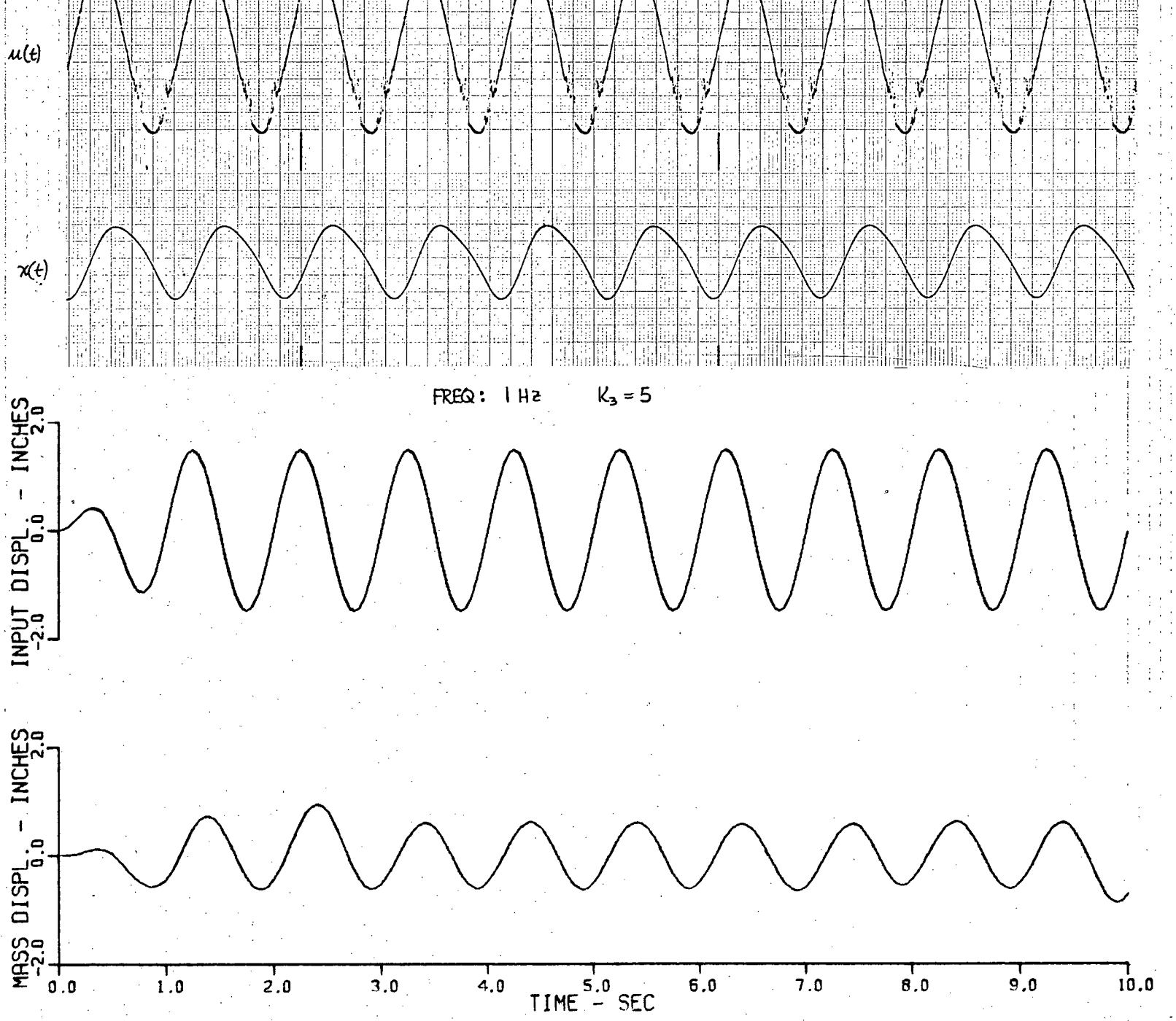
u(t)
x(t)
FREQ: 1 Hz
$K_3 = 5$
INPUT DISPL. - INCHES
2.0
0.0
-2.0
MASS DISPL. - INCHES
2.0
0.0
-2.0
0.0
1.0
2.0
3.0
4.0
5.0
6.0
7.0
8.0
9.0
10.0
TIME - SEC